

ROLE OF THE EBOLAVIRUS GLYCOPROTEIN IN COUNTERING TETHERIN

DURING VIRAL BUDDING

Nathan H. Vande Burgt

A DISSERTATION

in

Cell and Molecular Biology

Presented to the Faculties of the University of Pennsylvania

in

Partial Fulfillment of the Requirements for the

Degree of Doctor of Philosophy

2015

Supervisor of Dissertation

Paul F. Bates, Ph.D., Professor of Microbiology

Graduate Group Chairperson

Daniel S. Kessler, Ph.D., Associate Professor of Cell and Developmental Biology

Dissertation Committee

Ronald N. Harty, Ph.D., Professor of Pathobiology and Microbiology

Jeffery M. Bergelson, M.D., Professor of Pediatrics

Susan R. Weiss, Ph.D., Professor of Microbiology

Claude Krummenacher, Ph.D., Assistant Professor of Biological Sciences

ROLE OF THE EBOLAVIRUS GLYCOPROTEIN IN COUNTERING TETHERIN DURING VIRAL
BUDDING

COPYRIGHT

2015

Nathan H. Vande Burgt

This work is licensed under the
Creative Commons Attribution-
NonCommercial-ShareAlike 3.0
License

To view a copy of this license, visit

<http://creativecommons.org/licenses/by-nc-sa/3.0/>

DEDICATION PAGE

This thesis is dedicated to the memory of my grandfathers, Wilfred Vande Burgt and Howard Kooiman.

ACKNOWLEDGMENTS

There are many people I would like to thank who have participated in this research at every step, from designing experiments to writing the thesis.

I would like to thank members of the Bates lab, past and present, for their helpful advice, critiques, and support. They have made the Bates lab a stimulating and productive environment in which to pursue challenging scientific questions. I would especially like to thank my mentor Paul Bates, for his helpful and engaging role in every part of my thesis work. He has taught me how to critically assess my research and how to ask relevant questions to advance scientific knowledge.

I would like to thank the many labs within the Microbiology Department at the University of Pennsylvania for making a stimulating work environment, especially the Doms, Ross, Cherry, and Lopez labs for helpful advice and critiques. I would like to thank members of my thesis committee including Ronald Harty, PhD, Jeffery Bergelson, MD, Susan Weiss, PhD, and Claude Krummenacher, PhD.

I would like to thank my friends and family for all of their support during my time here at the University of Pennsylvania. My parents, Jerry and Margie Vande Burgt have listened and encouraged me to continue in my studies and I would not be here today without their support. My girlfriend, Natalie Hsiao Fang-Yen, has been very supportive and even participated in editing this document. This thesis would not be possible without her. My church, Spirit and Truth Fellowship CRC, and small group Bible study have also encouraged and prayed for me countless times.

I would like to also thank the various funding sources that made all of this research possible including the following grants: NIH R01-AI081913, NIH U54-AI57168, T32-GM07299, and T32-AI55400.

ABSTRACT

ROLE OF THE EBOLAVIRUS GLYCOPROTEIN IN COUNTERING TETHERIN DURING VIRAL BUDDING

Nathan H. Vande Burgt

Paul F. Bates

Ebola virus (EBOV) is the causative agent of Ebola virus hemorrhagic fever and initiates sporadic outbreaks with very high mortality rates of up to 90%. The only viral surface protein on EBOV virions, the EBOV Glycoprotein (GP_{1,2}), is a known antagonist of the intrinsic innate immune effector Tetherin, which prevents release of budded virions by “tethering” them to the cell. Unlike other Tetherin antagonists, GP_{1,2} does not degrade Tetherin, remove Tetherin from the cell surface, or sequester Tetherin in intracellular compartments. Thus, the mechanism of how GP_{1,2} counters Tetherin is not well understood. This study utilizes methods in molecular biology and microbiology to focus on the different domains of GP_{1,2} and understand their role in countering Tetherin. Using VP40 or HIV-1 Gag to produce virus-like particles (VLP), we show that the GP_{1,2} glycan cap and transmembrane domain are necessary for GP_{1,2} anti-Tetherin activity. Chimeric proteins containing alternative transmembrane domains in place of the GP_{1,2} transmembrane domain fail to counteract Tetherin and release VLP. Additionally, using widefield microscopy, alternative transmembrane domains do not change the surface localization of Tetherin and GP_{1,2}, suggesting that surface interactions may not be important for understanding how GP_{1,2} counters Tetherin. Other observations and experiments suggest an active role for GP_{1,2} in the formation of viral particles. In conclusion, we propose a model where the GP_{1,2} transmembrane domain assists in a budding process that does not allow for incorporation of Tetherin into the budding virions. The model suggests that the GP_{1,2} transmembrane domain functions to avoid Tetherin mediated restriction and to form viral particles independent of VP40 budding.

TABLE OF CONTENTS

DEDICATION PAGE	III
ACKNOWLEDGMENTS	IV
ABSTRACT	V
TABLE OF CONTENTS	VI
LIST OF ILLUSTRATIONS	VIII
CHAPTER 1 – INTRODUCTION AND BACKGROUND	1
Section 1.1 – Ebola Virus Epidemiology	1
Section 1.2 – Ebola Virus Pathogenesis	2
Section 1.3 – Antibody Therapy and Vaccines for Ebola Virus	3
Section 1.4 – Genomic Structure of Ebola Virus and Viral Proteins	4
Section 1.5 – Ebola Virus Entry & Replication	6
Section 1.6 – Ebola Virus Assembly & Budding	7
Section 1.7 – Structure and Functions of the Ebola Virus Glycoprotein.....	8
Section 1.8 – Cellular Anti-viral Intrinsic Innate Immune Effectors	13
Section 1.9 – Antiviral Functions of Tetherin	16
Section 1.10 – Viral Antagonists of Intrinsic Innate Immune Effectors	20
Section 1.11 – Viral Antagonists of Tetherin	22
Section 1.12 – Interactions between Ebola Virus Glycoprotein and Tetherin	24
CHAPTER 2 – REQUIREMENTS WITHIN THE EBOLA VIRAL GLYCOPROTEIN FOR TETHERIN ANTAGONISM	27

Section 2.1 – Abstract	27
Section 2.2 – Introduction	27
Section 2.3 – Materials and Methods	30
Section 2.4 – Results	34
Section 2.5 – Discussion	47
CHAPTER 3 –EBOLA VIRUS GLYCOPROTEIN CONSTRUCTS AND TETHERIN LOCALIZE INDEPENDENTLY AT THE CELL SURFACE	51
Section 3.1 – Abstract	51
Section 3.2 – Introduction and Background	51
Section 3.3 – Methods	53
Section 3.4 – Results	55
Section 3.5 – Discussion	61
CHAPTER 4 – CONCLUSIONS AND FUTURE DIRECTIONS	64
Section 4.1 – Formation of Ebola Virus Glycoprotein Induced Particles	64
Section 4.2 – Role of the Sialic Acid Residues in the Glycan Cap	67
Section 4.3 – How the Ebola Virus Glycoprotein Could Counter Tetherin	69
BIBLIOGRAPHY	74

LIST OF ILLUSTRATIONS

CHAPTER 1

Figure 1-1: Linear models of EBOV GP gene products.....	10
Figure 1-2: PBD models of EBOV GP _{1,2} and cathepsin cleaved GP _{1,2}	12
Figure 1-3: Model depicting Tetherin mediated restriction of viral particles.....	18

CHAPTER 2

Figure 2-1: C-terminal and N-terminal nucleotide sequence list.....	32
Figure 2-2: Comparing the ability of alternative msd to release VLP from Tetherin.....	35
Figure 2-3: Expression of glycoprotein in the cell lysates of Figure 2-2C.	36
Figure 2-4: Expression of glycoprotein in the cell lysates of Figure 2-2D.	38
Figure 2-5: Testing the role of GP _{1,2} cytoplasmic cysteine residues in antagonizing Tetherin.	40
Figure 2-6: Comparison of chimeric sGP glycoproteins in an HIV-1 Gag budding assay. .	42
Figure 2-7: Testing the ability of GP _{1,2} to counter Tetherin containing an alternative transmembrane domain.....	43
Figure 2-8: Testing the ability of Tetherin containing an alternative transmembrane in restricting VLP release.	45
Figure 2-9: Determining the role of the glycan cap in countering Tetherin.	47

CHAPTER 3

Figure 3-1: Representative immunofluorescence image slices of HT1080 cells.....	56
Figure 3-2: Geometric means of the fluorescence signal within image slices chosen for analysis.	57
Figure 3-3: Comparison of Tetherin and GP channels by PCC.	59
Figure 3-4: ICA plots comparing the intensities of the Tetherin and GP channels.	60
Figure 3-5: Comparing the intensities of the Tetherin and GP channels by ICQ.....	62

CHAPTER 4

Figure 4-1: Budding of VP40 VLP with sGP chimeras containing alternative transmembrane domains.....66

Figure 4-2: The effect of neuraminidase on sGP-TM(GP) mediated release of particles from Tetherin.68

Figure 4-3: Comparison of EBOV budding in three different models.70

CHAPTER 1 – INTRODUCTION AND BACKGROUND

Section 1.1 – Ebola Virus Epidemiology

Ebola virus is a filamentous negative-sense, single stranded RNA virus of the family *Filoviridae* (5, 123, 139). There are two major genera within *Filoviridae*, *Ebolavirus* and *Marburgvirus*, both of which have viral species capable of producing severe hemorrhagic fever in people. A third genus, *Cuevavirus*, has not been implicated in causing human disease (182). Within the *Ebolavirus* genus, there are currently five viral species with varying propensities to infect human populations and cause disease. The founding member of the genus, *Zaire ebolavirus* (EBOV), was originally described in 1976 as the causative agent of an outbreak responsible for 280 deaths in the Democratic Republic of the Congo (DRC), formerly Zaire (2). Additional viral species, such as *Sudan ebolavirus*, have caused outbreaks of similar size and severity (1). A third species *Bundibugyo ebolavirus*, is a relatively new species and has caused outbreaks with less mortality than seen with *Zaire* or *Sudan ebolavirus* (165). Two other species of *Ebolavirus*, *Tai forest ebolavirus* and *Reston ebolavirus*, have only been implicated in causing a few cases of infection in people (118, 142).

Outbreaks associated with these species occur sporadically, localizing primarily within central sub-Saharan Africa. Most recently, EBOV has caused a large outbreak in the West African countries of Guinea, Liberia and Sierra Leone (13). As of May 17, 2015, a total of 26,933 cases have been reported resulting in 11,120 deaths (3). Unlike previous isolated EBOV outbreaks, this epidemic spread to large urban communities with no previous history or experience with EBOV disease (75). Urbanization has likely assisted the increase of EBOV cases within West Africa and facilitated spread to other countries, such as the United States.

EBOV outbreaks are primarily sporadic and humans cannot sustain viral transmission from one outbreak to the next. Therefore, an animal reservoir has been implicated as the source of EBOV (30). Initially, primates were considered as a possible reservoir, since contact with

primates was often associated with the index case of EBOV outbreaks (70). However, infection of primates and other wildlife species with EBOV produces fatality rates similar to those seen in people (150). For example, EBOV has caused outbreaks that have severely depleted the Western gorilla (*Gorilla gorilla*) and chimpanzee (*Pan troglodytes*) population (22). Thus, primates are likely an intermediate host and not the ultimate source of EBOV. Several species of fruit bats have been found to contain EBOV genomes (149). Furthermore, contact with fruit bats has been connected to the 1995 outbreak of EBOV in the DRC (148). However, infectious EBOV has yet to be isolated from fruit bats, and there is currently no working animal model to study EBOV infection in fruit bats.

Section 1.2 – Ebola Virus Pathogenesis

The incubation period of EBOV can last anywhere from 2-21 days. In the majority of infected persons, early signs of EBOV disease progress as a typical viral infection with fever, chills, and malaise (32, 181). More severe symptoms present as the disease progresses including abdominal pain, diarrhea, vomiting, shortness of breath, internal hemorrhaging, or unexplained bleeding (4, 32, 181). In some earlier cases of EBOV, a large macropapular rash was noted on patients, however this was not observed in the recent West Africa outbreak (11, 32). Patients who succumb to the disease usually die within 6 to 16 days of hypovolemic shock and multi-organ failure. Survivors usually show signs of improvement within 6 to 11 days and often develop a humoral antibody response to EBOV. Overall mortality rates for patients with EBOV are unusually high, with an average mortality of 79% for all outbreaks from 1976 – 2012.

EBOV initiates infection by direct contact of exposed mucosal surfaces or skin breaks with contaminated surfaces or material (51). From the initial contact site, EBOV infects macrophages (M Φ) and dendritic cells (DC) (69). Once infected, these cells secrete cytokines and chemokines, such as MIP-1 α , MIP-1 β and TNF α , which results in attracting additional M Φ and DC to the site of infection, providing more infection targets for EBOV (86). From the initial

infection, MΦ and DC travel to the lymph nodes and spleen where EBOV is able to spread to other cell types, including fibroblasts, endothelial and epithelial cells (116, 215). One significant cell type predominately not infected by EBOV are lymphocytes (12). Despite this resistance to EBOV infection, lymphocyte populations crash a few days after EBOV infection (264). The mechanisms causing lymphocyte depletion are not well understood, but may involve production of nitric oxide or dysregulation of the innate immune system following EBOV infection (12, 102, 264). High levels of cytokines, such as IL-2, IFN-γ and TNFα, are detected in patients that succumb to EBOV, suggesting that an over-active immune response may contribute to mortality (256).

Section 1.3 – Antibody Therapy and Vaccines for Ebola Virus

Currently there are no licensed vaccines, anti-viral drugs, or antibody therapies available. The sporadic nature, high fatality rate, and isolated location typical of EBOV infections have hindered the development of treatments for EBOV. Most EBOV outbreaks occur in isolated locations lacking basic health care infrastructure, transportation networks, and electricity grids. Thus, treatment of patients consists primarily of supportive care such as providing drugs for pain and nausea (83). Typically, EBOV occurs in locations with malaria and other infectious diseases, so treatment often includes antibiotics or anti-malaria drugs (83). Where possible, a limited number of patients receive blood transfusions from recovering EBOV patients, which provides protective antibodies before newly infected patients can develop their own immune response (178). However, the small number of patients receiving these transfusions has made it difficult to determine the effectiveness of this treatment. Until the recent outbreak in West Africa, treatment of most EBOV patients was limited to supportive care and containment of infected individuals to prevent spread.

Several vaccines are in the process of being developed for EBOV. Two of the most successful, which have moved into phase 3 clinical trials, are recombinant viruses expressing the EBOV glycoprotein with either vesicular stomatitis virus (VSV-EBOV) or a defective chimpanzee

adenovirus type 3 (cAd3-EBO) as the backbone. The cAd3-EBO vaccine, when boosted with modified vaccinia Ankara (MVA), was able to protect 4/4 macaques from lethal EBOV challenge (238). In several phase 1 clinical trials, the vaccine demonstrated safety and immunogenicity after a single vaccination (133, 144, 206). In macaque challenge models, the VSV-EBOV vaccine proved protective and interestingly, could be administered post-challenge and still result in survival of some animals (58, 127). The VSV-EBOV vaccine was moved into phase 1 clinical trials and showed immunogenicity at all titers tested and production of neutralizing antibodies at higher doses (7, 209). Both of these vaccines are currently being tested in ongoing phase 2/3 clinical trials in Liberia. An interim report of one trial shows the VSV-EBOV vaccine to be highly efficacious, with an estimated vaccine efficacy of 100% (101).

In addition to vaccines, antibodies are currently being developed for treatment of infected individuals. One potential antibody drug, ZMapp, was tested in guinea pigs and non-human primates and showed good protection with 18/18 rhesus monkeys surviving after given lethal doses of EBOV (204). Zmapp is a drug formulation consisting of three monoclonal antibodies directed against the EBOV glycoprotein (204). Some patients who were treated in the United States for EBOV infection in 2014 received ZMapp (164). ZMapp is currently slated to begin clinical trials and possibly become one of the first licensed therapeutics for treatment of EBOV.

Section 1.4 – Genomic Structure of Ebola Virus and Viral Proteins

Filoviruses are single stranded, non-segmented, negative sense RNA viruses containing a genome approximately 18-19 kilobases long (59, 220). The EBOV genome, like other filoviruses, has seven genes organized in the following order: NP, VP35, VP40, GP, VP30, VP24, and L (59). From these seven genes, EBOV expresses nine proteins; a brief summary of each is given below (220, 258).

The NP gene expresses the Nucleoprotein that forms the core of the nucleocapsid structure and interacts with VP35 and VP24 to bind the viral RNA genome (109, 221).

Furthermore, Nucleoprotein also associates with VP40 to assist in incorporation of the genome into EBOV virions (189).

The VP35 gene produces the Polymerase cofactor VP35, which is thought to function as a phosphoprotein, analogous to the product of the P gene in rhabdoviruses (31). VP35 is known to associate with Nucleoprotein and VP40 and may have a role in bringing the EBOV polymerase to the nucleocapsid (109, 124). Importantly, VP35 is a potent antagonist of the interferon response (18). Several mechanisms by which VP35 counters interferon include binding double stranded RNA and preventing activation of PKR, inhibiting activation of interferon regulatory factor 3, and impairing the function of IKK ϵ and TBK-1 (17, 34, 60, 203).

The VP40 gene produces the matrix protein, VP40, which is primarily responsible for assembly and formation of filamentous virions (31). In fact, VP40 is capable of forming virus-like particles (VLP) independent of other viral proteins (20). VP40 forms multimers which can interact with the nucleocapsid, members of the ESCRT complex, and the plasma membrane (96, 227, 247).

The GP gene expresses three proteins by an unusual RNA editing event. The majority of the protein expressed from GP is the pre-secreted Glycoprotein (pre-sGP), which is post-translationally processed by cellular furin to generate the secreted Glycoprotein (sGP) and a small 40 amino acid peptide called delta-peptide (261). While the function of delta-peptide remains unclear, recent studies suggest that sGP acts as an immunogenic decoy to redirect immune responses to parts of sGP that are not present or inaccessible in the full-length Envelope Glycoprotein (GP_{1,2}) (176). Production of GP_{1,2} occurs when the RNA polymerase encounters a series of seven adenines and erroneously incorporates an eighth adenine, switching the open reading frame to generate GP_{1,2} (222, 258). GP_{1,2} is also processed by host furin into two subunits, GP₁ and GP₂; however, these subunits remain linked by a di-sulfide bond (120, 259). Three of these heterodimers interact to form the trimeric GP_{1,2} which is the only viral protein

expressed on the surface of EBOV (223). GP_{1,2} has many functions important for EBOV including mediating entry into target cells, shielding of viral and cellular epitopes, and countering Tetherin (35, 64, 129). The GP gene can also produce a third gene product, the Super small secreted Glycoprotein (ssGP), which is formed when the polymerase adds two additional adenines during transcription (258). Besides possibly functioning similar to sGP, this protein has no known function.

The VP30 gene expresses the Minor nucleoprotein VP30, which functions to associate with the nucleocapsid (95). VP30 also functions to allow transcription of viral RNA in the presence of an otherwise inhibitory RNA transcription secondary structure within the viral genome (266).

The VP24 gene produces the Membrane-associated protein VP24, which is required for nucleocapsid formation by associating with Nucleoprotein and VP35 (109). VP24 also functions to block cellular interferon production by preventing nuclear accumulation of STAT1 (210).

Finally, the L gene produces the large RNA-directed RNA polymerase L, which interacts with the nucleocapsid to drive virus replication and transcription (260).

Section 1.5 – Ebola Virus Entry & Replication

EBOV utilizes a number of cellular factors to bind cells and initiate uptake of virions into endocytic compartments where EBOV mediates fusion with the host cell. The surface glycoprotein of EBOV, GP_{1,2}, is heavily glycosylated with N and O-linked glycans (120). These glycans enable various C-type lectins including DC-SIGN and DC-SIGNR to bind GP_{1,2} and enhance infectivity of EBOV, but do not directly lead to cellular entry of virions (8, 234). EBOV virions are large filamentous particles with diameters up to 100 nm and lengths of up to 1500 nm. Uptake is mediated primarily by virion-induced macropinocytosis, although clatherin- or caveolar-mediated endocytosis pathways can be used as alternatives (23, 123, 179, 216). A member of the Tyro3 receptor kinase family, AXL, has been shown to stimulate macropinocytosis and lead to

enhanced viral entry; however, a direct interaction between AXL and GP_{1,2} has not been described and AXL does not stimulate macropinocytosis in all cell types (111, 232). Thus, it remains unclear exactly how EBOV induces macropinocytosis to stimulate uptake into host cells.

EBOV virions are transported through endocytic compartments to the late endosome where GP_{1,2} is processed by cellular cathepsins B and L (130, 225). Cathepsin cleavage removes the glycan cap and mucin domains of GP_{1,2} exposing the receptor binding domain, which interacts with the EBOV receptor, a cholesterol transporter called Niemann-Pick C1 (NPC1) (35, 44, 104). Interaction with NPC1, via a process that remains elusive, leads to insertion of the GP₂ internal fusion loops into the host lipid bilayer. Subsequently, the supporting triple helix collapses into a six-helix bundle, driving fusion and bringing the viral and cell membranes together (81, 268).

Inside the cell, EBOV proceeds to generate monocistronic mRNA which is translated and produces more viral proteins (219). Transcription of mRNA switches to genome replication once enough viral protein has accumulated, minimally Nucleoprotein, VP30, VP35, and L (177). As fully replicated negative sense genomes accumulate and associate with the nucleocapsid, Nucleoprotein levels drop and drive transcription to produce more mRNAs for protein production. Eventually, an equilibrium is reached and results in production of nucleocapsid coated viral genomic RNA.

Section 1.6 – Ebola Virus Assembly & Budding

Once viral RNA has replicated and produced enough viral protein, the nucleocapsid forms and covers the viral genome (177). Next, the matrix protein, VP40, interacts with Nucleoprotein and VP35 to drive incorporation of the nucleocapsid coated RNA and promote budding of EBOV particles (124, 154). VP40 adopts various conformational states corresponding to specific functions of VP40. At high concentrations, VP40 monomers initially oligomerize into hexamers; however, octamers form when bound to RNA, which readily incorporate into VP40

containing particles (76, 103, 246). Interestingly, VP40 octamer formation is essential for viral replication, yet VP40 is capable of producing particles with and without octamers (103). Thus, the role of VP40 oligomerization is not fully understood and remains to be clarified.

VP40 contains late-budding domains (L-domains), which allow VP40 to interact with cellular proteins that drive formation of viral particles during the late stages of virus replication (270). VP40 is able to recruit both Tsg101 and Nedd4 via an N-terminal peptide motif 7-PTAPPEY-13 (96, 170). Tsg101 is a component of the ESCRT-I complex, and is recruited to budded EBOV particles by recognizing and interacting with the PTAP motif in VP40 (10, 131, 155, 170). The proximal VP40 sequence PPEY also interacts with Nedd4, an ubiquitin ligase responsible for ubiquitinating VP40 oligomers and redirecting VP40 to sites of EBOV budding (247). Interestingly, VP40 L-domains, while enhancing virion production, are not essential for production of infectious EBOV virions (185). Thus, other viral proteins may allow EBOV to produce particles and bud independent of VP40 L-domains.

Other EBOV proteins are also known to be important for budding EBOV virions. Nucleoprotein associates with VP40 to enhance production of virions (154). EBOV GP_{1,2} can also enhance virion production in the presence of VP40 (154). GP_{1,2} mediated enhancement is likely due to the anti-Tetherin activity of GP_{1,2} (129). However, expression of EBOV Glycoprotein alone allows cells to produce unstructured, pleomorphic particles (136, 188). Whether or not this ability of GP_{1,2} to produce particles is important for infectious EBOV remains open for further investigation.

Section 1.7 – Structure and Functions of the Ebola Virus Glycoprotein

The EBOV Glycoprotein (GP_{1,2}) is the only viral protein expressed on the surface of EBOV particles (223). Functional GP_{1,2} predominately forms trimers on EBOV particles and when expressed in tissue culture cells (223). The full-length GP_{1,2} gene encodes 676 amino acids. The first 501 residues comprise the GP₁ subunit. The remaining 175 amino acids consist of the GP₂

subunit, as shown in Figure 1-1. Within GP₁, residues 1-32 are the signal peptide, which allows GP_{1,2} to be expressed on the cell and viral surface (220). The next 167 residues form the core of GP_{1,2} and also function as the receptor-binding region. Adjacent to the receptor-binding region is the glycan cap. The glycan cap spans residues 200-304 and contains six N-linked and unknown numbers of O-linked glycosylation sites (120, 220). In the native structure, this domain sits atop the core of GP_{1,2} and occludes the receptor-binding region (145). The mucin domain comprises residues 305-501 and, similar to the glycan cap, is heavily glycosylated, containing 14 N-linked glycosylation sites besides additional O-linked glycans (120, 220). Unlike the rest of GP₁, which forms a rigid structure, the mucin domain is disordered and unstructured (145). The mucin domain appears to form a propeller-like structure extending above and beyond the rest of GP_{1,2} (97). This extended structure may explain the ability of the mucin domain to occlude epitopes on GP_{1,2} and other cellular surface proteins (64, 235). The other subunit, GP₂, wraps around the GP₁ core and primarily consists of coiled-coil domains that function to drive fusion of the virus with the cell membranes (268, 269). The GP₂ subunit contains a transmembrane domain, which anchors GP_{1,2} to the plasma membrane and may have a role in GP_{1,2} mediated cytopathic effects (90). The cytoplasmic tail of GP_{1,2} is only four amino acids long and contains acylated cysteine residues similar to other viral type I fusion proteins (114). However, preventing acylation of these residues does not decrease the infectivity of EBOV pseudotypes, and thus, the importance of acylation remains to be discovered (114).

GP_{1,2} undergoes several processing events within the host cell. First, as a single pass type I transmembrane protein, the initial 32 amino acids, which function as a signal peptide for insertion into the ER membrane, are removed from mature GP_{1,2} by host cell machinery (220). In addition to promoting GP_{1,2} plasma membrane expression, this sequence also modulates GP_{1,2} glycosylation, which in turn, affects GP_{1,2} binding to DC-SIGN and DC-SIGNR (171). Second, the immature glycoprotein GP₀ contains a consensus furin site at residues 498-501, which results in

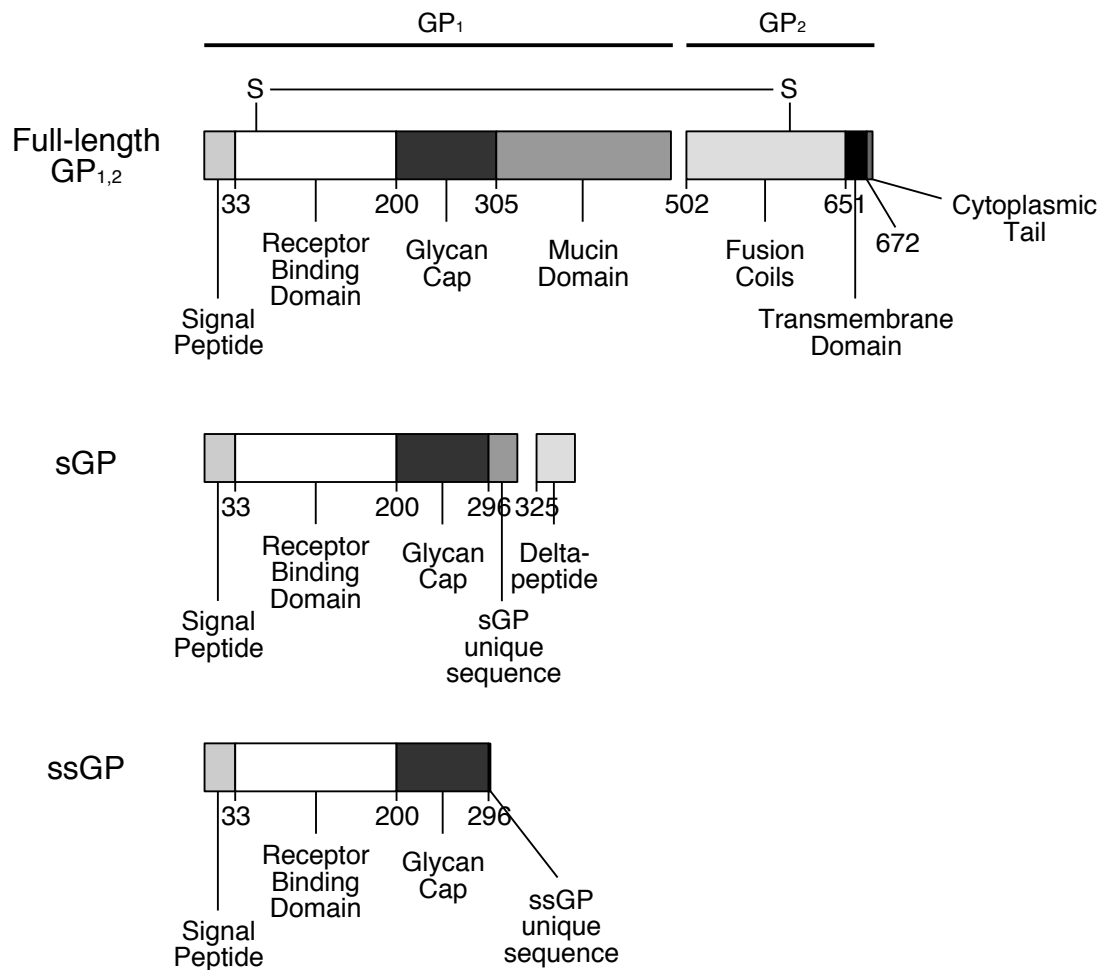


Figure 1-1: Linear models of EBOV GP gene products. The majority of polypeptides produced are sGP, the secreted glycoprotein, that lacks a transmembrane domain. Full-length GP_{1,2} is produced about 20% of the time and is processed by furin to produce two subunits, GP₁ and GP₂, which are held together by a disulfide bond. A small amount of ssGP is also produced.

formation of two subunits, GP₁ and GP₂ when cleaved by furin (223, 259). Post-processing, these subunits remain associated with each other by a di-sulfide bond to form mature GP_{1,2} (259). Interestingly, preventing the cleavage of GP_{1,2} into GP₁ and GP₂ by mutation of the cleavage site or producing pseudotypes in furin-deficient cell lines does not reduce the infectivity of GP_{1,2} pseudotypes (271). Finally, after EBOV entry into cells, GP_{1,2} requires processing by cellular cathepsins in the acidic late endosomes, notably Cathepsins B and L (36, 130, 225). Cathepsins recognize and cleave a disordered loop within GP₁, as shown in Figure 1-2, resulting in removal of the glycan cap and mucin domains of GP_{1,2} (35, 44, 104, 145). There is also an additional requirement for cathepsins, independent of proteolytic cleavage, which is not fully understood (14).

The primary function of EBOV GP_{1,2} is to mediate entry of viral particles into host cells. GP_{1,2} can bind to several cellular factors that improve infectivity by enhancing attachment of virions to the host cell, including dendritic cell-specific intercellular adhesion molecule-3-grabbing non-integrin (DC-SIGN and DC-SIGNR) (8, 234). GP_{1,2} likely stimulates AXL to enhance macropinocytosis of virions and allow for uptake into late endosomes; however, a direct interaction between AXL and GP_{1,2} has not been shown (111, 232). None of these interactions are sufficient to allow GP_{1,2} to mediate fusion with host cells. To fuse in the late endosomes, cathepsin-cleaved GP_{1,2} must interact with Niemann-Pick C1 (NPC1) (35, 44).

The EBOV GP_{1,2} also has a role in subverting the host immune system. The GP_{1,2} mucin domain has been shown to mask its own epitopes as well as other surface proteins from antibody and immune cell recognition. Initially, it was thought that the GP_{1,2} mucin domain down-regulated proteins from the cell surface (63, 235). However, the apparent down-regulation of GP_{1,2} could be reversed by probing with antibody epitopes that were not affected by the mucin domain (64). Thus, a shielding model has been proposed that explains how GP_{1,2} can block immune recognition of its own epitopes and prevent recognition of other surface markers on infected cells

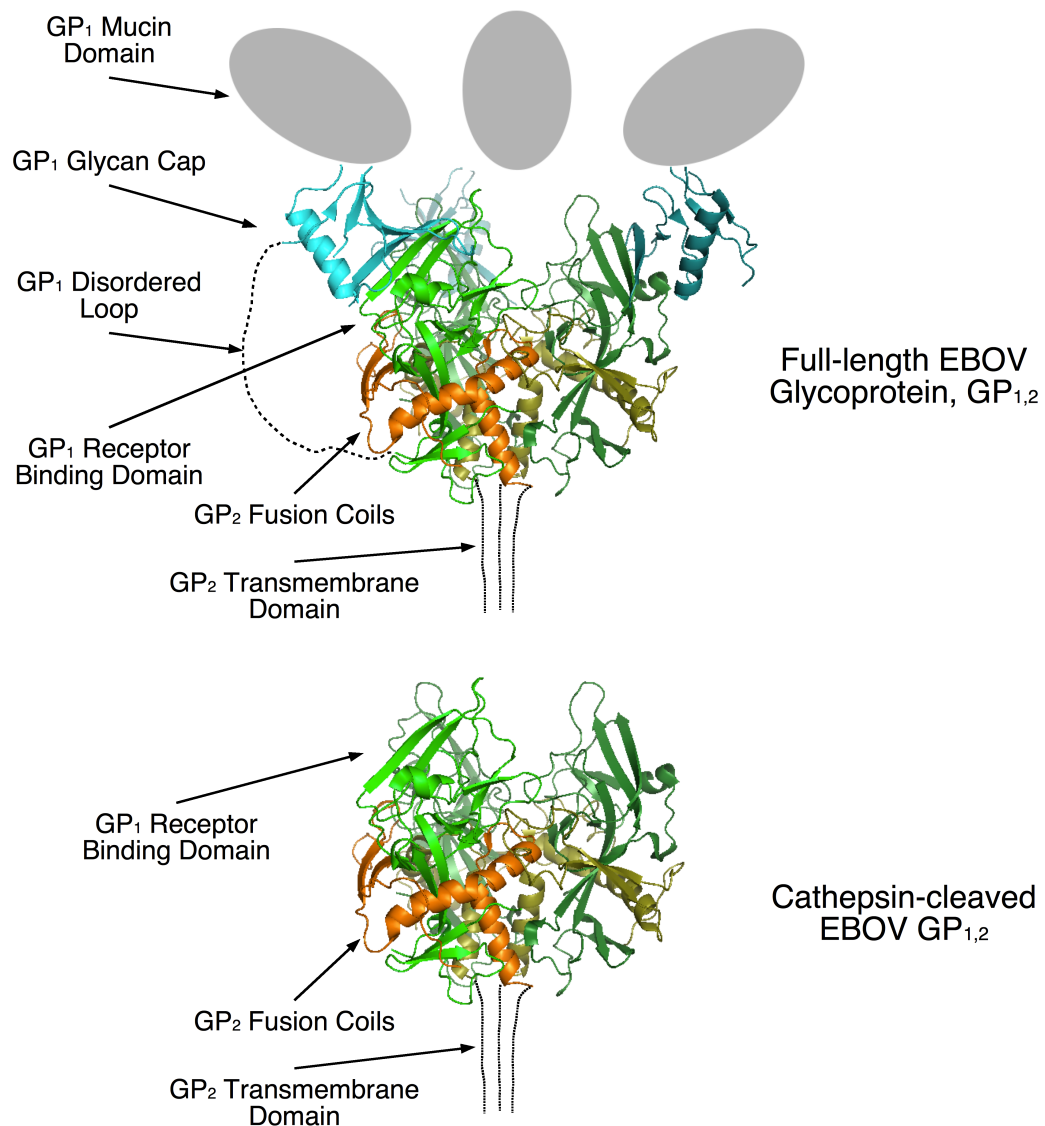


Figure 1-2: PBD models of EBOV GP_{1,2} and cathepsin cleaved GP_{1,2}. The crystal structure data for the full-length EBOV glycoprotein (PDB accession number 3CSY deposited by Lee et al.) was displayed using Jmol. Each of the three monomers of GP_{1,2} is displayed in either bright colors, dull colors, or shadowed colors. Green represents the receptor binding domain of GP₁. Blue represents the glycan cap domain of GP₁, which is connected to the receptor binding domain by a disordered loop. The disordered loop is not represented in the structure, but is displayed here as a black dotted line. The mucin domain above the glycan cap domain is also a disordered region not shown in the structure and is displayed here as a grey circle. The orange represents the fusion coils of GP₂. The transmembrane domain for each monomer is not seen in the structure, but is shown here as a fine dotted line. The GP_{1,2} structure shown below full-length GP_{1,2} represents a model of GP_{1,2} after cathepsin processing in the disordered loop, which results in removal of the mucin and glycan cap domains.

(64). One additional consequence of shielding is the induction of cell rounding, which is not an indicator of toxicity as originally thought (243, 273). Instead, this phenotype is simply a loss of adherence, likely due to shielding of $\beta 1$ integrins and other surface adhesion proteins (63). Also, although the mechanism is poorly understood, GP_{1,2} has an important function in countering the anti-viral factor Tetherin to allow for release of particles from the cell surface (129).

An additional interesting and underappreciated function of GP_{1,2} is its ability to produce membrane blebs similar in size to VP40 virions, but not in shape (136, 188). Unlike VP40-derived virions, which have a uniform diameter, GP_{1,2} particles are much more pleomorphic (188). The mechanism that GP_{1,2} uses to bud independent of VP40 remains unknown, although, budding may be dependent on the ability of GP₂ to form filaments (90). GP_{1,2} does not have any late domains or direct interactions with members of the ESCRT pathway, in contrast to VP40, which utilizes its late domains to recruit TSG101 and Nedd4 (96, 170, 247).

As mentioned in section 1.4, the full-length GP_{1,2} protein is not the major product of the GP gene. Instead, the majority of the glycoprotein made from the GP gene is the secreted glycoprotein (sGP); full-length GP_{1,2} is only produced as a result of an mRNA editing event (222, 258). The editing event occurs just before the mucin domain, and thus, sGP encodes most features of GP₁, including the glycan cap. However, unlike the full-length version, sGP predominately forms dimers, instead of trimers (223). The apparent function of sGP during EBOV infection is primarily as an immunological decoy to redirect the immune response away from targeting full-length GP_{1,2} (176).

Section 1.8 – Cellular Anti-viral Intrinsic Innate Immune Effectors

Mammalian cells express many cellular anti-viral factors, which can be activated and expressed, even if the host cell does not function primarily as a component of the immune system. While some of these proteins are constitutively active in the absence of virus, many are upregulated in the context of viral infection. Thus, these factors have been termed Intrinsic Innate

Immune Effectors (IIIE). IIIE do not function primarily as signaling molecules that suppress viral replication by upregulating other anti-viral factors. Instead, they act directly on viral components or processes to inhibit virus infection and spread within the host. IIIE can affect many steps of the virus life cycle and often form a critical part of the barrier preventing cross-species transmission of viruses.

There are a number of factors that inhibit the entry process of viruses. One of the first described IIIE is the murine restriction factor Friend virus susceptibility gene (Fv1), which restricts replication of Friend Murine Leukemia Virus (MLV) (156). Functionally similar genes have been identified in humans such as Tripartite Motif 5 α (TRIM5 α), which is active against lentiviruses, including HIV-1 (98, 132, 250). TRIM5 α is able to recognize incoming viral capsid and, via a mechanism not fully understood, inhibit virions by accelerating the uncoating process or initiating proteasomal degradation of the virus (38, 228, 241). TRIM5 α is just one of a large family of TRIM proteins, consisting of more than 70 members. Although mechanistic insight is lacking in most cases, at least 20 other TRIMs, including TRIM11, TRIM19, TRIM26, and TRIM31, also have anti-viral functions targeting *Arenaviridae*, *Herpesviridae*, *Orthomyxoviridae*, and *Rhabdoviridae* families (187, 208, 252). The Interferon-Induced Transmembrane Proteins (IFITM) are another family of proteins that affect the early events in viral infection by inhibiting entry and trafficking of viruses (117). IFITM are also broadly acting and restrict many virus families including *Coronaviridae*, *Filoviridae*, *Flaviviridae*, and *Orthomyxoviridae* (29, 108). Although the exact mechanism is unclear, IFITM may inhibit viruses by interfering with trafficking of early or late endosomal compartments needed by virions to enter the host cell (57, 108).

Two more examples of IIIE that inhibit HIV-1 replication through very distinct mechanisms are APOBEC3G and SAMHD1. APOBEC3G, a member of the Apolipoprotein B mRNA Editing Enzyme, Catalytic Polypeptide-like (APOBEC) protein family, can prevent HIV-1 replication by inducing viral genome hypermutation via cytosine deamination or by directly blocking reverse

transcription of HIV-1 genomic RNA (85, 94, 153, 186, 230, 278). While APOBEC3G was originally shown to target HIV-1, APOBEC3G and other APOBECs can inhibit other *Retroviridae* members and HBV of *Hepadnaviridae* (47, 84, 167, 251). Another protein, SAM domain and HD domain-containing protein 1 (SAMHD1), was also discovered to block HIV-1 replication by limiting the pool of dNTPs needed for HIV-1 to complete reverse transcription of its genome (74, 212). While most studies have focused on the role of SAMHD1 in countering HIV-1, SAMHD1 has also been demonstrated to block infection of HBV and HTLV-1 (39, 242).

Other steps of the virus life cycle can be affected by IIE including transcription and translation. One class of proteins, the Interferon-induced proteins with Tetratricopeptide Repeats (IFIT), inhibit viruses by reducing the efficiency of cap-dependent translation, binding uncapped or incompletely capped viral RNA, and directly binding and sequestering viral proteins (46, 110, 199, 245). Another way cells inhibit RNA translation is through the RNaseL/Oas system (40, 105). RNaseL recognizes and cleaves single stranded RNAs, thus shutting down all protein synthesis, including those producing viral proteins (62, 272). Protein Kinase R (PKR) is another virally induced protein that impairs cellular translation by phosphorylation of EIF2 α (56, 233). This prevents the EIF2 complex from returning to an active state and shuts down global translation of mRNAs. In mice, another interferon-induced protein, Myxovirus Resistance protein, Mx1, inhibits primary transcription of Influenza virus, while the human homologue MxA blocks Influenza at an undefined later step of replication (6, 157, 196). The anti-viral activity of MxA has been extended to many other virus families including *Bunyaviridae*, *Hepadnaviridae*, and *Rhabdoviridae* (65, 77, 197). Recently, another Mx protein, MxB, has been shown to specifically inhibit a late post-entry step of HIV-1 infection (80). MxB prevents HIV-1 integration by blocking HIV-1 import into the nucleus or by destabilizing the HIV-1 DNA (80, 159).

Finally, there are also a limited number of factors that have been implicated in blocking viral assembly and budding processes. There are several TRIM family member proteins that

block the later stages of virus infection (252). Another factor, Interferon-Stimulated Gene 15 (ISG15), blocks EBOV VLP budding by interfering with Nedd4 ligase activity (190). Other viruses including Influenza virus, JEV, and HIV-1 are also affected by ISG15 (106, 107, 200). Viperin (Virus Inhibitory Protein, Endoplasmic Reticulum-associated, Interferon-Inducible) has an unusual anti-viral function in preventing virus assembly by disrupting lipid-raft formation or preventing lipid droplet formation (100, 122, 262). However, the exact mechanism used by Viperin to inhibit viruses remains uncertain. Tetherin also inhibits budding of HIV-1 virions by preventing release of budded virions from the cell surface (184).

Section 1.9 – Antiviral Functions of Tetherin

Tetherin is a type II transmembrane glycoprotein consisting of 180 amino acids with a molecular weight of 29 to 33 kD that was originally described as a marker on B-cells without any associated function and is known by several names: HM1.24, Bone marrow stromal antigen 2 (BST-2), and Cluster of Differentiation 317 (CD317) (78, 113, 279). Tetherin is an unusual type II transmembrane protein in that it contains both an N-terminal cytoplasmic tail and a C-terminal glycosylphosphatidylinositol (GPI) anchor (113, 140). There are two N-linked glycosylation sites in the extracellular domain of Tetherin, which consists primarily of a long coiled-coil domain (113, 152, 184). Both the GPI anchor and the coiled-coil domain participate in localizing Tetherin to lipid rafts, while the N-terminal transmembrane domain is excluded from lipid rafts (24, 92, 140). There are three cysteines within the extracellular domain, which, along with the structural motif of the coiled-coil domain, assist in formation of Tetherin dimers, and potentially higher order tetramer structures (9, 226).

Before being identified as an anti-viral factor, Tetherin had few well-defined functions. Early work suggested that Tetherin, as a marker on B-cells, had a role in B-cell development (113). Initially, Tetherin was of interest to the cancer field because multiple myeloma cells upregulated expression of Tetherin and thus, Tetherin could be used as a marker to locate and

destroy these tumors (191, 192). Tetherin has also been shown to associate with RhoGAP interacting with CIP4 homologs protein 2 (RICH-2), a protein that can provide a physical link between membrane proteins and the actin cytoskeleton (213). Due to the unique topology, interaction with RICH-2 and association with lipid rafts, Tetherin may also have a role in organizing the micro-domains of lipid rafts on the cell surface (25, 213).

In 2008, Tetherin was shown to have anti-viral activity by inhibiting budding of HIV-1 particles (183, 184). Shortly thereafter, our lab demonstrated that EBOV particles are also retained in a Tetherin-dependent manner (129). Unlike other IIIE that inhibit cellular pathways leading to budding of virions, Tetherin acts directly at the step of viral-host membrane scission and does not require other proteins for its anti-viral activity (254). When virions are budding from the cell, as shown in Figure 1-3, the GPI anchor of Tetherin preferentially incorporates into the viral particles, while the Tetherin N-terminal transmembrane domain remains associated with the cell membrane (9, 61, 254). This results in the virion, while having a membrane discontinuous with the cellular membrane, remaining in close proximity to the cell because of the Tetherin proteins (93, 198). Some studies suggest that virions are subsequently endocytosed into the cell and degraded in the lysosome; however this step of Tetherin's anti-viral activity has yet to be demonstrated clearly (67, 184). Thus, Tetherin primarily inhibits cell-free virus spread, while cell-cell spread is generally not affected by Tetherin (112, 125).

The range of viruses that Tetherin can inhibit is very diverse; theoretically, Tetherin could inhibit any enveloped virus that buds from a membrane containing Tetherin. Also, many viruses have ways to counter Tetherin, as will be described in section 1.11. Thus, determining whether or not a virus is affected by Tetherin is not always simple. Enveloped virus restriction by Tetherin has been best studied using HIV-1 (184). Additional viruses from the *Retroviridae* family, such as SIV, RSV, HERV-K, and HTLV are also inhibited by Tetherin (128). Notably, Tetherin blocks release of *Filoviridae* virus particles, including both EBOV and Marburg virus (128, 129). Viruses

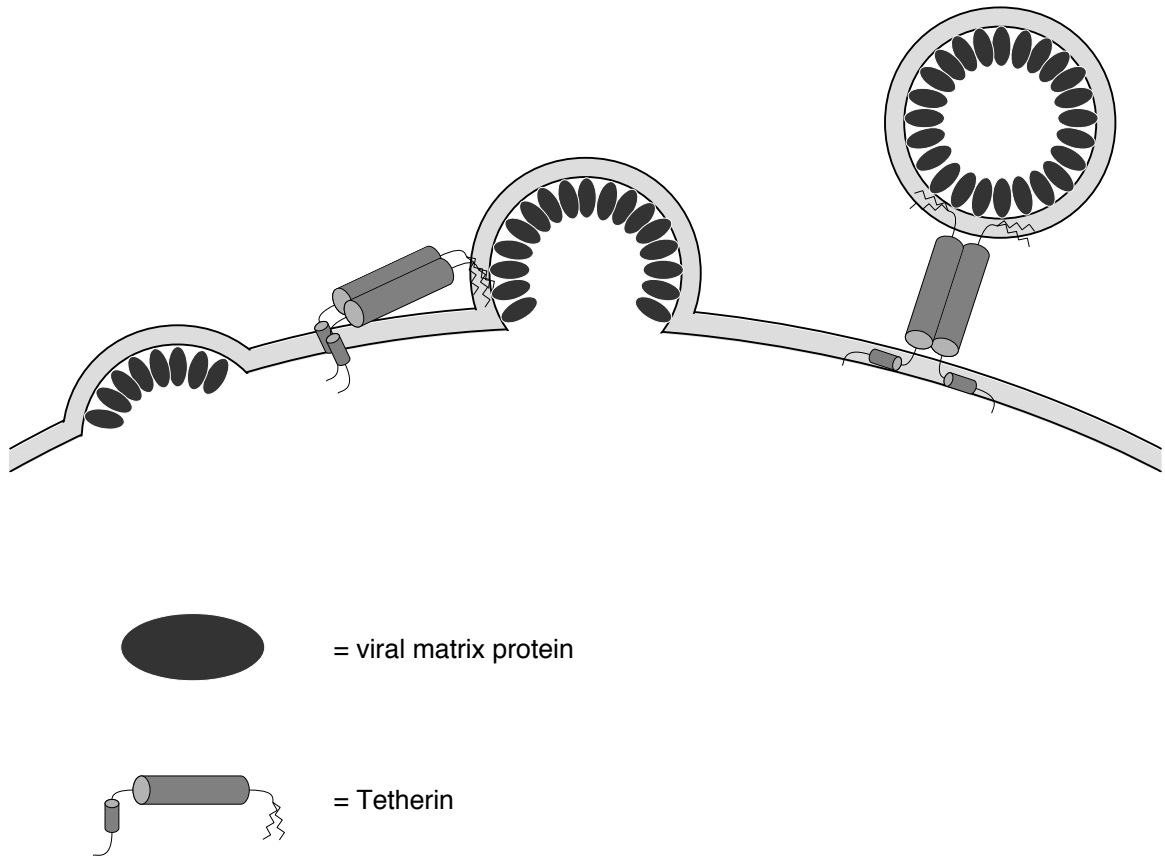


Figure 1-3: Model depicting Tetherin mediated restriction of viral particles. As the virions bud from the cell surface, Tetherin oligomers incorporate into the budding particle, preferentially the end with the C-terminal GPI anchor. The virus completes budding while the transmembrane domain of Tetherin remains associated with the cellular membrane. Thus, the virion, although having a membrane discontinuous with the cell, remains “tethered” to the cell surface.

from other families are also restricted by Tetherin including Lassa from *Arenaviridae*, HCV and Dengue from *Flaviviridae*, HSV-1, HSV-2, and KSHV from *Herpesviridae*, VSV from *Rhabdoviridae*, Nipah virus and Sendai virus from *Paramyxoviridae*, Influenza from *Orthomyxoviridae*, and Chikungunya from *Togaviridae* (27, 45, 126, 137, 158, 193, 205, 217, 263, 265). Interestingly, entry of CMV seems to be enhanced by Tetherin via an undetermined mechanism, while budding remains unaffected (257).

Besides functioning to target viruses directly, Tetherin has also been implicated in regulation of innate immune responses, including type-I interferon (IFN-1) and nuclear factor kappa-light-chain-enhancer of activated B cells (NFκB). Upon activation by TLR 7 or 9, plasmacytoid dendritic cells (pDC) can become stimulated to produce large amounts of IFN-1 in humans (201). When Immunoglobulin-like transcript 7 (ILT7) on pDC interacts with Tetherin, ILT7 can signal to inhibit production of IFN-1 in pDC (33). However, this inhibition may be dependent on how pDC are stimulated, as Tetherin-ILT7 interactions cannot inhibit all IFN-1 produced by pDC (21, 244).

Tetherin also has the ability to regulate production of NFκB. One unique feature of Tetherin is the presence of two methionine residues at position 1 and 13. Interestingly, the first methionine has a weak Kozak translation initiation motif, which allows the translating ribosome to periodically initiate the polypeptide chain at the second methionine instead of the first one. These two isoforms of Tetherin both have the ability to restrict viral budding, however, the product produced from the first methionine, long-Tetherin (l-Tetherin), can initiate signaling via the NFκB pathway, while the other isoform, short-Tetherin (s-Tetherin) cannot (42). Tetherin signaling is TAK1 and TRAF6 dependent indicating that L-Tetherin signals through the canonical NFκB pathway (67, 248).

The mechanism detailing how l-Tetherin can initiate NFκB signaling is still unclear. One possibility is that the cytoplasmic tail of l-Tetherin could function as a hemi-immunoreceptor

tyrosine-based activation motif (hemi-ITAM) (68). ITAMs are a pair of the amino acid sequences YxxL/I spaced six to eight amino acids apart that are important for initiating signaling events by phosphorylation of the tyrosine residues (211, 218). I-Tetherin contains two tyrosines at amino acid residues 6 and 8, and while neither residue fits the YxxL/I motif exactly, mutation of the tyrosine at position 6 completely prevents the ability of I-Tetherin to signal through NFκB, and mutation of the other tyrosine partially inhibits signaling (68, 248). Thus, the ability of Tetherin to form dimers and tetramers could allow several hemi-ITAM motifs on the N-terminal tails to group together and form a functional ITAM (68). Experiments have also shown that Tetherin immunoprecipitates with spleen tyrosine kinase (Syk), which could be phosphorylating the hemi-ITAM motif on I-Tetherin and initiating signaling (68).

The current model provides a good start to understanding how I-Tetherin is able to initiate NFκB signaling. However, the model needs clarification in a few areas. For example, a direct interaction with Syk has not yet been demonstrated; it is possible that I-Tetherin could be recruiting additional factors that Syk acts upon, instead of binding Syk directly. Furthermore, experiments in our lab suggest that additional mutations in the N-terminal tail can allow I-Tetherin, without tyrosine residues at position 6 and 8, to signal better than I-Tetherin containing the tyrosine residues (41). These experiments and others show that I-Tetherin does not act as a hemi-ITAM and suggest that I-Tetherin interacts with another protein to recruit Syk and initiate NFκB signaling.

Section 1.10 – Viral Antagonists of Intrinsic Innate Immune Effectors

While the cellular IIE are able to restrict many viruses, most viruses that establish successful infections have evolved ways to overcome these barriers. These viruses typically express one or more proteins that specifically counteract the various IIE expressed in the host cell. Alternatively, viruses may inhibit the signaling pathways that induce expression of IIE; these

factors will not be discussed here. As there are many pathogenic viruses and many IIIIE, the following section highlights only a few of the viral antagonists that have been identified to date.

HIV-1 encodes several accessory genes that are not necessary for replication in most tissue culture cell lines (54). Two of these accessory genes are Viral Infectivity Factor (Vif) and Viral Protein Unique (Vpu) (43, 207, 240). Vif recognizes and binds the cellular IIIIE APOBEC3G, which prevents APOBEC3G from incorporating into virions, and subsequently recruits a host ubiquitin ligase complex (239, 275). APOBEC3G is ubiquitinated by the complex and degraded efficiently by host proteasomes (169, 231). The other gene, Vpu, has a function in recognizing and degrading Tetherin and will be examined in more detail in section 1.11 (184).

Another virus with well-characterized IIIIE antagonists is Influenza A, from the *Orthomyxoviridae* family. Influenza A expresses Non-structural protein 1 (NS1), which has many anti-viral functions (141). NS1 binds double-stranded RNA (dsRNA) produced during Influenza replication and prevents OAS recognition of dsRNA and thus, blocks subsequent digestion by RNaseL (162, 174). To allow translation, NS1 binds PKR and prevents PKR from phosphorylating EIF2 α (162). Together, these NS1 activities and others allow for Influenza A to replicate in cells that express IIIIE.

Vaccinia, a double-stranded DNA virus of the *Poxviridae* family, has a large genome that encodes many IIIIE antagonists. One such protein, Protein E3 (E3L) has activity against both PKR and ISG15 (37, 73). E3L binds dsRNA and prevents PKR from recognizing and degrading Vaccinia dsRNA (48). E3L also sequesters ISG15 and prevents ISG15 from blocking budding of Vaccinia (82). Another Vaccinia protein, Protein K3 (K3L) mimics the structure of EIF2 α and acts as a decoy for PKR to allow translation to occur in the presence of PKR (48, 49).

Finally, EBOV also encodes proteins that counter IIIIE. As mentioned before, VP35 binds dsRNA and also prevents activation of PKR (34, 60). The EBOV full-length GP_{1,2} also counters Tetherin, which will be discussed in more detail in section 1.12 (129).

Overall, the diversity of proteins and mechanisms used by these viral agents to establish infection in host cells highlights the importance of these IIIE in regulating and controlling viral replication. Understanding viral infections requires an investigation into the functions and interactions between IIIE and their viral antagonists.

Section 1.11 – Viral Antagonists of Tetherin

Similar to the other IIIE, viruses also encode proteins that target Tetherin and allow viral budding in the context of cellular Tetherin expression. To date, several viral antagonists of Tetherin have been discovered, however the underlying mechanisms are only known for a few Tetherin antagonists. Three of these antagonists, Vpu, Nef, and Env, representing the variety of mechanisms used to counter Tetherin, are described below.

HIV-1 Group M Vpu was the first described Tetherin antagonist and is the best characterized. Vpu was known to enhance virus release for both HIV-1 and other retroviral capsids many years before the being discovered as a counter of Tetherin (79, 184). The mechanism describing how Vpu counters Tetherin has been well described. Numerous residues within Vpu are required to recognize three Tetherin transmembrane domain residues, I34, L37, and L41, within a very specific orientation (87, 135, 163, 237, 255). Once bound to Tetherin, Vpu recruits Beta-Transducin repeat Containing E3 Ubiquitin Protein Ligase (β -TrCP, also known as F-box/WD repeat-containing protein 1A) which ubiquitylates amino acids 3-5 (STS) of Tetherin (50, 166, 249). Vpu recruits HRS, a member of the ESCRT-0 complex, and Tetherin is subsequently downregulated from the cell surface, trafficked through the lysosomal pathway and degraded (115, 119, 175). Importantly, since Vpu requires the STS sequence of Tetherin, Vpu can only counter Tetherin multimers containing the l-Tetherin isoform; s-Tetherin is resistant to Vpu mediated degradation (42). While this mechanism shows how Vpu utilizes β -TrCP to degrade Tetherin and release virions, Vpu may also sequester Tetherin in peri-nuclear

compartments, away from sites of viral budding; this pathway is independent of β -TrCP mediated degradation (53, 99).

Not all viruses within *Retroviridae* encode the Vpu gene, yet they bud from cells using mechanisms similar to HIV-1 Group M and thus, utilize other proteins to counter Tetherin (28). Most other SIV and HIV-1 Group O utilize Protein Nef (Nef) to counter Tetherin (134, 277). SIV Nef binds sequences in the Tetherin cytoplasmic tail, DDIWK (224, 229, 276). The sequence DDIWK is not present in human Tetherin, so HIV-1 Group O Nef evolved to recognize sequences adjacent to the missing motif (134). After binding Tetherin, Nef initiates a clathrin-dependent downregulation of Tetherin from the cell surface, resulting in accumulation of Tetherin in lysosomal compartments (121, 229).

Both HIV-2, and *Chlorocebus tantalus* SIV (SIVtan) use their Envelope protein (Env) to antagonize Tetherin through a degradation-independent mechanism (88). Unlike Vpu and Nef, Env does not recognize or require the Tetherin transmembrane domain and cytoplasmic tail; instead Env likely binds and recognizes the Tetherin ectodomain (99). An endocytosis motif in the Env cytoplasmic tail, GYxx θ , subsequently downregulates Tetherin from the cell surface and relocalizes Tetherin to intracellular compartments without causing Tetherin degradation (87, 143). Since Env recognizes the Tetherin ectodomain, Env counteracts both I-Tetherin and s-Tetherin isoforms (267). Also, because Tetherin is only relocalized and not degraded, Tetherin could continue to mediate signaling and activate NF κ B; however, this function in the presence of Env remains to be shown by experimental data.

Other viruses, besides members of *Retroviridae*, also encode Tetherin antagonists including K5 from Kaposi's sarcoma-associated herpesvirus, Glycoprotein M from Herpes simplex virus, HA and NA from Influenza virus, proteins F and HN from Sendai virus, and nsP1 from Chikungunya virus, (15, 27, 72, 126, 168, 274). Some of these antagonists use similar

mechanisms as described for Vpu, Nef, or Env, specifically, degradation of Tetherin or removal of Tetherin from the cell surface, away from sites of viral budding.

Section 1.12 – Interactions between Ebola Virus Glycoprotein and Tetherin

In 2009, our lab published data showing that EBOV GP_{1,2} also functioned as a Tetherin antagonist (129). Since then, research by us and others has focused on understanding the GP_{1,2} Tetherin interaction and asking these questions. What are the domains of Tetherin needed for GP_{1,2} to recognize Tetherin? Conversely, what are the domains of GP_{1,2} needed to counter Tetherin? Finally, what is the mechanism by which GP_{1,2} can allow budding in the presence of Tetherin?

GP_{1,2} does not recognize or require the Tetherin transmembrane domain or cytoplasmic tail to counter Tetherin; instead GP_{1,2} is thought to recognize residues of the ectodomain, which have yet to be determined (161). GP_{1,2} binds and forms complexes with Tetherin as shown by immunoprecipitation assays; however, this interaction is primarily with the immature form of the glycoprotein species (129). Also unlike Vpu, GP_{1,2} can counter human Tetherin, and other Tetherin proteins from divergent species, such as murine, African green monkey, Rhesus macaque, and gorilla Tetherin (129, 138). This ability to counter multiple Tetherin species may contribute to the wide pathogenic range of EBOV.

Mutational analysis of various domains within GP_{1,2} have been used to determine which regions are required for anti-Tetherin activity. Similar to many other glycoproteins, much of GP_{1,2} is folded in a rigid, complex structure and thus, making large deletions within GP_{1,2} remains difficult (145). The mucin domain of GP_{1,2}, which is required for the GP_{1,2} epitope shielding function and is largely unstructured, is not necessary for allowing GP_{1,2} to counter Tetherin (89, 129). The transmembrane domain of GP_{1,2} is required for function; mutants without transmembrane domains, or transmembrane domains from other viral glycoproteins fail to counter Tetherin (71, 129). One study attempted to determine whether or not the transmembrane

domain is sufficient to counter Tetherin. They found that the transmembrane domain was not sufficient by placing the EBOV transmembrane domain onto Lassa virus Glycoprotein (71). Furthermore, one study also found that binding seems to be mediated by the GP₂ rather than the GP₁ subunit (138). However, these chimeras could not produce infectious pseudotypes, so this question remains unanswered. The short cytoplasmic tail of GP_{1,2}, which is only 4 amino acids long, contains two cysteine residues that are acetylated, but to date, no definitive function has been attributed to acetylation (114). These residues, as well as the entire cytoplasmic tail, are dispensable for anti-Tetherin function (71, 160). In summary, the specific domains of GP_{1,2} that are needed to counter Tetherin need to be better understood and this thesis attempts to clarify the role of the GP_{1,2} domains.

The mechanisms used by most anti-Tetherin viral proteins are readily observable and easily understood. However, unlike antagonists such as Vpu or Nef, GP_{1,2} does not degrade Tetherin, as Tetherin protein expression does not decrease in the presence of GP_{1,2} (129, 138). Also, unlike other antagonists, GP_{1,2} does not remove Tetherin from the cell surface or relocalize Tetherin out of lipid rafts (138, 160, 161). GP_{1,2} does not remove Tetherin from budding particles; in fact, levels of Tetherin in VLPs seem to increase in the presence of GP_{1,2} (89). GP_{1,2} does need to localize properly to exert anti-Tetherin activity, as ER-retained GP_{1,2} does not release Tetherin held VLPs (129). Furthermore, immunofluorescence images of Tetherin staining patterns, which normally localize to the cell surface and Golgi network, do not seem to change in the presence of GP_{1,2} (129, 140). Recent data shows that GP_{1,2} can change the localization of Tetherin and VP40 (71). Thus, GP_{1,2} may be able to relocalize Tetherin away from VP40 and allow VP40 to function and produce VLPs. To date many studies have illuminated the things that GP_{1,2} does not do, however, overall, the mechanism used by GP_{1,2} to counter Tetherin remains unclear. The experiments and questions asked in this thesis do not fully explain this mechanism, but do provide a much more detailed understanding of the required domains in EBOV GP_{1,2} and

some insight in the mechanism whereby GP_{1,2} functions to produce VLPs in the presence of Tetherin.

CHAPTER 2 – REQUIREMENTS WITHIN THE EBOLA VIRAL GLYCOPROTEIN FOR TETHERIN ANTAGONISM

Reprinted with minor changes from the manuscript in submission:

Vande Burgt NH, Kaletsky RL, and Bates P., (2015) Requirements within the Ebola viral glycoprotein for Tetherin antagonism. *Virology*.

Section 2.1 – Abstract

Tetherin is an interferon-induced, intrinsic cellular response factor that blocks release of numerous viruses, including Ebola virus, from infected cells. As with many viruses targeted by host factors, Ebola virus employs a tetherin antagonist, the viral glycoprotein (EboGP), to counteract restriction and promote virus release. Unlike other tetherin antagonists such as HIV-1 Vpu or KSHV K5, the features within EboGP needed to overcome tetherin are not well characterized. Here we describe sequences within the EboGP ectodomain and membrane spanning domain (msd) as necessary to relieve tetherin restriction of viral particle budding. Fusing the EboGP msd to a normally secreted form of the glycoprotein effectively promotes Ebola virus particle release. Cellular protein or lipid anchors could not substitute for the EboGP msd. The requirement for the EboGP msd was not specific for filovirus budding, as similar results were seen with HIV particles. Furthermore trafficking of chimeric proteins to budding sites did not correlate with an ability to counter tetherin. Additionally, we find that a glycoprotein construct, which mimics the cathepsin-activated species by proteolytic removal of the EboGP glycan cap and mucin domains, is unable to counteract tetherin. Combining these results suggests an important role for the EboGP glycan cap and msd in tetherin antagonism.

Section 2.2 – Introduction

The innate immune system is the first line of defense against viral pathogens. Consequently, mammalian cells employ numerous innate cellular mechanisms to inhibit viral

replication and spread. Intrinsic antiviral factors comprise a form of innate immunity that directly limit viral entry, replication or assembly. These factors are often ubiquitously expressed, but can be further induced during viral infection, generally by interferon. Tetherin (also referred to as BST-2, CD317, or HM1.24) is an interferon-inducible host intrinsic antiviral protein that acts at least in part by retaining budded enveloped virions on the cell surface and preventing virion release into the extracellular media (184).

Although discovered as an intrinsic immune factor because of its effect upon HIV-1 replication, the ability of tetherin to disrupt virion budding is not specific for HIV-1. Ebola virus viral particle release is effectively blocked by tetherin (129, 184). Indeed egress of a range of enveloped viruses including simian lentiviruses, Lassa virus, Kaposi sarcoma-associated herpesvirus, influenza A virus, vesicular stomatitis Indiana virus, Chikungunya virus, and hepatitis C virus are impacted by tetherin expression (126, 184, 195, 217, 274). Tetherin's ability to inhibit viral particle release from infected cells is dependent upon the protein's unusual cellular topology which consists of an extracellular coiled coil domain anchored on both ends by a N-terminal transmembrane domain and a C-terminal GPI anchor (140). During HIV assembly, tetherin is seen to localize to sites of viral budding (93) and block viral egress by forming a physical linkage between the virion and the host cell (254).

For many of the viruses affected by tetherin, antagonists have been identified that impede the anti-viral activity of tetherin. Some of these antagonists, such as HIV-1 Vpu, recognize the transmembrane region of tetherin and modify residues in the cytoplasmic tail of tetherin, resulting in the down-regulation and degradation of tetherin (253). K5 from KSHV targets residues in the cytoplasmic tail of tetherin for ubiquitination and subsequent proteasomal degradation (168), whereas the envelope proteins of HIV-2 and a subset of SIVs require sequences in the tetherin ectodomain for recognition and surface downregulation (88, 99).

Ebola virus is a member of the species *Zaire ebolavirus* within the *Filoviridae* family and a causative agent of outbreaks of hemorrhagic fever in sub-Saharan Africa primarily due to zoonotic transmission of virus from a presumptive natural reservoir in fruit bats (149, 202). Prior to the 2014 epidemic in Western Africa, these outbreaks were infrequent and of limited scope (146). Ebola virus infection fatality rates are unusually high, ranging from 59-88%, while disease progression occurs rapidly; on average, patients succumb to infection 10 days after showing symptoms (32, 70, 123).

Ebola virus infection produces several proteins from the viral glycoprotein (GP) gene. The primary product from the viral GP gene is a 323 residue nonstructural, soluble glycoprotein (sGP) that exists as a homodimer. Polymerase stuttering incorporates an additional nucleotide in a small percentage of the GP transcripts causing a frameshift and production of the full-length, virion associated glycoprotein (EboGP) (223, 259). Due to this method of production, sGP and EboGP share 295 N-terminal residues, including regions within EboGP needed for receptor recognition and cell binding as well as a domain called the glycan cap. EboGP forms trimers and is cleaved into two subunits, GP₁ and GP₂, such that GP₂ is membrane anchored by a hydrophobic membrane spanning domain (msd) (259).

Structural analysis of EboGP shows that the GP₂ subunit contains the fusion machinery and forms a stalk that holds GP₁, the globular receptor-binding region (145). Within GP₁ is the glycan cap, a moderately glycosylated region that, together with a heavily glycosylated mucin domain, sits atop the trimeric glycoprotein spike and covers the receptor binding domain of EboGP (52, 145). While EboGP shares the N-terminal 295 residues with sGP, the proteins are markedly different in their structure; EboGP forms trimers, while sGP exists as homodimers (16, 55, 259).

EboGP has been identified as an inhibitor of intrinsic immunity based upon its ability to act as an antagonist of tetherin (129). While the mechanism of action for tetherin antagonism by

EboGP is poorly understood, tetherin degradation or relocalization from the cell surface is likely not involved (160, 161). Recent reports suggest that EboGP may prevent tetherin from localizing with VP40 (89). Specific EboGP domains have been implicated in interacting with or counteracting tetherin. Within GP₁, the mucin domain can be removed without affecting EboGP anti-tetherin activity (129). Furthermore, FRET analysis of the interaction between EboGP and tetherin has suggested that the GP₂ subunit appears to interact with tetherin (138). Similarly recent chimeric protein analysis demonstrated a role for the EboGP msd within GP₂ in tetherin antagonism (71). sGP is unable to affect tetherin antiviral function (129).

Here the domains within the Ebolaviral glycoproteins required to antagonize tetherin antiviral activity are further characterized. We define a minimal 320 residue portion of the Ebola glycoprotein ectodomain, containing the receptor binding domain and glycan cap regions of EboGP, that when anchored to the cell surface is sufficient to antagonize tetherin activity. Moreover, there is a specific requirement for the EboGP msd, as anchoring sGP by other cellular msd sequences or by a GPI anchor does not antagonize tetherin activity. Finally, deletion of the glycan cap region by proteolytic processing renders EboGP unable to promote viral budding suggesting that the glycan cap is important for tetherin antagonism.

Section 2.3 – Materials and Methods

Cell Lines, Plasmid Vectors, and Antibodies

293T cells were grown in DMEM (Invitrogen) supplemented with 5% fetal bovine serum (Invitrogen) and 2 mM L-Glutamine (Invitrogen). Vectors used to transfect cells were constructed as described below. The vector pcDNA3.1 furin expressing human furin was previously described (26). To express HIV Gag, psPAX2 was obtained from Addgene. Human tetherin, in the vector pCMV Sport6 Tetherin was obtained from Open Biosystems. An AU1 tagged cytoplasmic tail and transmembrane domain of mouse transferrin receptor one (mtfr1) and the human tetherin ectodomain were combined to generate mtfr1-tetherin in a pCB6 backbone

(Figure 2-7B). To express and detect viral protein products, we cloned sequences into the pCAGGS vector and, where specified, appended a C-terminal FLAG, V5, or polyhistidine tag to generate these constructs: pCAGGS VP40 (FLAG tagged), pCAGGS EboGP (V5-His tagged), pCAGGS GP-primed (V5-His tagged), and pCAGGS sGP. EboGP lacking a glycan cap (GP-primed) was generated by replacing EboGP residues 203-206 (VNAT) with a consensus furin cleavage site (RRKR) as previously described (91). EboGP constructs with amino acid point mutations C670A and C672A were generated both individually and in combination. To generate sGP chimeras, an XbaI restriction site (or XhoI for sGP-TM_(TVA)) was introduced at the C-terminus of sGP after residue 320, immediately before the furin RVRK cleavage site. Sequences encoding the transmembrane domain from EboGP, human ACE2, the chicken TVA receptor, or a GPI anchored form of the TVA receptor were appended to sGP after the XbaI site. Sequence details of all constructs produced are shown in Figure 2-1. Antibodies used include the mouse IgG2a anti-V5 antibody (Invitrogen 46-0705), rabbit anti-FLAG antibody (Sigma F7425), rabbit polyclonal sera (R12) produced against EboGP, and mouse anti-tetherin antibody (Biolegend RS38E). HRP-conjugated, Alexa Fluor 488, or Alexa Fluor 647 secondary antibodies against mouse or rabbit Fc were used where indicated.

Virus-like Particle (VLP) Budding Assay

293T cells were seeded in a 24-well plate at a density of 1.0×10^5 cells per well. Using Lipofectamine 2000 (Invitrogen) or polyethylenimine (PEI) (PolySciences Inc.), 293T cells were transfected with plasmids encoding VP40 or psPAX2, tetherin, and filovirus GP or an empty vector. When GP-primed was used, pcDNA3.1 furin was added to all transfected wells. VLPs in the supernatants were harvested at 48 hours post-transfection and, after a clarifying spin at 1700 rcf, were purified through a 20% sucrose cushion by centrifugation in a TLA120.1 rotor at 40,000 rpm for 30 minutes. Concurrently, the cells were lysed in 1% Triton lysis buffer and cleared by

MSD and N-terminal Sequences

EboGP	1912	O G D N D N W W T G W R Q W I P A G I G V T G V V I A V I A L F C I C K F V F P CAGGGGACAATGACAATTG GTGGACAGGATGGAGACAAT <u>GGATACCGGCAGGTATTGSA GTTACAGCGCTTCTAATTGC AGTTATCGCTTTATCTGTA TATGCAAAATTGCTTTCCG</u> Ectodomain EboGP Transmembrane Domain Cytoplasmic Tail
	2032	R F E G K P I P N P L L G L D S T R T G H H H H H * <u>CGSTTCGAGGTTAGCCTAT CCCTAACCTCTCCTCGETC TCGATTCTACGCTACCGGT CATCATCACCARCACCATG A</u> V5-His tag
sGP	946	K T S V V R V R R E L L P T Q O G P T Q Q L K T T K S W L O K I P L Q W F K C T V <u>AAAACATCAGTGGTCTCTAG ACAGGGGACAATGACAATT GGTGGACAGGATGGAGACAA TGGATACCGGCAGGTATTGG AGTTACAGCGCTTCTAATTGC CAGTTATCGCTTTATCTGTA</u> sGP Furin Cut Site Delta Peptide EboGP Transmembrane Domain
	1066	K E G K L Q C R I * AAGGAAGGAAGCTGCAGTG TCGCATCTAA
sGP-TM (GP)	946	K T S V V S R O G D N D N W W T G W R Q W I P A G I G V T G V V I A V I A L F C <u>AAAACATCAGTGGTCTCTAG ACAGGGGACAATGACAATT GGTGGACAGGATGGAGACAA TGGATACCGGCAGGTATTGG AGTTACAGCGCTTCTAATTGC CAGTTATCGCTTTATCTGTA</u> sGP XbaI EboGP Ectodomain EboGP Transmembrane Domain
	1066	I C K F V F * <u>ATAATGCAAAATTTGCTTTTA G</u> EboGP Cytoplasmic Tail
sGP-TM (ACE2)	946	K T S V V S R Q P T L G P P N O P P V S I W L I V F G V V M G V I V V G I V I L <u>AAAACATCAGTGGTCTCTAG ACAGGCAACACTTGGACCTC CTAACACGCCCCCTGTTTC ATATGGCTGATGTTTTGG AGTTGTGATGGGATGATAG TGGTGGCATTTGCATCTCG</u> sGP XbaI ACE2 Ectodomain ACE2 Transmembrane Domain
	1066	I F T G I R D R K K K N K A R S G E N P Y A S I D I S K G E N N P G F Q N T D D <u>ATCTTCACTGGGATCAGAGA TCGGAAGAAGAAAAATAAG CAAGAAGTGGAGAAATCCT TATGCTCCATCGATATTAG CAAAGGAGAAAAATAATCCAG GATTCCAAAACACTGATGAT</u> ACE2 Cytoplasmic Tail
	1186	V Q T S F * GTTTCAGACCTCTCTTTAG
sGP-TM (TVA)	946	K T S V V L E P T D N G T E A P T V P A P G R A L P A R N H G R M W M L I T A V <u>AAAACATCAGTGGTCTCTAG GCCCAGGACAACGGCAGC AGGCTCCCACTGTCCCTGG TCCTGGACCTGCTCTGCCAGC CAGGAATCAGGCCCGCATGT GGATGCTGATCACTGCAGTG</u> sGP XhoI TVA Ectodomain
	1066	L L C C L V A V G G I A A W G K S K A K S R S D I F S L E S A S K E L L V P D K <u>CTCTGGCTCTCTGCTGATG TGGGGTGGTATCGCTGCAT GGGGGAATCCAAAGCAA AAGCAGCTGACATCTTCAG TCTTGAAGCGCATCCAGG AGCTGCTGGTCCGTGACAAG</u> TVA Transmembrane Domain TVA Cytoplasmic Tail
	1186	S O A D L F S * AGCCAGGAGACTTGTCTCT CTGA
sGP-GPI (TVA)	946	K T S V V S R P T D N G T E A P T V P A P G R A L P A R N H G R M W M L I T A G <u>AAAACATCAGTGGTCTCTAG ACCCAGGACAACGGCAGC AGGCTCCCACTGTCCCTGG TCCTGGACCTGCTCTGCCAGC CAGGAATCAGGCCCGCATGT GGATGCTGATCACTGCAGTG</u> sGP XbaI TVA Ectodomain and GPI anchor signal sequence
	1186	I F C C E L V R W D * ATCTTTTGTGTGAGCTGGT GAGATGGGACTGA
Tetherin	1	M A S T S Y D Y C R V P M E D G D K R C K L L L L G I G I L V L L I I V I L G V P ATGGCATCTACTTCTGATGA CTATTGCAGAGTCCCCATGG AAGACGGGATAAGCGCTGT <u>AAGTCTCTGTGGGATAGG AATTCTGGTCTCTGATCA TCGTGATTTGGGGTGGCC</u> Tetherin Cytoplasmic Tail Tetherin Transmembrane Domain
	121	L I I F T I K A N S <u>TTGATTAATCTTACCATCAA GGCCAACAGC</u>
mtfr1-Tetherin	1	M D T Y R Y I M D Q A R S A F S N L F G G E P L S Y T R F S L A R Q V D G D N S <u>ATGATACATATCGATACAT TATGGATCAAGCCAGATCAG CATTCTTAACCTGTTTGGT GGGGAACCATGTCATACAC CCGTTTAGCCTTGCTCGGC AAGTAGATGGAGATAACAGT</u> AUL tag mtfr1 Cytoplasmic Tail
	121	H V E M K L A A D E E E N A D N N M K A S V R K P K R F N G R L C F A A I A L V CATGTGGAGATGAACCTGGC TGCAGATGAAGAAGAAATG CCGACATAACATGAAGCT AGTGTCCGAAAACCAAGAG GTTTAATGGAAGACTCTGCT <u>TTCCAGCTATTGCATGACTG</u>
	241	I F F L I G F M S G Y L G T I K A N S <u>ATTTTCTTCTGATTTGATT CATGATGGCTACTGGSCA CCATCAAGGCCAACAGC</u> mtfr1 Transmembrane Domain

Figure 2-1: C-terminal and N-terminal nucleotide sequence list. A nucleotide sequence list comparing the unique C-terminal or N-terminal domains for each construct used in this study. The amino acid translation is given above each sequence and annotations are indicated below each sequence.

centrifugation at 18,000 rcf for 3 minutes. Cell lysates and purified VLPs were then analyzed by immunoblot.

Immunoprecipitation Assay

293T cells were seeded in a 6-well plate at a density of 2.2×10^5 cells per well. Using Lipofectamine 2000, 293T cells were transfected with plasmids encoding tetherin, GP, or empty vector. 48 hours post-transfection, cells were lysed in a 1% Triton buffer and, after clearing the lysate at 18,000 rcf for 3 minutes, rocked with Protein A conjugated agarose beads overnight at 4°C. Concurrently, Protein A conjugated agarose beads were also rocked overnight at 4°C with antibodies to tetherin (RS38E) or GP (R12). After incubation, the antibody bound agarose beads were washed twice in 1% Triton buffer. The naked agarose beads were cleared from the rocking cell lysates, replaced with antibody bound agarose beads, and rocked overnight at 4°C. Protein adhering to the antibody bound agarose beads were washed four times in 0.1% Triton buffer and subsequently analyzed by immunoblot.

Immunoblot Analysis

Samples were loaded and run on a 4-15% Tris-HCl polyacrylamide gel (Bio-Rad) and subsequently transferred to a PVDF membrane by electroblotting. Membranes were blocked in 5% non-fat dry milk with Tris-buffered saline (Blotto) and then rocked overnight at 4°C with a 1:10,000 dilution of antibody. After washing with Blotto, appropriate HRP conjugated secondary antibodies were added to the membranes and rocked for one hour. Membranes were washed in Blotto and Tris-buffered saline with 0.1% Tween-20 and subsequently imaged on a chemiluminescent imager (Fujifilm LAS-1000). Where indicated in experiments, membranes were stripped with Restore Western blot stripping buffer (Thermo Scientific) and re-probed with antibodies. All experiments shown are representative of immunoblots repeated at least three times.

Flow Cytometry Analysis

293T cells were seeded at a density of 1.05×10^5 cells per well into a 24-well plate. Cells were transfected using Lipfectamine 2000 with 600ng of plasmids encoding GP, a chimeric GP or pCAGGS empty vector. 48 hours post-transfection, cells were lifted off the plate with 5 mM EDTA in PBS-/- and kept at 4°C throughout the analysis. Cells were spun at 150xg for 5 min and resuspended in Flow Wash (PBS-/- with 1% FBS and 0.05% NaAz) and probed with an appropriate primary and secondary antibody for 1 hour. Cells were washed 2X with Flow Wash, fixed and permeabilized with BD Fix/Perm (BD Biosciences) for 20 minutes, washed 2X with BD Perm/Wash (BD Biosciences), and probed again with appropriate primary and secondary antibody for 1 hour. Cells were washed 2X with BD Perm/Wash, resuspended in PBS-/- and analyzed by on a FACS Calibur (BD Biosciences). Post acquisition analysis was performed on FlowJo software (FlowJo LLC).

Section 2.4 – Results

Requirements within EboGP for Tetherin Antagonism

To define the minimal requirements within the Ebola virus glycoprotein needed to antagonize tetherin function, we employed an Ebola virus-like particle (VLP) budding assay, with a panel of plasmids including full-length EboGP, sGP, an sGP chimera (Figure 2-2A and 2-2B). Previously we found that neither sGP nor secGP, a soluble version of EboGP cleaved at the extracellular base by tumor necrosis factor-converting enzyme (TACE) protease [31], could effectively counteract tetherin (129). The membrane spanning domain (msd) represents a significant difference between full-length EboGP and secGP; we therefore sought to determine whether the msd was a determinant of anti-tetherin activity. A chimeric glycoprotein was produced by appending the msd from EboGP onto the C-terminus of sGP creating sGP-TM_(GP) (Figure 2-2A and 2-2B). Flow cytometry and immunoblot analysis confirmed the expression of the chimeric protein (Figures 2-2E and 2-3). Analysis of budded Ebola VP40 particles demonstrated that sGP-TM_(GP) was able to effectively antagonize tetherin activity by promoting

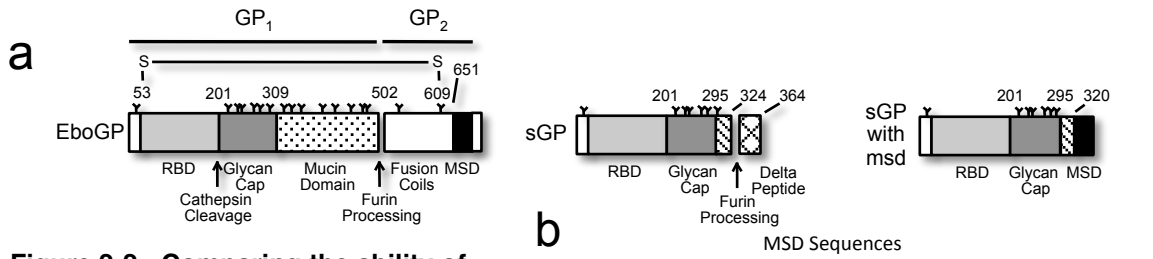
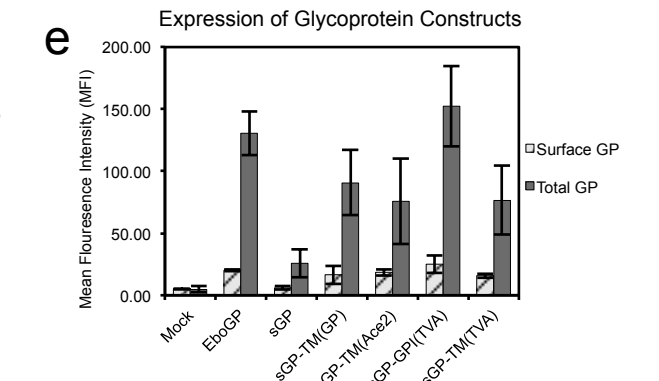
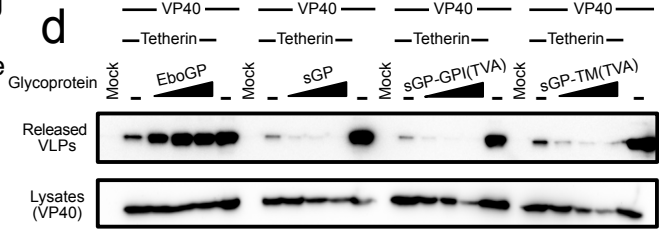


Figure 2-2: Comparing the ability of alternative msd to release VLP from Tetherin. (a) A schematic diagram of the constructs used in this study showing the domains of EboGP, sGP, and a chimeric sGP with an appended membrane spanning domain (msd), either a protein transmembrane (TM) domain or a GPI anchor, to the C-terminus. (b) Amino acid sequences of the constructs employed, highlighting the C-terminal regions appended to the chimeric sGPs. Where known, the msd sequence is annotated. (c) An Ebolavirus-like particle (VLP) budding assay comparing the anti-Tetherin activity of EboGP, sGP and chimeric sGPs. 293T cells were transfected with plasmids encoding VP40-FLAG, human Tetherin and varying amounts of the GP constructs as indicated. *Top Panel:* Purified VLPs were analyzed by SDS-PAGE and immunoblot using a FLAG-tag antibody to detect VLPs released into the media. *Bottom Panel:* Cell lysates were analyzed by SDS-PAGE and immunoblot probed with an antibody to FLAG to evaluate VP40 expression in the transfected cells. (d) A VLP budding assay comparing the anti-Tetherin activity of EboGP, sGP, and sGP with either a GPI anchor or a proteinaceous msd from TVA. *Top Panel:* Purified VLPs were detected by immunoblot and probed with an antibody to the FLAG tag of VP40. *Bottom Panel:* VP40 expression in the 293T cell lysates was confirmed by using an antibody to FLAG in the immunoblot. Results are representative of at least 3 independent experiments. (e) A bar chart depicting the relative expression of the GP constructs in 293T cells, as measured by flow cytometry, after staining with polyclonal antibody (R12) to GP. Surface GP was detected on fixed cells without permeabilizator while for total GP, staining was performed after permeabilization.

b

MSD Sequences

EboGP	638	QGDNDNWWTG	WRQWIPAGIG	VTGVVIVAVIA	LFCICKFVFP	RFEFGKPIPNP
			EboGP TM Domain			
	688	LIIGLDSTRTC	HHHHHH*			
			V5-His Tag			
sGP	316	KTSVVRVRE	LLPTQGPTQQ	LKTTKSWLQK	IPLQWFKCTV	KEGKLQCRI*
		sGP Furin Site		Delta Peptide		
sGP-TM (GP)	316	KTSVVSRRQGD	NDNWWTGWRQ	WIPAGIGVTC	VVIIVAVIALEFC	ICKFVF*
		sGP		EboGP TM Domain		
sGP-TM (ACE2)	316	KTSVVSRRQPT	LGPPNQPPVS	TWLVYRGVVM	GVIVYVGIIVL	IFTGIRDRC
		sGP		ACE2 TM Domain		
	366	KKNKARSGEN	PYASIDISKG	ENNPGFQNTD	DVQTSF*	
sGP-TM (TVA)	316	KTSVIVLEPTD	NGTEAPTTPA	PGRALPARNH	GRMWMLITAV	LLCCLVAVG
		sGP		TVA TM Domain		
	366	GIAAWGKSKA	KSRSDIFSLE	SASKELLVPD	KSQADLFS*	
sGP-GPI (TVA)	316	KTSVVSRRPTD	NGTEAPTTPA	PGRALPARNH	GRMWMLITAG	IFCCELVRW
		sGP				
	366	D*				



(e) A bar chart depicting the relative expression of the GP constructs in 293T cells, as measured by flow cytometry, after staining with polyclonal antibody (R12) to GP. Surface GP was detected on fixed cells without permeabilizator while for total GP, staining was performed after permeabilization.

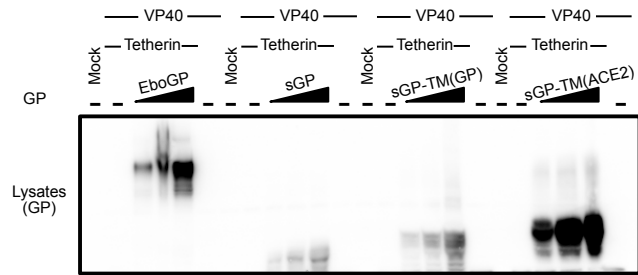


Figure 2-3: Expression of glycoprotein in the cell lysates of Figure 2-2C. Immunoblot of 293T cell lysates depicting the expression of the glycoproteins used in the budding assay from Figure 2-2C. The immunoblot of the cell lysates from Figure 2-2C was stripped and reprobed with the R12 antibody to detect verify expression of the constructs in the budding assay.

VLP release across a range of sGP-TM_(GP) expression levels (Figure 2-2C). As controls, we confirmed that sGP could not promote virion release, even at the highest levels of sGP expression utilized, while EboGP effectively antagonized tetherin and prompted virion release (Figure 2-2C). sGP and EboGP expression in transfected 293T cells were verified by flow cytometry (Figure 2-2E) and by immunoblot of cell lysates and supernatants (Figure 2-3). Cellular lysate expression of sGP appears lower than EboGP because sGP does not contain an msd and thus, is secreted from cells and not retained on the cell surface (Figure 2-2E). Overall these experiments define a minimal 320 residue portion of the Ebola glycoprotein ectodomain, containing the receptor binding domain and glycan cap regions of EboGP, that when anchored to the cell surface is sufficient to antagonize tetherin activity. Conversely, these data indicate that the mucin domain and the extracellular region of the GP₂ subunit of EboGP are dispensable for anti-tetherin activity.

Chimeras Reveal a Specific Requirement for the EboGP Membrane Spanning Domain (msd)

To differentiate whether the activity of sGP-TM_(GP) was due to the physical anchoring of EboGP N-terminal region to the membrane or if there was a specific requirement for the Ebola virus msd, chimeras were constructed with heterologous membrane anchoring domains from other type I membrane proteins appended to the C-terminus of sGP (Figure 2-2A and 2-2B). The msd from the avian glycoprotein TVA and from human ACE2 were appended to sGP creating sGP-TM_(TVA) and sGP-TM_(ACE2) respectively. The expression of these chimeras was analyzed by flow cytometry (Figure 2-2E) and immunoblot analysis (Figures 2-3 and 2-4) and all of the chimeras were expressed, albeit at varying levels. One construct, sGP-TM_(TVA), seemed to express poorly in the cell lysates when assessed by immunoblot (Figure 2-4). However, flow cytometry analysis shows that sGP-TM_(TVA) is well expressed on the cell surface (Figure 2-2E). The ability of the chimeras to promote virion release was assessed using an Ebola VLP budding assay as described above. In contrast to the results with the Ebola msd, sGP-TM_(ACE2) and sGP-

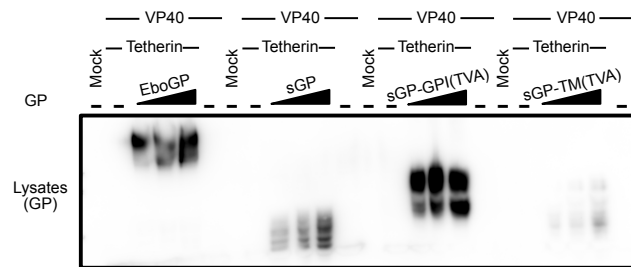


Figure 2-4: Expression of glycoprotein in the cell lysates of Figure 2-2D. Immunoblot showing glycoprotein expression in the 293T cell lysates from the budding assay in Figure 2-2D. Immunoblot from the budding assay in Figure 2-2D was stripped and re-probed with the R12 antibody to confirm expression of the new constructs.

TM_(TVA) were unable to antagonize tetherin activity as judged by their inability to significantly promote particle release even at the highest level of expression (Figures 2-2C and 2-2D).

Both full-length Ebola glycoprotein and tetherin have been reported to localize to glycolipid-enriched or lipid raft regions of the membrane (20, 140, 172). We hypothesized that the msd and short cytosolic domain of EboGP might provide lipid raft localization to the sGP–TM_(GP) chimera thus facilitating tetherin antagonism. To address this theory, sequences for an alternatively spliced form of avian TVA that encodes a glycosylphosphatidylinositol (GPI)-linked anchor (19, 180) were appended onto sGP to produce sGP–GPI_(TVA) (Figure 2-2A and 2-2B). Western blot and flow cytometry analysis demonstrated that this chimera was expressed and routed to the cell surface (Figure 2-2E and 2-4). Expression of this chimera with Ebola VP40 and tetherin demonstrated that it is unable to promote virion release in the presence of tetherin (Figure 2-2D). In sum, these results demonstrate that fusion of 39 residues containing the msd from the GP₂ subunit of EboGP onto 320 residues of the ectodomain is sufficient to effectively antagonize human tetherin. Moreover, they reveal a specific requirement for the 39 residues of the EboGP msd.

A notable feature of the Ebola msd is the presence of cysteine residues near the inner membrane surface. In EboGP these two cysteine residues are reported to be acylated, however the functional consequences of acylation remain unknown (114). To determine if these residues contributed to the observed anti-tetherin function of GP, we replaced amino acids C670 and C672 with alanine residues both individually and in tandem. Similar to other reports, we found that replacing either or both cysteines with alanine residues did not alter the ability of EboGP to release tethered VLPs in a budding assay (Figure 2-5) (71, 160).

The Ebola msd Requirement is not Specific for Filoviral Budding

To address whether the requirement for the EboGP msd is specific for budding of Ebola VP40 or if the EboGP msd is able to promote release of other viral particles that are restricted by

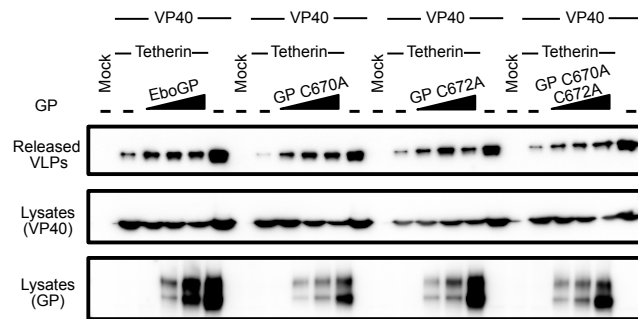


Figure 2-5: Testing the role of GP_{1,2} cytoplasmic cysteine residues in antagonizing Tetherin. A VP40 VLP budding assay assessing the ability of EboGP to antagonize tetherin with either one or both membrane proximal cysteines modified to an alanine. *Top Panel:* An immunoblot depicting purified VLPs released by each of the glycoproteins, suggesting that modification of the cysteine residues at 670 and 672 do not affect VLP release. *Middle Panel:* Cellular lysates were also analyzed by immunoblot to verify the expression of VP40. *Bottom Panel:* The middle panel immunoblot was stripped and reprobed with the R12 antibody to detect glycoprotein expression in the cellular lysates.

Tetherin, we tested several of the EboGP chimeras for their effect upon HIV-1 VLP budding in the presence of human tetherin. Similar to the results with VP40, the sGP-TM_(GP) chimera allowed budding of HIV particles from tetherin expressing cells (Figure 2-6, top panel). As was the case for filamentous Ebola VP40 particles, neither the ACE2 or TVA heterologous membrane spanning regions, nor the TVA GPI anchor could substitute for the msd of EboGP to promote efficient HIV-1 budding (Figure 2-6, top panel). Although the sGP-TM_(TVA) chimera was poorly expressed in these experiments, which might account for its inability to counteract tetherin, both sGP-TM_(ACE2) and sGP-GPI_(TVA) were well expressed (Figure 2-6 fourth panel) yet unable to promote HIV-1 particle budding.

One possible reason for the failure of these chimeras to relieve tetherin restriction could be that they are unable to localize to the particle budding sites. To address this hypothesis the incorporation of EboGP msd chimeras into HIV-1 particles in the absence of tetherin was analyzed. As can be seen in Figure 2-6 (third panel, left hand lanes), sGP-TM_(GP), sGP-TM_(ACE2) and sGP-GPI_(TVA) were effectively incorporated into HIV-1 particles while sGP-TM_(TVA) was poorly expressed and incorporated. This finding demonstrates that these chimeric glycoproteins, which are unable to relieve tetherin restriction, are not excluded from sites where HIV-1 viral particles bud and suggests that an ability to move the EboGP ectodomain into the site of budding is not sufficient to relieve tetherin restriction. While the exact nature of the features critical for release of tetherin restricted virions within the Ebola virus msd remain to be elucidated, overall, these chimera studies point to a critical role of the EboGP msd for function as a tetherin antagonist. Moreover, they identify the amino terminal 295 residues of sGP, when appended to the EboGP msd, as sufficient for tetherin antagonism.

The Tetherin Amino-terminal Region is not Required for EboGP Recognition

A specific requirement for the EboGP msd might suggest direct recognition of the tetherin msd by EboGP. To test this hypothesis, the tetherin msd and N-terminal cytoplasmic domains

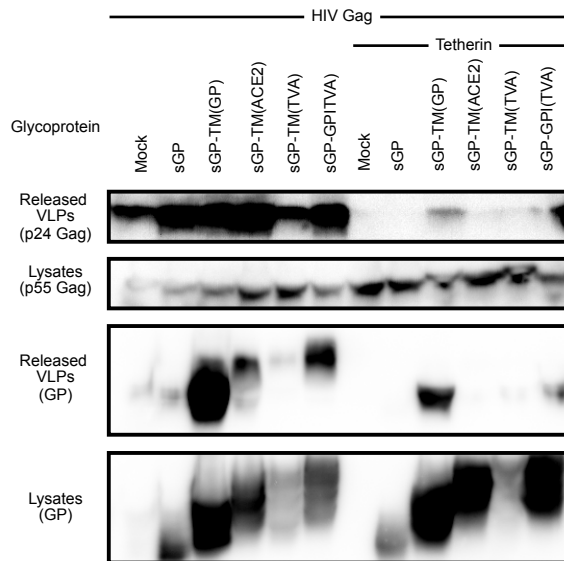


Figure 2-6: Comparison of chimeric sGP glycoproteins in an HIV-1 Gag budding assay. *Top Panel:* Released HIV-1 VLPs were analyzed by SDS-PAGE and detected by immunoblot for HIV-1 Gag (p24) in supernatant of 293T cells transfected with an HIV-1 Gag encoding vector plus chimeric sGPs with or without Tetherin. *Second Panel:* Expression of HIV Gag. Cell lysates of the transfected cells were analyzed by immunoblot for expression of HIV Gag (p55). *Third Panel:* Incorporation of GPs into VLPs. The immunoblot in the top panel was stripped and probed with a polyclonal antibody against EboGP. *Fourth Panel:* Expression of sGP and chimeric sGPs. The immunoblot from the second panel was stripped and expression of GP was analyzed in the cell lysates. These results are representative of two independent experiments.

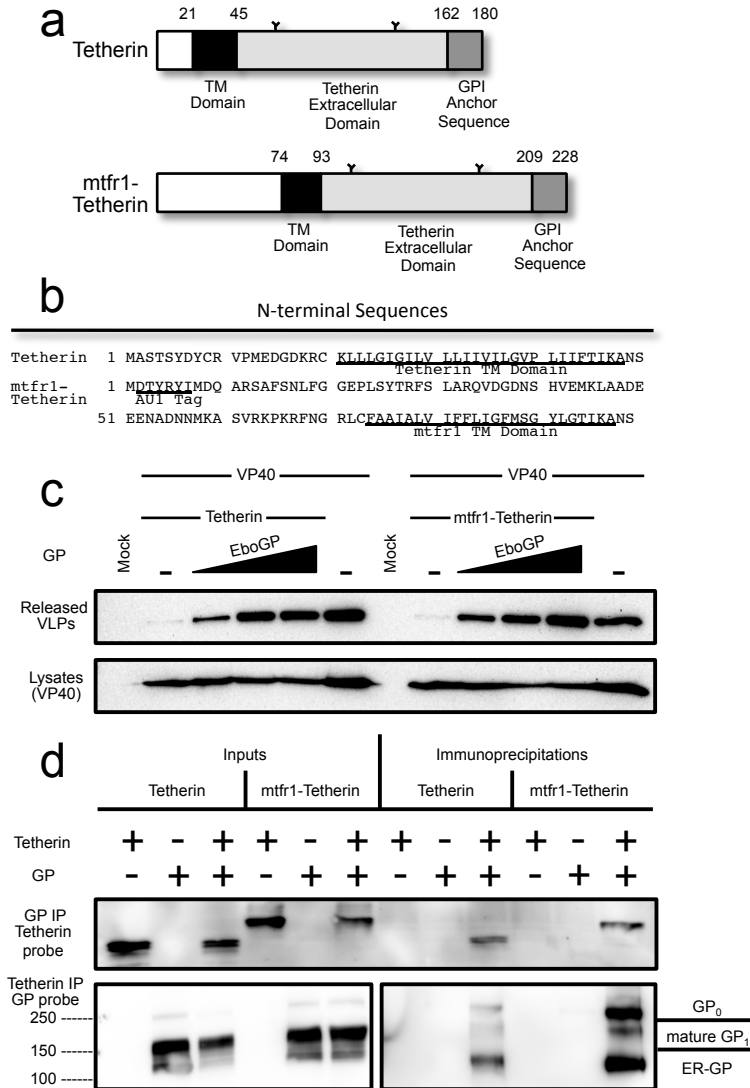


Figure 2-7: Testing the ability of GP_{1,2} to counter Tetherin containing an alternative transmembrane domain. (a) Schematic diagram of human tetherin and the chimeric mtfr1-tetherin containing a cytoplasmic tail and transmembrane domain from mouse transferrin receptor 1 (mtfr1). (b) A comparison of the N-terminal amino acid sequence of tetherin and mtfr1-tetherin. (c) A budding assay comparing the ability of the Ebolavirus glycoprotein to release VLPs retained by tetherin or mtfr1-tetherin. 293T cells were transfected with VP40-FLAG and increasing amounts of EboGP with either human tetherin or chimeric mtfr-tetherin as indicated. *Top Panel:* Purified VLPs were analyzed by SDS-PAGE/immunoblot using an anti-FLAG antibody for detection. *Bottom Panel:* 293T cell lysates were analyzed by SDS-PAGE/immunoblot, and probed with the anti-FLAG antibody to confirm VP40 expression. (d) Co-immunoprecipitation analysis comparing the ability of tetherin and mtfr1-tetherin to interact with EboGP. Lysates from 293T cells expressing tetherin and/or EboGP were analyzed by SDS-PAGE/immunoblot either directly (Inputs) or after immunoprecipitation with antibody specific for GP (top panel) or tetherin (bottom panel). Molecular mass is shown to the left in kD. The left middle panel is a lower exposure of the right middle panel to visualize the overexposed lanes.

were replaced with the domains from mouse transferrin receptor protein 1 to generate a chimeric protein, mtf1-tetherin (Figure 2-7A and 2-7B). Previous studies with similar chimeras have shown that the specific msd of tetherin is dispensable for tetherin function (161, 198). To confirm that mtf1-tetherin retained the ability to restrict virion release, a VLP budding assay was employed (Figure 2-8). The chimera was able to block VLP release, although the activity was slightly reduced based on expression level compared to wild-type (wt) tetherin. Having demonstrated that this chimeric tetherin is active, the ability of EboGP to counteract the activity of mtf1-tetherin was assessed using a VLP budding assay. As seen in Figure 2-7C, EboGP was able to promote VLP release similarly from cells expressing wt tetherin or mtf1-tetherin. This result suggests that EboGP does not require the tetherin msd in order to recognize tetherin and impair its activity.

Previously, EboGP and tetherin have been shown to interact by co-immunoprecipitation (IP) (129). To determine whether EboGP physically interacts with the chimeric mtf1-tetherin, wt tetherin or the mtf1-chimera were co-expressed with EboGP in 293T cells. Cell lysates were immunoprecipitated with a polyclonal anti-EboGP antibody followed by western blot analysis for tetherin. As seen in Figure 2-7D, EboGP effectively immunoprecipitates both wt and the chimeric tetherin proteins. To verify the interaction, the reciprocal IP was performed using an antibody that reacts with the ectodomain of tetherin to precipitate, followed by western analysis for EboGP (Figure 2-7D). As was previously noted (129), it appears that the immature forms of EboGP preferentially interact with tetherin – and here this finding is seen for both wild type and the chimeric mtf1-tetherin. These experiments demonstrate that while the msd domain of EboGP is required for tetherin antagonism, recognition does not require specific intra-membrane sequences in tetherin.

The Glycan Cap of EboGP is Required to Antagonize Tetherin

Among filoviruses, the glycan cap is a moderately conserved (~55% identity) glycosylated domain within the viral glycoprotein GP₁ subunit. This region is proteolytically cleaved by cellular

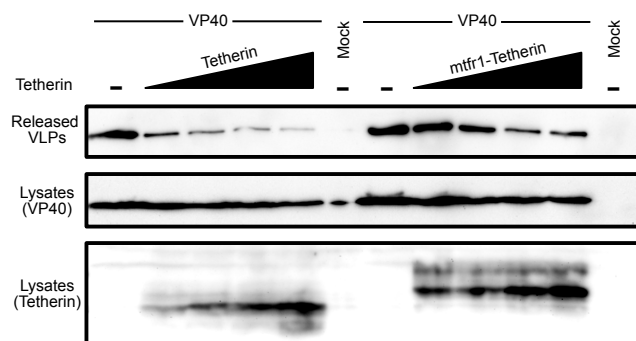


Figure 2-8: Testing the ability of Tetherin containing an alternative transmembrane in restricting VLP release. A VP40 VLP budding assay comparing the ability of tetherin and mtrf1-tetherin to prevent release of VLPs into the supernatant. *Top Panel:* VLPs analyzed by immunoblot showing the effectiveness of both tetherin and mtrf1-tetherin in retaining budded particles. *Middle Panel:* An immunoblot showing the expression of VP40 in the corresponding cellular lysates. *Bottom Panel:* The immunoblot from the middle panel was reprobbed for glycoprotein expression using the R12 antibody.

cathepsins during filoviral entry to reveal a binding site for NPC1, the conserved receptor (35, 44, 145). Aside from occluding the receptor-binding site, no other function has been ascribed to the glycan cap. Indeed, virus produced in which the cap domain is removed by *in vitro* proteolysis is more infectious than wt virions, demonstrating that this domain is dispensable for the cell entry function of EboGP (36, 130, 225). To examine the role of this domain in antagonizing tetherin, an EboGP mutant was constructed such that sequences encoding the glycan cap could be readily removed (130). This was accomplished by inserting a consensus furin cleavage site at the point in a disordered loop where cathepsin cleavage usually occurs generating GP-primed (Figure 2-9A). The added furin site allows GP-primed to be cleaved by host proteases during production of the glycoprotein, thus mimicking the cleavage produced by cathepsins during entry (130). To determine the role of the glycan cap in promoting virion release, a VLP budding assay was used to compare EboGP and GP-primed. As seen in Figure 2-9B, GP-primed did not promote release VLPs even at the highest levels of expression tested.

To ascertain whether the glycan cap domain participates in the EboGP–tetherin interaction, we compared the ability of EboGP and GP-primed to immunoprecipitate tetherin. EboGP and tetherin were co-expressed in 293T cells and the interaction was assessed by co-IP with antibodies to EboGP. The interaction was also verified by performing the reciprocal IP. Both the inputs and immunoprecipitated protein were analyzed by Western blot (Figure 2-9C). We were able to confirm the EboGP–tetherin interaction, as shown in previous work (129). Surprisingly, in contrast to the VLP release data, IP of cells expressing GP-primed effectively co-precipitated tetherin. However, an IP with a tetherin antibody precipitated only pre-processed immature GP and not the cleaved form lacking the glycan cap or the mature full-length glycoprotein. Thus, while the glycan cap seems to be important for the anti-tetherin activity of EboGP, it remains unclear whether or not the glycan cap has a role in mediating the tetherin interaction.

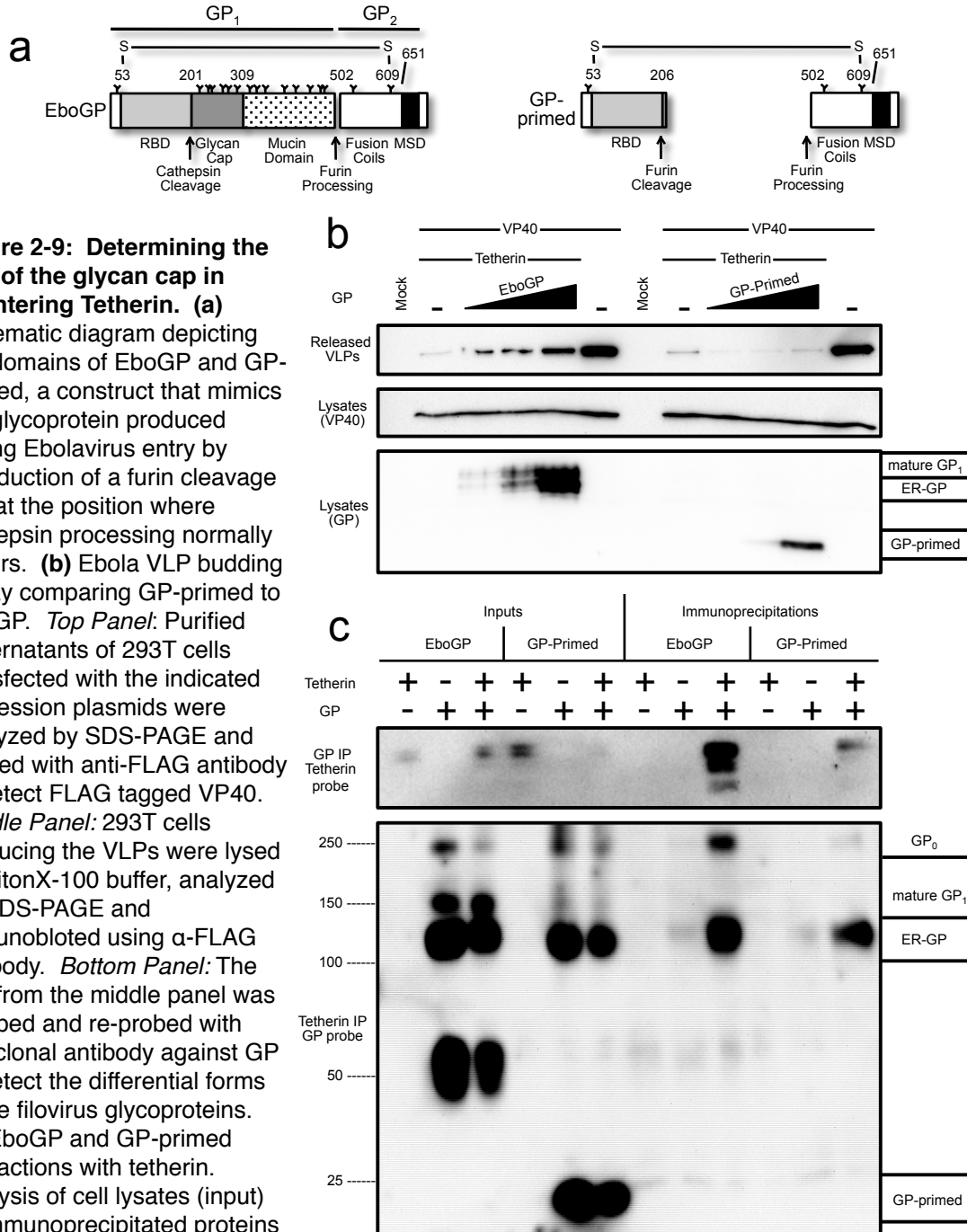


Figure 2-9: Determining the role of the glycan cap in countering Tetherin. (a)

Schematic diagram depicting the domains of EboGP and GP-primed, a construct that mimics the glycoprotein produced during Ebolavirus entry by introduction of a furin cleavage site at the position where cathepsin processing normally occurs. **(b)** Ebola VLP budding assay comparing GP-primed to EboGP. *Top Panel:* Purified supernatants of 293T cells transfected with the indicated expression plasmids were analyzed by SDS-PAGE and probed with anti-FLAG antibody to detect FLAG tagged VP40. *Middle Panel:* 293T cells producing the VLPs were lysed in TritonX-100 buffer, analyzed by SDS-PAGE and immunoblotted using α -FLAG antibody. *Bottom Panel:* The blot from the middle panel was stripped and re-probed with polyclonal antibody against GP to detect the differential forms of the filovirus glycoproteins. **(c)** EboGP and GP-primed interactions with tetherin.

Analysis of cell lysates (input) or immunoprecipitated proteins from 293T cells transfected with tetherin and EboGP or GP-primed as indicated. *Top Panel:* Precipitation using polyclonal α -EboGP sera flowed by SDS-PAGE and detection with an α -tetherin monoclonal antibody. *Bottom Panel:* A reciprocal analysis, using an α -tetherin antibody for immunoprecipitation and detection with α -EboGP sera. Molecular mass is shown in kD. Indicated on the right are the immature form of the Ebolavirus glycoprotein, GP₀ and the mature forms of GP-primed and EboGP.

Section 2.5 – Discussion

Tetherin represents an important barrier to replication of a number of enveloped viruses; consequently viruses have evolved a variety of specific tetherin antagonists. The Ebola virus envelope glycoproteins are effective tetherin antagonists (99, 129, 184) and have been shown to promote viral spread in tetherin expressing cells (138). Here we dissect the requirements within the Ebola glycoproteins that are important to counteract tetherin activity. Overall, we find that regions in both the ectodomain and membrane spanning domain of the Ebola virus glycoprotein are necessary and, when expressed as a chimeric protein, sufficient to antagonize tetherin activity.

Analysis of chimeric GP envelope proteins in which the membrane-spanning region of EboGP is replaced by heterologous sequences indicates that this region of the GP₂ subunit is required for tetherin antagonism. Our findings are similar to recent studies (71) where it was found that the membrane-spanning domain from an arenavirus glycoprotein was unable to replace the EboGP msd. In other studies, it was suggested from co-IP analysis that the GP₂ subunit is sufficient for an interaction with tetherin (138). In contrast, our analysis demonstrates that the ability of EboGP to counteract tetherin also requires sequences from the GP₁ subunit. This discrepancy likely reflects the different assays used in the analysis or may suggest that the interaction measured by IP is not a surrogate for anti-tetherin activity.

HIV-1 Vpu utilizes sequences within the membrane spanning domain to directly interact with human tetherin (87, 135, 214). Indeed this sequence specificity determines the restricted host range of Vpu (173, 224). Given that EboGP also requires the membrane-spanning region of GP₂ it is tempting to speculate that the Ebola virus glycoprotein also directly recognizes tetherin via the membrane spanning sequences. However, data presented here and elsewhere argue against this hypothesis. First, EboGP recognizes divergent tetherin species where there is low conservation of the tetherin membrane spanning sequence. For example, mouse tetherin has

only 38% identity with human, yet it is still effectively antagonized by EboGP (129). Similarly, data presented here shows that replacing the tetherin membrane spanning region and cytoplasmic tail with mouse transferrin receptor sequences still allows tetherin antagonism. These results are similar to data from Lopez et al. analyzing chimeric tetherin proteins (161). Overall these data suggest that if the EboGP membrane-spanning region recognizes tetherin, it likely does so in a sequence independent manner.

The ability of sGP-TM_(GP) to promote virus release suggests that recognition of tetherin requires the amino terminal 320 residues of the Ebola envelope surface glycoprotein but not the extracellular sequences from the GP₂ subunit. Although the structure of sGP is not determined, by comparison with the crystal structure of full length Ebola GP, sGP-TM_(GP) includes the receptor binding and glycan cap domains of GP₁ (145). Removal of the glycan cap region of EboGP in the GP-primed mutant by incorporation of a furin protease cleavage site at position 206, abrogates EboGP tetherin antagonist activity. This mutant glycoprotein is analogous to the cathepsin-processed form of EboGP that is fully functional for entry into host cells (52, 130). The inability of GP-primed to affect tetherin activity might suggest that the glycan cap region may have another role in addition to occluding the receptor binding domain – namely tetherin antagonism. Exactly how this region recognizes tetherin, or if it can directly promote Ebola GP interaction with tetherin, remains to be determined. Finally, the differential anti-tetherin activities of the sGP-TM_(GP) chimera and GP-primed mutant demonstrate that the tetherin antagonist function can be separated from a role in viral entry.

Ebola viral particles are believed to bud from cholesterol-rich lipid rafts where both the viral matrix and glycoproteins localize (194). The GPI anchor of tetherin is required for antiviral function (184) and likely acts at least in part by directing the protein to sites of budding (140). However, anchoring sGP via a GPI tail did not confer anti-tetherin function. Thus localizing sGP at the site of viral budding and tetherin activity does not appear to be sufficient to antagonize

tetherin reinforcing our finding that the membrane spanning region of EboGP plays a critical role. Interestingly, although HIV-1 Vpu also localizes to lipid rafts, raft-association is not required to antagonize tetherin activity and promote HIV-1 release (66, 160). This supports the notion that features within the EboGP msd other than lipid raft association are important for antagonism; however the nature of these features or the mechanism by which they act remain obscure. For the HIV-2 and SIV envelope proteins, extracellular determinants have also been shown to govern tetherin specificity, however with EboGP, the exact nature of the extracellular region needed remains unclear. Additionally, for SIV and HIV-2 envelope proteins, antagonism requires recognition of tetherin through the ectodomain and a highly conserved endocytosis motif in the cytoplasmic tail (143). In contrast, the short four residue cytoplasmic tail of EboGP has no similar motif, thus GP directed endocytosis is not a likely role for the Ebola msd in the sGP-TM_(GP) chimera. Moreover, SIV and HIV-2 envelope proteins appear to restrict tetherin to the trans Golgi network (99, 143) whereas no such relocalization has been seen for EboGP (138, 161). Overall the precise mechanism by which these various viral glycoproteins act upon tetherin is obscure. However our studies localize anti-tetherin activity to 320 ectodomain residues plus 39 amino acids of the EboGP msd. The Ebola viral glycoprotein and the chimeras and mutants we describe provide a platform for addressing these mechanistic questions.

CHAPTER 3 –EBOLA VIRUS GLYCOPROTEIN CONSTRUCTS AND TETHERIN LOCALIZE INDEPENDENTLY AT THE CELL SURFACE

Section 3.1 – Abstract

The *Zaire ebolavirus* (EBOV) glycoprotein (GP_{1,2}) counters the anti-viral factor Tetherin by an obscure mechanism. Since EBOV buds from the cell surface, how GP_{1,2} and Tetherin localize on the cell surface may be important. However, the mucin domain of GP_{1,2} can mask epitopes and impede microscopy analysis. The EBOV secreted glycoprotein (sGP), which lacks a mucin domain, can gain anti-Tetherin activity when given a transmembrane domain from GP_{1,2}, sGP-TM(GP), but not ACE2, sGP-TM(ACE2). Here we analyze transient expression of these proteins in HT1080 cells using widefield fluorescence microscopy with fluorophore-conjugated antibodies to determine how Tetherin localization is affected by these proteins. As expected based on prior analysis, we found that both Tetherin and the sGP chimeric proteins express on the cell surface. However, Tetherin and sGP-TM(GP) staining did not co-localize; instead correlation analysis suggests that they localize to the surface independent of each other. When we expressed Tetherin with sGP-TM(ACE2), which lacks anti-Tetherin activity, both proteins continued to localize independently. Furthermore, expression of sGP-TM(ACE2) reduced glycoprotein-mediated filamentous particle production. Overall, our findings suggest that the EBOV glycoprotein counters Tetherin without localizing with Tetherin at the cell surface and that the transmembrane domain of GP_{1,2} may function to promote production of filamentous particles.

Section 3.2 – Introduction and Background

The *Zaire ebolavirus* (EBOV) full-length glycoprotein (GP_{1,2}) is the only viral protein on the surface of EBOV virions and has many important roles in viral infections (220, 258). GP_{1,2} functions as a receptor-binding protein by interacting with the cellular receptor NPC-1 and triggering fusion of the viral and cellular membranes (35, 44). When GP_{1,2} is expressed on the cell surface, the large disordered region within GP_{1,2}, the mucin domain, shields GP_{1,2}, MHC, and

other epitopes from recognition by the immune system (64, 145). During virus assembly, GP_{1,2} counters the anti-viral factor, Tetherin, and allows for release of virions from cells expressing Tetherin (129).

Tetherin is an interferon-induced intrinsic innate immune effector that prevents budded virions from leaving the cell surface (184). In addition to GP_{1,2}, a number of other viral proteins have been identified that also counteract Tetherin. For some of these antagonists, a mechanism has been described detailing how Tetherin is countered. For example, HIV-1 Vpu antagonizes Tetherin by recognizing the transmembrane domain of Tetherin and recruiting an E3 ligase, β -TrCP to ubiquitinylate Tetherin (135, 175, 184). This results in removal of Tetherin from the cell surface, sequestration into an intracellular compartment, and proteosomal degradation (50, 99).

However, for EBOV GP_{1,2}, a detailed mechanism has not been described. GP_{1,2} does not change levels of Tetherin within the cell, nor does GP_{1,2} downregulate Tetherin from the cell surface (129, 138, 161). Tetherin and GP_{1,2} co-immunoprecipitate with each other, however, Tetherin interacts predominately with an immature ER form of GP_{1,2} (129). Both GP_{1,2} and Tetherin have been shown to localize to the surface, and tagged GP_{1,2} seems to co-localize with Tetherin (138, 140, 160, 161). However, recent microscopy data describes GP_{1,2} as not co-localizing with Tetherin, but preventing Tetherin from localizing with VP40, the matrix protein of EBOV (89). Two significant difficulties in using microscopy to assess GP_{1,2} localization with other proteins on the cell surface are the ability of the GP_{1,2} mucin domain to shield epitopes from antibody recognition and to cause cell rounding by high level GP_{1,2} expression (64, 243).

Here, we utilized two unique constructs derived from the EBOV secreted glycoprotein (sGP) to assess localization of Tetherin and the EBOV glycoprotein. The sGP protein is the primary product of the EBOLV glycoprotein gene, which produces full-length GP_{1,2} after an mRNA transcriptional editing event that occurs for ~20% of transcripts (223). Unlike GP_{1,2}, sGP cannot counteract Tetherin (129). However, these sGP constructs have an appended C-terminal

transmembrane domain from either GP_{1,2}, sGP-TM(GP), or Angiotensin-Converting Enzyme 2, sGP-TM(ACE2). sGP lacks a mucin domain; likewise, these sGP constructs do not cause rounding of cells and cannot shield epitopes from antibody recognition (243). Previous experiments in section 2.4 (Figure 2-2 C) showed that sGP-TM(GP) acquired the ability to antagonize Tetherin, while sGP-TM(ACE2) does not affect Tetherin activity. Thus, we were able to assess Tetherin and GP localization in the presence of a functional and non-functional EBOV glycoprotein.

Using widefield fluorescence microscopy in the context of VP40 and Tetherin expression, we found that both sGP-TM(GP) and sGP-TM(ACE2) could localize to the surface of HT1080 cells. HT1080 cells are an adherant human epithelial cell line that remain relatively flat on glass surfaces and do not endogenously express Tetherin. Interestingly, however, neither glycoprotein seemed to co-localize with Tetherin. Instead, both of the sGP constructs and Tetherin localized randomly and independent of each other, suggesting that the mechanism used by the EBOV glycoprotein to counter Tetherin does not involve direct interactions with Tetherin on the cell surface.

Section 3.3 – Methods

Cells Lines, Plasmids, and Antibodies

HT1080 cells were maintained at 37°C in 5% CO₂ in DMEM with 10% FBS and 2 mM L-glutamine. The plasmids pCAGGS, pCAGGS VP40-GFP, pCMV-Sport6 Bst2, pCAGGS sGP-TM(GP), and pCAGGS sGP-TM(ACE2) were described in section 2.3 and previous work (42, 96). Primary antibodies used include mouse monoclonal anti-Tetherin (Biolegend RS38E) and rabbit polyclonal anti-GP (R12 rabbit sera). Secondary antibodies used include goat anti-mouse-PE (Invitrogen) and goat anti-rabbit-Alexa 647 (Invitrogen).

Transfection and Preparation of Cells for Microscopy

Glass coverslips were incubated for one hour with 100 µg/mL poly-D-lysine (Sigma P6407), washed 5 times with dH₂O, dried, and stored at 4°C. 24 hours before transfection, 7.5x10⁴ HT1080 cells were plated in a 24-well plate containing poly-D-lysine coated coverslips and then transfected with 750 ng of total plasmid DNA and 1.875 µL of Lipofectamine 2000 (Invitrogen) per well. No more than 100 ng of pCAGGS VP40-GFP, 50 ng of pCMV Sport6 Bst2, or 300 ng of vectors containing a glycoprotein were used. Empty vector pCAGGS was used where needed. 36 hours post-transfection, cells were fixed in 4% PFA at 37°C for 10 minutes. Post-fixation, cells were kept at 4°C and washed 3-5X with PBS^{+/+} between all subsequent steps. Coverslips were blocked in PBS^{+/+} with 5% goat serum (Sigma G9023) and 2% BSA (EquiTech-Bio Inc). Cells were stained with primary antibody in blocking solution overnight and stained with secondary antibody in blocking solution for 2 hours. The coverslips were mounted on glass slides with Vectashield Mounting Media with DAPI (Vector Laboratories).

Microscopy and Software Analysis

Within 24-48 hours after the slides were prepared, images were collected on a Leica DM6000 upright widefield microscope (Leica Microsystems) with the following filter sets installed: Chroma 49000 for DAPI (Chroma Technology Corp), L5 for Alexa 488 (Leica Microsystems), Chroma 49008 for Alexa 594 (Chroma Technology Corp), and Y5 for Alexa 647 (Leica Microsystems). Post-acquisition image stacks were analyzed using FIJI (Fiji Is Just ImageJ) software. All stacks were bleach corrected using a simple ratio. Next, using a theoretical PSF (Point Spread Function) generated from the Diffraction PSF 3D plugin, stacks were deconvolved with the Iterative Deconvolve 3D plugin. Compensation for detection of sGP in the Tetherin channel was also performed. Representative slices from each deconvolved stack were chosen, and within each slice, regions of biological interest were selected for further analysis. Slices were log (base10) transformed and the mean intensity compared to background was calculated. C-

localization analysis, plot generation, and calculation of Pearson's Correlation Coefficient (PCC) and Li's Intensity Correlation Quotient (ICQ) were done using the Coloc2 plugin (151).

Section 3.4 – Results

Addition of a Transmembrane Domain causes sGP and Tetherin to Express on the Cell Surface

Immunofluorescence microscopy was used to determine the surface localization of sGP-TM(GP) and sGP-TM(ACE2) in the context of a virus-like particle budding system using VP40 and Tetherin. As shown in the representative histograms in Figure 3-1, VP40, Tetherin, and each of the sGP constructs were detected in transfected non-permeabilized HT1080 cells. Expression of VP40 (row 1 column 2 of Figure 3-1) resulted in formation of filamentous structures, as expected. However, co-expression with sGP-TM(ACE2) (row 6 column 2 of Figure 3-1) generally reduced the number of cell-free filaments, while co-expression with sGP-TM(GP) (row 5 column 2 of Figure 3-1) resulted in filaments produced with VP40, sGP-TM(GP), or both proteins. Both sGP constructs and Tetherin were detected on the cell surface (column 3 and 4 Figure 3-1).

Identification of Tetherin positive cells co-expressed with the sGP constructs was difficult, not only because Tetherin expression was lower, but because the fluorophore-conjugated (Alexa 647) secondary antibodies for sGP were also detected with the filter set used to detect Tetherin. Therefore, after deconvolution and other post-acquisition corrections, compensation was performed on all of the Tetherin images to minimize cross-channel bleedthrough and a subset of the resulting images are displayed in Figure 3-1.

To compare the level of expression between the different proteins, which utilize different fluorophores, the ratio of the fluorescence positive signal was compared to the background signal for each image stack. The resulting ratios were plotted and averaged across all images in a histogram as shown in Figure 3-2, confirming the results seen visually with the subset of images shown in Figure 3-1. VP40 levels were consistent across all samples, while Tetherin and the sGP constructs were generally expressed well, when included in the transfection, although

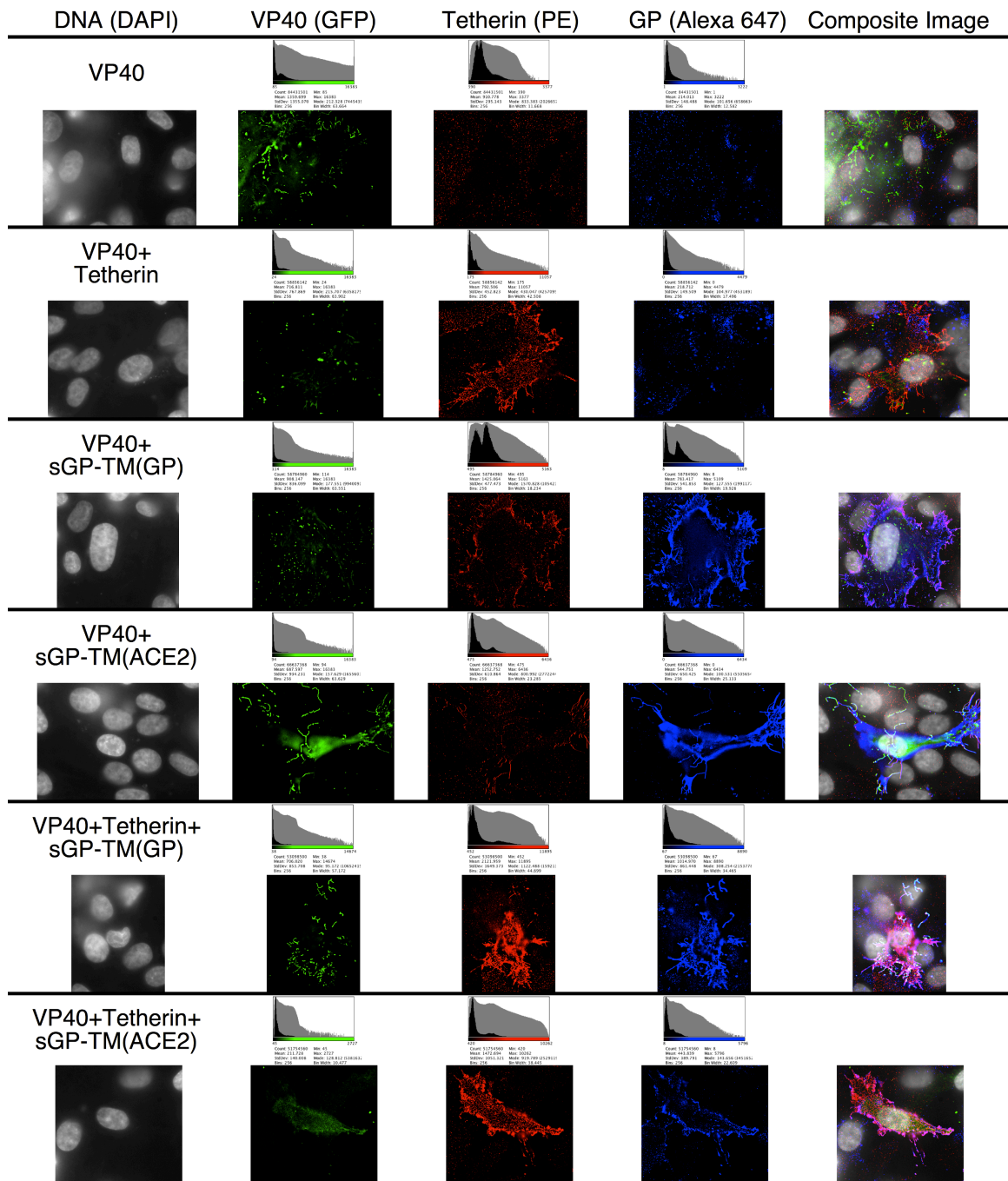


Figure 3-1: Representative immunofluorescence image slices of HT1080 cells. The left-most column indicates the plasmid combination that the cells received. All cells were stained with antibodies to Tetherin and GP, and then with secondary antibodies conjugated to PE and Alexa 647 respectively. DAPI was included in the mounting media and GFP indicates the VP40-GFP fusion protein. The top row indicates which fluorophore or dye is shown in the images. The histograms above the images depict original image intensities before processing of the image stacks. The plots show pixel count on the y-axis and pixel intensities on the x-axis, with black values plotted on a normal scale and gray values on a log scale.

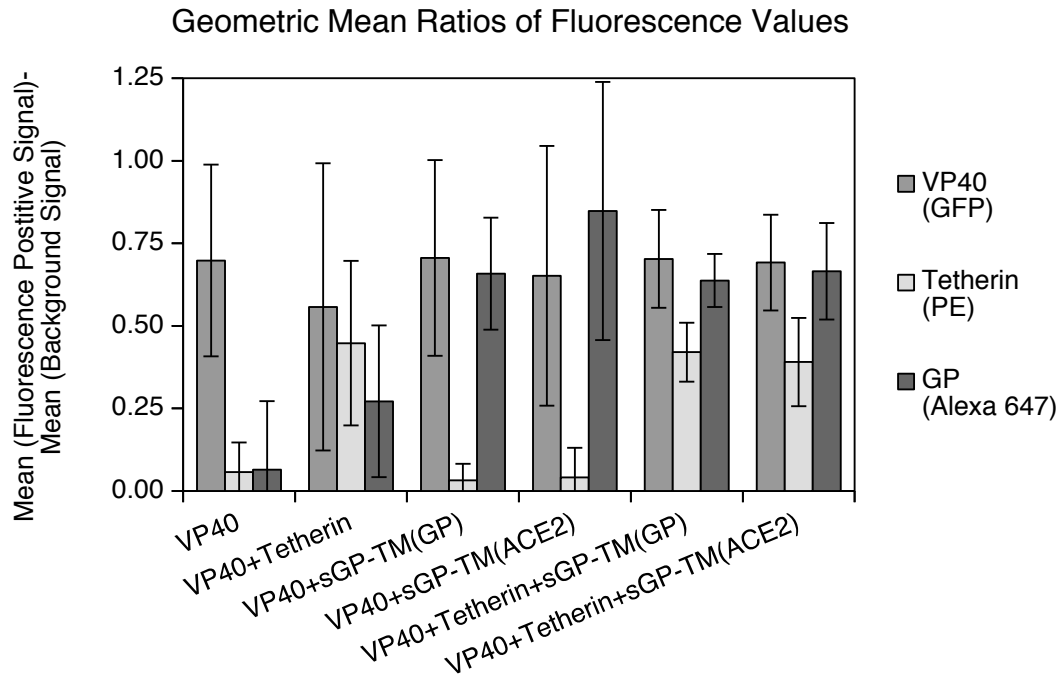


Figure 3-2: Geometric means of the fluorescence signal within image slices chosen for analysis. A histogram depicting the average ratios of the geometric mean (log transformed) fluorescence signal over background. HT1080 cells transfected with plasmids encoding the proteins are indicated on the x-axis. After image processing, areas of positive fluorescence signal in each image were manually selected and compared to the unselected areas within each image. This ratio is displayed in the y-axis as a general comparison of fluorescence intensity across all images. The error bars represent 2 S.E. (~95% confidence interval) and n=3, except for VP40+Tetherin+sGP-TM(GP) n=6, and VP40+Tetherin+sGP-TM(ACE2) n=5.

Tetherin levels were lower than either VP40 or the sGP constructs. A few of the images transfected with VP40+Tetherin had non-specific background staining in the GP channel that did not overlap with Tetherin staining. For the VP40+Tetherin images, this non-specific staining causes the mean fluorescence in the GP channel to be higher, but is not an indication of channel bleed-over from the Tetherin channel. This staining does not appear in the other images and does not impact downstream analysis.

Transmembrane Domain Containing sGP Constructs Localize Randomly with Tetherin

Two methods were used to measure the level of correlation between Tetherin and the two GP constructs. First, the pixel intensities of the two channels were compared directly. The intensity of pixels from the Tetherin and GP channels at each location were plotted against each other to generate the 2D intensity histograms as shown in Figure 3-3A. Then, using the formula shown in Figure 3-3B, Pearson's Correlation Coefficient (PCC) was calculated for the fluorescence positive area within each image. PCC values can range from 1 (correlation) to -1 (anti-correlation). The average of the calculated PCC values was plotted on a histogram in Figure 3-3C. Interestingly, Tetherin localization did not correlate or anti-correlate with either of the sGP constructs. This suggests that while the sGP constructs and Tetherin staining may have some overlap in the images, this apparent co-localization is not different than expected from a random distribution.

A second method used to assess co-localization is a method developed by Li et al., which works on the following principle (151). For a given set of values, the sum of the differences from the mean will be zero: $\sum_i(X_i - \bar{X}) = 0$. For two such sets that are not correlated or anti-correlated, the sum of the product of the differences from the mean will also tend to be zero: $\sum_i(X_i - \bar{X})(Y_i - \bar{Y}) \approx 0$. For sets that are correlated, this sum will be greater than zero $\sum_i(X_i - \bar{X})(Y_i - \bar{Y}) > 0$, and for anti-correlated sets, less than zero $\sum_i(X_i - \bar{X})(Y_i - \bar{Y}) < 0$. Thus, for each image, the product of the differences from the means was calculated for the pixel intensities of the Tetherin and GP

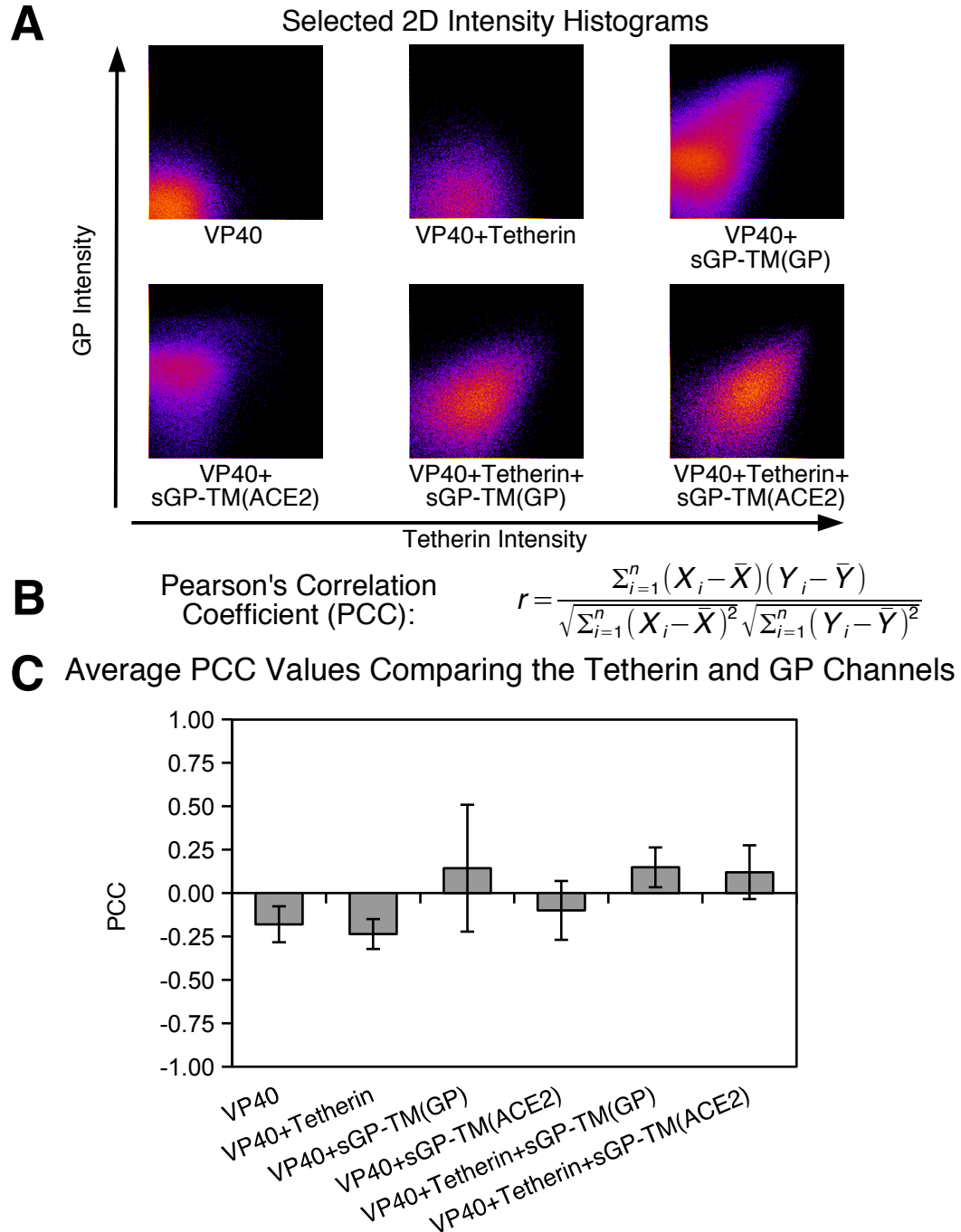


Figure 3-3: Comparison of Tetherin and GP channels by PCC. **A)** Representative images showing the pixel intensities from the Tetherin channel and the GP channel at each location plotted against each other. **B)** The equation used to calculate the PCC for each image file. **C)** Histogram of the average PCC for all image files when comparing the Tetherin and GP channels. The average PCC value is plotted on the y-axis, while the x-axis indicates which plasmids the HT1080 cells received during transfection. The error bars represent 2 S.E. (~95% confidence intervals) while n=3 for all samples except n=6 for VP40+Tetherin+sGP-TM(GP) and n=5 for VP40+Tetherin+sGP-TM(ACE2).

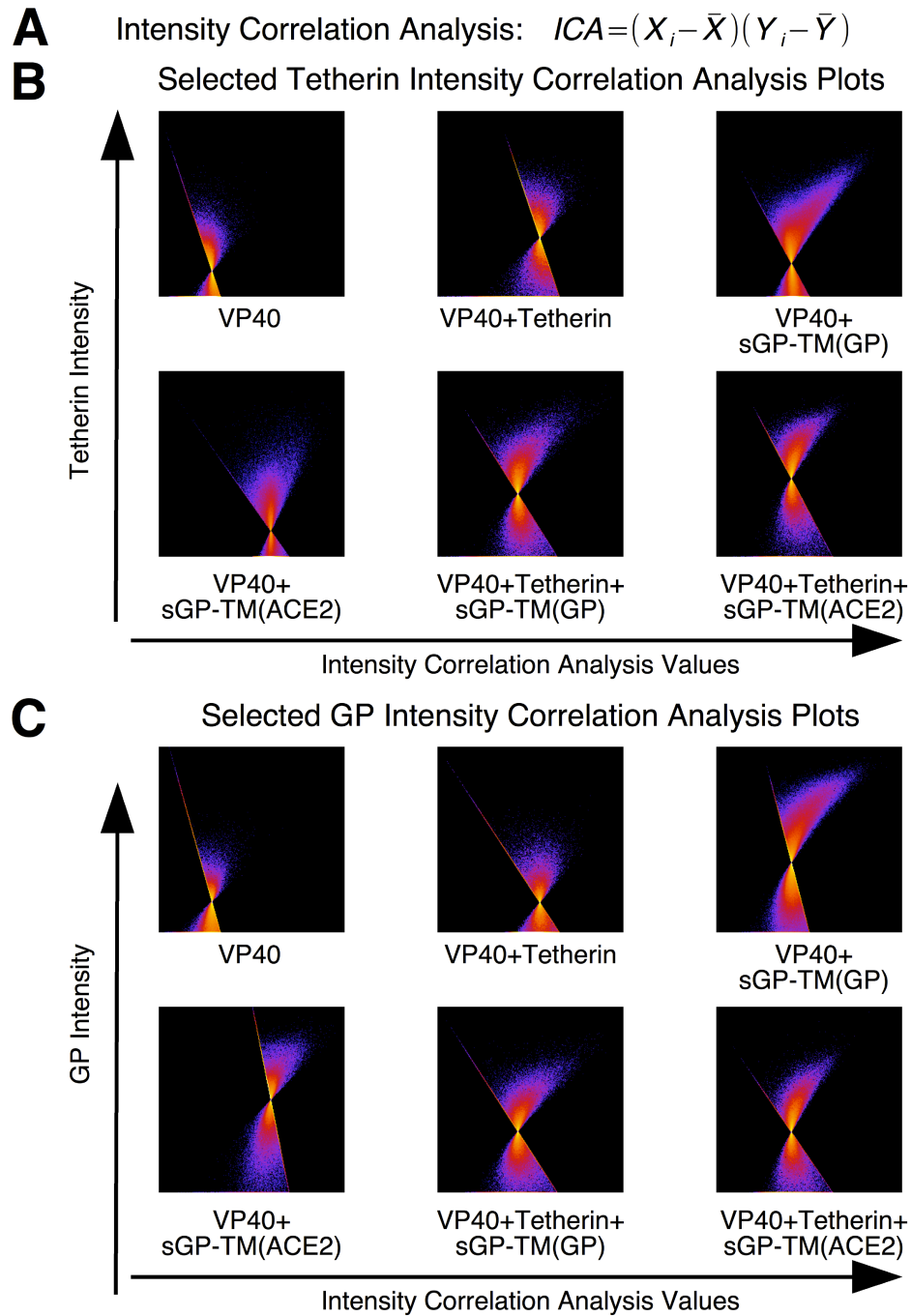


Figure 3-4: ICA plots comparing the intensities of the Tetherin and GP channels. A) The formula used to calculate Intensity Correlation Analysis (ICA) values where X_i and Y_i , the two channel intensity values of a pixel at one location, are compared to the mean intensities, to calculate the ICA value. **B)** Representative plots comparing the intensity of the pixels in the Tetherin channel on the y-axis with the calculated ICA value on the x-axis. The name beneath each plot describes the plasmids that the HT1080 cells were transfected with. **C)** ICA plots similar to B) but comparing the intensity of the pixels in the GP channel to the ICA values instead.

channels, to give an Intensity Correlation Analysis (ICA) value, as shown in Figure 3-4A. Next, plots were generated by comparing the intensity of the pixels in the Tetherin channel with the calculated ICA value, as shown in Figure 3-4B. Similar plots were generated in Figure 3-4C using the GP channel instead. These hourglass shaped plots can be visually interpreted; plots that tilt to the right indicate dependent staining, while plots that tilt to the left indicate segregated staining. In general, all of these plots show neither dependent nor independent staining.

A more quantitative analysis was performed by using the formula shown in Figure 3-5A to generate an Intensity Correlation Quotient (ICQ). ICA plots that tilt to the right exhibiting correlation will have a positive ICQ value of up to 0.5, while plots that tilt to the left showing anti-correlation will have a negative ICQ value. As seen in Figure 3-5B, the ICQ data matches closely with the data from Figure 3-3B. All of the ICQ values are close to zero, again suggesting that Tetherin and both sGP constructs display staining independent of each other and any observed overlap in the images is likely random and not correlative.

Section 3.5 – Discussion

Our results show that, Tetherin and the EBOV glycoprotein do not have a significant interaction, based on localization measured at the cell surface. Additionally, the localization of Tetherin and an EBOV glycoprotein does not change when the glycoprotein is unable to prevent Tetherin-mediated restriction of viral particles.

Some of these data contrast with earlier microscopy results published by others that suggested EBOV GP_{1,2} and Tetherin localize closely with each other on the cell surface (138, 160). Our analysis evaluated the localization of all glycoprotein and Tetherin on the cell surface, rather than simply looking for staining overlap of glycoprotein and Tetherin. Additionally, our results were not dependent on using tagged forms of GP_{1,2} or Tetherin, which could alter the localization as seen with tagged proteins used in other studies. Furthermore, the location of these tags necessitates permeabilization of the cells, which complicates colocalization analysis

A Intensity Correlation Quotient: $ICQ = \frac{\text{Number of positive ICA values}}{\text{Total number of ICA values}} - 0.5$

B ICQ Averages Comparing Tetherin and GP Channels

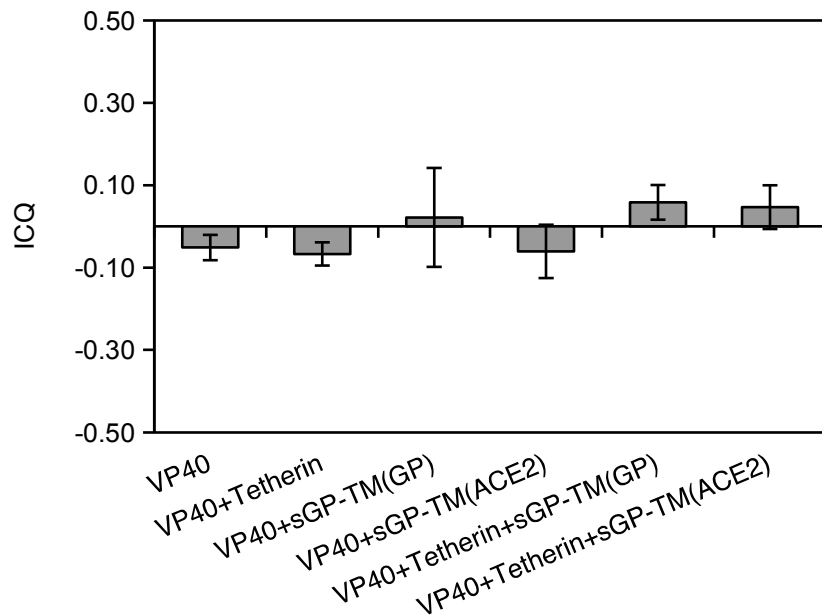


Figure 3-5: Comparing the intensities of the Tetherin and GP channels by ICQ. **A)** Formula to calculate the Intensity Correlation Quotients (ICQ) using the ICA values calculated in the previous figure. **B)** Histogram of the average ICQ values for all image files when comparing the Tetherin and GP channels. The average ICQ value is plotted on the y-axis, while the x-axis indicates which plasmids the HT1080 cells received during transfection. The error bars represent 2 S.E. (~95% confidence intervals) while n=3 for all samples except n=6 for VP40+Tetherin+sGP-TM(GP) and n=5 for VP40+Tetherin+sGP-TM(ACE2).

by obfuscating surface and internal proteins. One study by Gustin et al., attempted microscopy with non-permeabilized cells, but found that GP_{1,2} shielded Tetherin epitopes from antibody detection; a known function of the GP_{1,2} mucin domain (64, 89). Use of sGP derived constructs lacking a mucin domain allowed us to avoid the shielding effect seen with GP_{1,2}. Thus, the different microscopy methods and glycoprotein constructs used by earlier groups could account for the discrepancies seen when compared to our results.

Within the microscopy images, we detected filamentous structures containing VP40 as expected. We also found filamentous structures containing only sGP-TM(GP), similar to previous reports with full-length Ebola glycoprotein (188). Interestingly, we observed fewer structures containing sGP-TM(ACE2), which differs from sGP-TM(GP) only in the transmembrane domain and cytoplasmic tail portions. Studies by Hacke et al. have identified a GXXXA motif within the GP_{1,2} transmembrane domain that, along with cholesterol, allows GP_{1,2} to produce filamentous structures (90). The GXXXA motif is present in sGP-TM(GP), but is lacking the sGP-TM(ACE2) construct, which is consistent with our finding that sGP-TM(ACE2) produces fewer filamentous structures in our images. Overall, our observations support a role for the GP_{1,2} transmembrane domain in producing filamentous particles. Further experimentation is required to determine if the filament production ability of the EBOV glycoproteins is causally related to Tetherin antagonism.

CHAPTER 4 – CONCLUSIONS AND FUTURE DIRECTIONS

Section 4.1 – Formation of Ebola Virus Glycoprotein Induced Particles

Several EBOV proteins, including VP40, Nucleoprotein, VP35, and GP_{1,2} interact to form viral particles capable of assembling and budding from the cell membrane (124, 154). The primary driver of EBOV budding, the matrix protein VP40, oligomerizes and, independent of other viral proteins, forms filamentous particles similar in size and shape to infectious EBOV virions (31, 194, 227). These VP40 induced particles have been termed virus-like particles (VLP) and are used by the field to study many aspects of EBOV budding including interactions with host factors in the ESCRT pathway and Tetherin (20, 96, 129). VLP budding is dependent on VP40 late domains that interact with ESCRT pathway members such as TSG101 and NEDD4 (170, 247).

VP40-driven budding, however, is not always sufficient or even necessary to produce VLP. For example, VLP are sensitive to the anti-viral factor Tetherin and require a Tetherin antagonist, such as GP_{1,2}, to release VLP held by Tetherin on the cell surface (129, 184). GP_{1,2} is capable of enhancing VLP production even when VP40 contains mutations in the late-domain that prevent interaction with ESCRT pathway components, which suggests that these particles can utilize alternative host budding pathways (154, 185). Together, these observations suggest an important role for GP_{1,2} in budding and formation of viral particles.

The ability of GP_{1,2} to promote budding and formation of filamentous particles is a less appreciated function of the glycoprotein. As mentioned above, GP_{1,2} can enhance budding of VP40 particles and allow for ESCRT independent budding of VLP (154). Interestingly, GP_{1,2} can also induce the formation of filamentous particles similar in size, although not necessarily in shape, to VP40 derived particles (188). Unlike VP40 produced VLP, which form flexible rod-like particles with varying lengths and uniform diameters, the GP_{1,2} particles are of a similar size, but with less structure and lack a uniform shape (188).

Recently, experiments by Hacke et al., have suggested that the ability of GP_{1,2} to produce filamentous particles is dependent upon features within the GP₂ subunit of GP_{1,2} (90). A specific motif, GXXXXA, within the transmembrane domain allows production of particles via interactions with elevated levels of cholesterol at the plasma membrane. Their model hypothesizes that the association of cholesterol and the GP₂ subunit drives formation of a lattice-like network that contains GP_{1,2} and excludes other proteins.

As described earlier in section 2.4, we produced a panel of sGP constructs with transmembrane domains from other proteins including ACE2 and TVA. As shown previously in section 2.4 (Figure 2-2 C and D), none of the glycoproteins containing alternative transmembrane domains were able to counter Tetherin, even though they were able to incorporate onto HIV Gag particles in the absence of Tetherin (Figure 2-6). Complicating this analysis is the observation that some of these chimeric glycoproteins do not allow for VP40 budding in the absence of Tetherin. As shown in Figure 4-1, VP40 particles do not bud when sGP contains the transmembrane domain from ACE2. The immunoblots in Figure 4-1 demonstrate results similar to the observations in section 3.4 (Figure 3-1 row 6 column 2); in presence of the sGP-TM(ACE2) production of VP40 containing particles is reduced. Interestingly, as shown earlier in section 2.4 (Figure 2-1), the ACE2 transmembrane domain sequence lacks a GXXXXA motif, while both TVA and GP_{1,2} contain the motif. Thus, even though VP40 can form VLP in the absence of a glycoprotein, these data support the hypothesis that in the presence of both VP40 and GP_{1,2}, the GXXXXA motif is required on the glycoprotein transmembrane domain to produce particles.

To address this hypothesis, additional experiments will be needed to determine whether the GXXXXA motif within GP_{1,2} is important for producing GP particles or allowing for VP40 budding. Similar to the experiments by Hacke et al., the GXXXXA transmembrane motif in sGP-TM(GP) or full-length GP_{1,2} can be mutated to IXXXI and tested in a VP40 VLP budding assay (90). I would hypothesize that glycoproteins containing the GXXXXA motif would incorporate onto

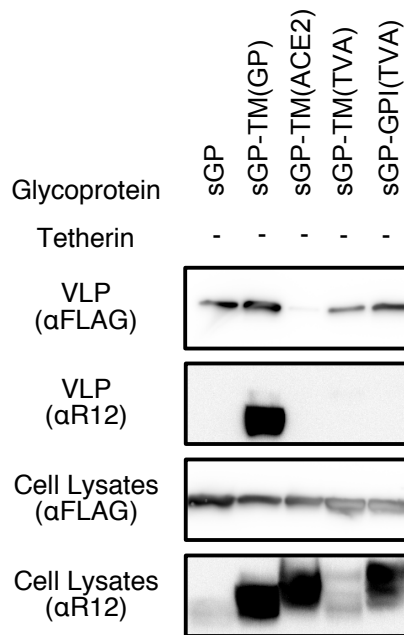


Figure 4-1: Budding of VP40 VLP with sGP chimeras containing alternative transmembrane domains. A VP40 based VLP budding assay, comparing the ability of various glycoproteins to incorporate and allow for VP40 budding in the absence of Tetherin. Using PEI, 293T cells were transfected with VP40-FLAG and each of the glycoproteins shown in the immunoblot. The immunoblots were probed with antibodies to FLAG, to detect VP40, and after stripping the blots, with R12, to detect the sGP glycoprotein.

VP40 particles while glycoproteins containing the IXXXI motif would not. Additionally, I would look for glycoprotein particle formation in the absence of VP40; again anticipating a loss of glycoprotein particle formation when the GXXXA motif is lost. These experiments would highlight the importance of the glycoprotein and the GXXXA motif in production of an understudied viral particle. However, it is likely that additional features within the GP_{1,2} membrane spanning domain are also required as sGP-TM(TVA) does not antagonize Tetherin.

Section 4.2 – Role of the Sialic Acid Residues in the Glycan Cap

A critical function of the EBOV glycoprotein is mediating entry of the EBOV virion into the host cell (220). GP_{1,2} contains a large number of glycosylation sites, most of which are located within the mucin domain and glycan cap domains of the protein (120, 259). These glycans interact with cellular lectins such as dendritic cell-specific intercellular adhesion molecule-3-grabbing non-integrin (DC-SIGN) and DC-SIGNR (8, 234). Lectin interactions and GP_{1,2} induced macropinocytosis allow for uptake and trafficking of the filamentous virion to endosomes containing cathepsins and the receptor NPC-1 (111). Cathepsin B, and possibly Cathepsin L, cleave GP_{1,2} within a disordered loop resulting in release of the glycan cap and mucin domain (36, 225). Removal of these domains exposes the receptor binding portion of GP_{1,2} allowing for an interaction with NPC-1 and subsequent fusion with the cellular membrane (35, 44).

In addition to functioning in entry, the glycan cap, but not the mucin domain, has a role in countering Tetherin during assembly and budding. As described earlier in section 2.4 (Figure 2-9 B), removal of the glycan cap prevents GP_{1,2} from promoting viral particle release in the presence of Tetherin. Although the constructs used lack both a glycan cap and mucin domain, the mucin domain does not influence Tetherin restricted budding (129). Thus, while the glycan cap is needed to counter Tetherin, a mechanism explaining the role GP_{1,2} glycan cap in countering Tetherin has not been described.

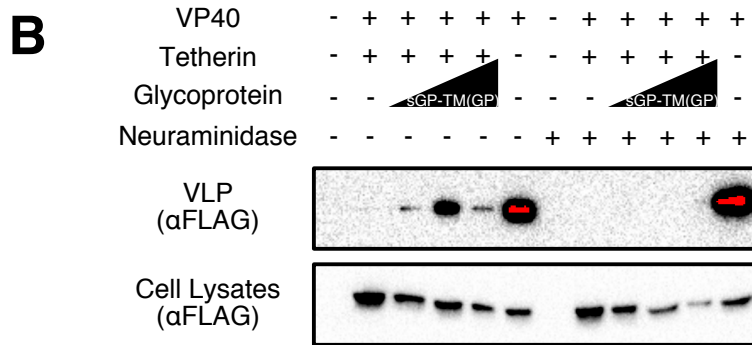
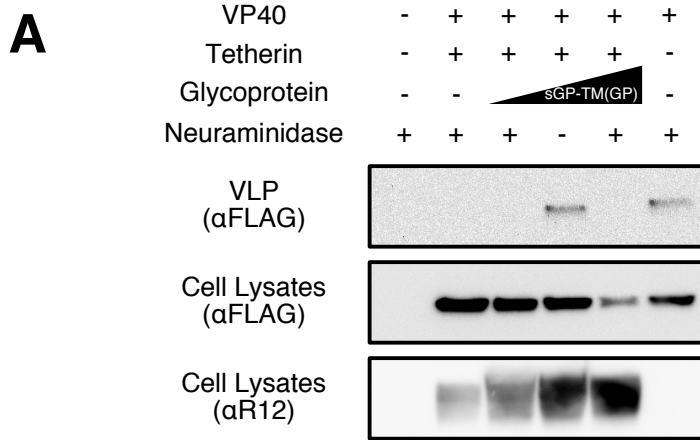


Figure 4-2: The effect of neuraminidase on sGP-TM(GP) mediated release of particles from Tetherin. A) A VP40 VLP budding assay in 293T cells showing the effect of neuraminidase on the ability of sGP-TM(GP) to release VLP held by Tetherin. Neuraminidase was added exogenously to all of the lanes except for the one lane as indicated. The immunoblots were probed with antibodies to FLAG to detect VP40, and after stripping, with R12 to detect sGP. **B)** Another VLP budding assay in 293T cells comparing the ability of VLP to bud with or without exogenous neuraminidase added to the media. The immunoblots were probed with antibodies to FLAG to detect VP40. The red line in the immunoblot indicates overexposure of the blot for that lane.

Interestingly, recent experiments have suggested that neuraminidase activity can prevent EBOV glycoprotein countering of Tetherin during budding. As shown in the budding assays in Figure 4-2, treatment of 293T cells with neuraminidase prevents the antagonist, sGP-TM(GP) from countering Tetherin and allowing for VLP release. It is possible that neuraminidase is cleaving the sialic acid residues on the many N-linked or O-linked glycosylations on the glycan cap of sGP-TM(GP). In turn, this could affect the ability of sGP-TM(GP) to counter Tetherin.

In order to clarify the role of sialic acid residues, I would propose to utilize a series of GP_{1,2} mutants in which the N-linked glycosylation sites are mutated singly and in combinations (147). These constructs could be used in a VP40 budding assay to determine if the glycan cap carbohydrates have a role in countering Tetherin. Additional experiments may be needed as well, since neuraminidase could be cleaving sialic acid residues on other proteins, such as Tetherin, to prevent sGP-TM(GP) from countering Tetherin.

Section 4.3 – How the Ebola Virus Glycoprotein Could Counter Tetherin

Currently, the mechanism by which GP_{1,2} counters Tetherin is not clear. Unlike the mechanisms used by other antagonists, GP_{1,2} does not degrade Tetherin, remove Tetherin from the surface of cells, or relocalize Tetherin away from lipid rafts (129, 160, 161). Our mutational analysis has revealed two domains within GP_{1,2} that influence anti-Tetherin activity: the glycan cap and the transmembrane domain (section 2.4, Figure 2-2 and Figure 2-9) (71, 138). While removal of the glycan cap is important during entry of EBOV, no other roles have been attributed to the glycan cap during assembly or budding of EBOV (36, 130, 145). However, the GP_{1,2} transmembrane domain actively functions to produce filamentous membranes that may be important for budding of EBOV virions (90, 188). Shown in Figure 4-3 are three models to summarize and compare the role of both VP40 and GP_{1,2} in budding.

In the first model, which is the most studied, VP40 oligomers interact, via late-domains, with components of the ESCRT pathway to drive formation of VLP (20, 96, 194). The VLP

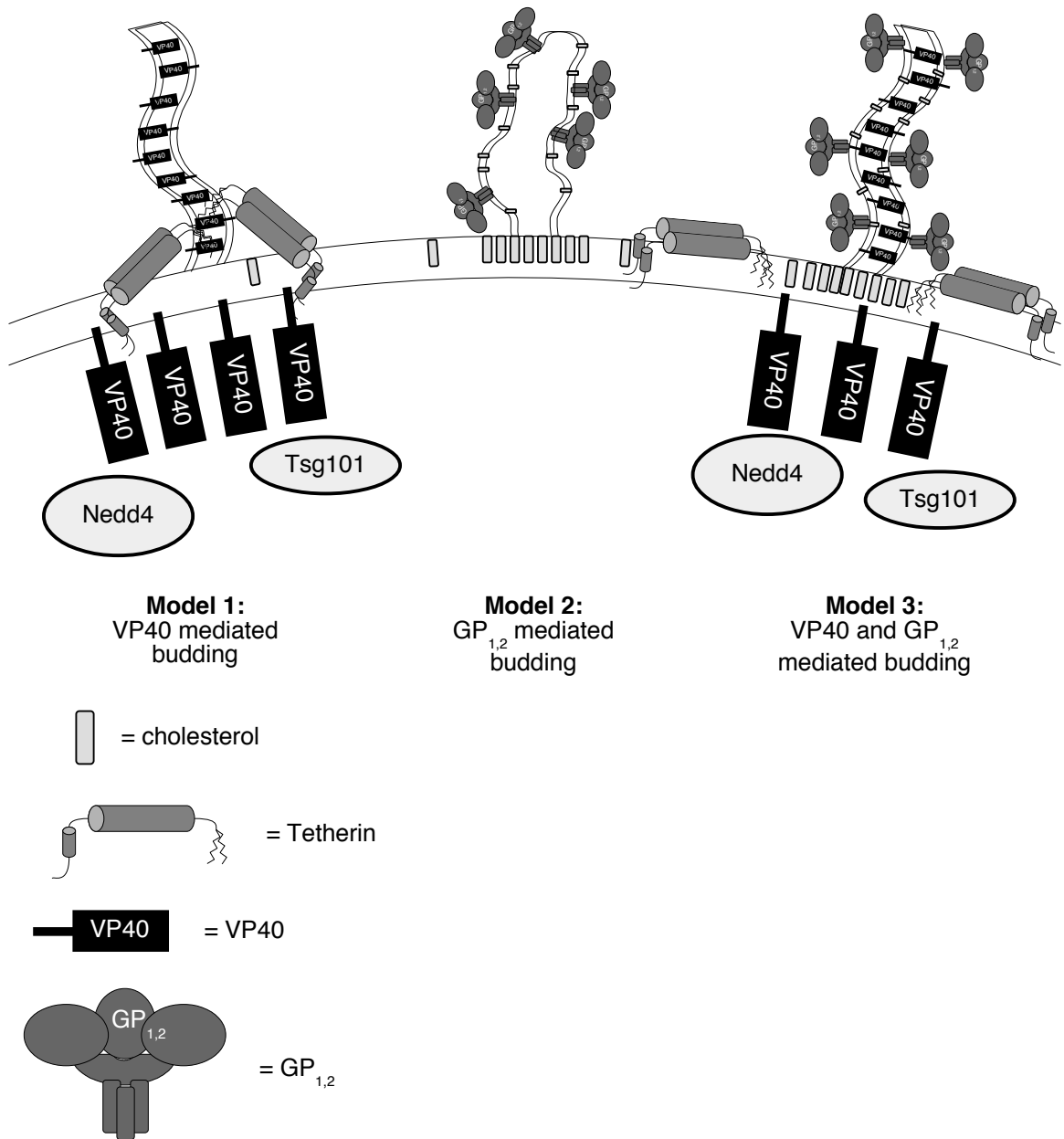


Figure 4-3: Comparison of EBOV budding in three different models. Three models of EBOV budding with VP40 alone, GP_{1,2} alone, and VP40 with GP_{1,2}. The first model depicts VP40 VLP budding, which is dependent on interactions with NEDD4 and TSG101, members of the ESCRT pathway and is inhibited by Tetherin. The second model depicts GP_{1,2} mediated budding, which is not inhibited by Tetherin and utilizes a GXXXA motif in the GP_{1,2} transmembrane domain to recruit cholesterol and produce less structured filaments. The third model depicts budding in the presence of both VP40 and GP_{1,2}, which is not inhibited by Tetherin and may not require ESCRT components.

formed by VP40 are filamentous particles of varying lengths with uniform diameters and are similar to infectious EBOV particles seen by electron microscopy (123, 188). Interactions between VP40 and VP35, the polymerase co-factor, are sufficient to package EBOV minigenomes (124). While these VLP serve as a good model for studying EBOV, this model is incomplete. Budding of VP40 VLP can be inhibited by Tetherin, requiring a Tetherin antagonist such as GP_{1,2} or HIV-1 Vpu to release particles (129, 184). Furthermore, the late domains within VP40 are not required for replication of infectious EBOV (185). Thus, another model is needed to understand EBOV budding.

The second model in Figure 4-3 depicts GP_{1,2} mediated production of pleomorphic particles; a process that has been observed, but is understudied compared to the first model (188). While similar in overall size to VP40 VLP, these particles appear less structured and lack a uniform diameter. Formation of GP_{1,2} particles is dependent on cholesterol and a GXXXA motif within the GP_{1,2} transmembrane domain (90). Also unlike VP40 VLP, GP_{1,2} particles can form in the presence of Tetherin. This model is supported by observations that mature GP_{1,2} does not interact or localize with Tetherin at the cell surface, as described in section 2.4 (Figure 2-7 D), section 3.4 (Figure 3-5 B), and elsewhere (161). However, the filament forming ability of GP_{1,2} has not yet been linked experimentally to its anti-Tetherin activity. Since the GP_{1,2} filament formation is dependent on the GXXXA motif within the GP_{1,2} transmembrane domain, I hypothesize that mutation of the GXXXA motif to IXXXI would also prevent GP_{1,2} from countering Tetherin in a budding assay. Showing that the GXXXA motif is required to counter Tetherin would strongly support the model described here. Additionally, I have already generated constructs with alternative transmembrane domains on sGP, some of which lack a GXXXA motif and have varied abilities to counter Tetherin. Testing the ability of these constructs to produce GP_{1,2} particles in a budding assay would further clarify the role of the GP_{1,2} transmembrane domain in particle production. However, VLP lacking VP40 are not likely to be sufficient for forming viral particles in

the context of an EBOV infection. Incorporation of other viral components, such as the nucleocapsid and RNA genome, depends on interactions with VP40 (124).

The final model in Figure 4-3 shows VP40 and GP_{1,2} interacting to form VLP. These particles can incorporate both VP40 and GP_{1,2}, and appear similar in morphology to infectious EBOV particles (188). Since budding of these particles is mediated by GP_{1,2}, and GP_{1,2} is a known Tetherin antagonist, Tetherin does not prevent budding of these particles (129). However, while Tetherin can inhibit and incorporated into VP40 VLP, it is not clear whether or not Tetherin is excluded from particles containing GP_{1,2}. Additional experiments utilizing sGP constructs with alternative transmembrane domains will be useful in determining the amounts of incorporated Tetherin within viral particles. Interestingly, Tetherin localizes to lipid rafts on the surface, while GP_{1,2} does not (160). Yet, both GP_{1,2} filament formation in HeLa cells and lipid rafts are dependent on cholesterol (90, 236). If Tetherin can incorporate into particles without inhibiting them, then perhaps production of VP40 and GP_{1,2} containing particles alters local cholesterol levels, causing disruptions in lipid raft formation. This could allow Tetherin to localize to EBOV particles without inhibiting them. Additional experiments will be needed to test this hypothesis. Also, while VP40 late domains can interact with ESCRT pathway components, such interactions are not necessary for budding of these particles (185). The active role of GP_{1,2} in budding may explain the observation that GP_{1,2} enhances EBOV particle production in the presence of VP40 containing late-domain mutations (154).

In conclusion, the mechanism by which GP_{1,2} counters Tetherin is unusual and distinct from other antagonists. GP_{1,2} seems to promote virion release without targeting Tetherin for degradation or relocalization. Experiments in this thesis suggest a role for the GP_{1,2} glycan cap and transmembrane domain. Furthermore, the GP_{1,2} transmembrane domain may have a more active role in production of filaments than previously thought. Together, these results suggest a model whereby GP_{1,2} directly promotes formation of viral particles in a manner that prevents

Tetherin from inhibiting viral release. Additional experiments will be needed to verify this model and further clarify the function of GP_{1,2} as a Tetherin antagonist.

BIBLIOGRAPHY

1. 1978. Ebola haemorrhagic fever in Sudan, 1976. Report of a WHO/International Study Team. *Bull World Health Organ* **56**:247-270.
2. 1978. Ebola haemorrhagic fever in Zaire, 1976. *Bull World Health Organ* **56**:271-293.
3. 5/27/2015 2015, posting date. Ebola Situation Report. World Health Organization. [Online.]
4. 2014. Ebola virus disease in West Africa--the first 9 months of the epidemic and forward projections. *N Engl J Med* **371**:1481-1495.
5. 2012. Family - Filoviridae, p. 665-671. In A. M. Q. King, M. J. Adams, E. B. Carstens, and E. J. Lefkowitz (ed.), *Virus Taxonomy*. Elsevier, San Diego.
6. **Aebi, M., J. Fah, N. Hurt, C. E. Samuel, D. Thomis, L. Bazzigher, J. Pavlovic, O. Haller, and P. Staeheli.** 1989. cDNA structures and regulation of two interferon-induced human Mx proteins. *Mol Cell Biol* **9**:5062-5072.
7. **Agnandji, S. T., A. Huttner, M. E. Zinser, P. Njuguna, C. Dahlke, J. F. Fernandes, S. Yerly, J. A. Dayer, V. Kraehling, R. Kasonta, A. A. Adegnika, M. Altfeld, F. Auderset, E. B. Bache, N. Biedenkopf, S. Borregaard, J. S. Brosnahan, R. Burrow, C. Combescure, J. Desmeules, M. Eickmann, S. K. Fehling, A. Finckh, A. R. Goncalves, M. P. Grobusch, J. Hooper, A. Jambrecina, A. L. Kabwende, G. Kaya, D. Kimani, B. Lell, B. Lemaitre, A. W. Lohse, M. Massinga-Loembe, A. Matthey, B. Mordmuller, A. Nolting, C. Ogwang, M. Ramharter, J. Schmidt-Chanasit, S. Schmiedel, P. Silvera, F. R. Stahl, H. M. Staines, T. Strecker, H. C. Stubbe, B. Tsofa, S. Zaki, P. Fast, V. Moorthy, L. Kaiser, S. Krishna, S. Becker, M. P. Kieny, P. Bejon, P. G. Kremsner, M. M. Addo, and C. A. Siegrist.** 2015. Phase 1 Trials of rVSV Ebola Vaccine in Africa and Europe - Preliminary Report. *N Engl J Med*.
8. **Alvarez, C. P., F. Lasala, J. Carrillo, O. Muniz, A. L. Corbi, and R. Delgado.** 2002. C-type lectins DC-SIGN and L-SIGN mediate cellular entry by Ebola virus in cis and in trans. *Journal of virology* **76**:6841-6844.
9. **Andrew, A. J., E. Miyagi, S. Kao, and K. Strebel.** 2009. The formation of cysteine-linked dimers of BST-2/tetherin is important for inhibition of HIV-1 virus release but not for sensitivity to Vpu. *Retrovirology* **6**:80.
10. **Babst, M., G. Odorizzi, E. J. Estepa, and S. D. Emr.** 2000. Mammalian tumor susceptibility gene 101 (TSG101) and the yeast homologue, Vps23p, both function in late endosomal trafficking. *Traffic* **1**:248-258.
11. **Bah, E. I., M. C. Lamah, T. Fletcher, S. T. Jacob, D. M. Brett-Major, A. A. Sall, N. Shindo, W. A. Fischer, 2nd, F. Lamontagne, S. M. Saliou, D. G. Bausch, B. Moumie, T. Jagatic, A. Sprecher, J. V. Lawler, T. Mayet, F. A. Jacqueroiz, M. F. Mendez Baggi, C. Vallenias, C. Clement, S. Mardel, O. Faye, B. Soropogui, N. Magassouba, L. Koivogui, R. Pinto, and R. A. Fowler.** 2015. Clinical presentation of patients with Ebola virus disease in Conakry, Guinea. *N Engl J Med* **372**:40-47.
12. **Baize, S., E. M. Leroy, M. C. Georges-Courbot, M. Capron, J. Lansoud-Soukate, P. Debre, S. P. Fisher-Hoch, J. B. McCormick, and A. J. Georges.** 1999. Defective humoral responses and extensive intravascular apoptosis are associated with fatal outcome in Ebola virus-infected patients. *Nat Med* **5**:423-426.
13. **Baize, S., D. Pannetier, L. Oestereich, T. Rieger, L. Koivogui, N. Magassouba, B. Soropogui, M. S. Sow, S. Keita, H. De Clerck, A. Tiffany, G. Dominguez, M. Loua, A. Traore, M. Kolie, E. R. Malano, E. Heleze, A. Bocquin, S. Mely, H. Raoul, V. Caro, D. Cadar, M. Gabriel, M. Pahlmann, D. Tappe, J. Schmidt-Chanasit, B. Impouma, A. K.**

- Diallo, P. Formenty, M. Van Herp, and S. Gunther.** 2014. Emergence of Zaire Ebola virus disease in Guinea. *N Engl J Med* **371**:1418-1425.
14. **Bale, S., T. Liu, S. Li, Y. Wang, D. Abelson, M. Fusco, V. L. Woods, Jr., and E. O. Saphire.** 2011. Ebola virus glycoprotein needs an additional trigger, beyond proteolytic priming for membrane fusion. *PLoS Negl Trop Dis* **5**:e1395.
 15. **Bampi, C., L. Rasga, and L. Roux.** 2013. Antagonism to human BST-2/tetherin by Sendai virus glycoproteins. *The Journal of general virology* **94**:1211-1219.
 16. **Barrientos, L. G., A. M. Martin, P. E. Rollin, and A. Sanchez.** 2004. Disulfide bond assignment of the Ebola virus secreted glycoprotein SGP. *Biochem Biophys Res Commun* **323**:696-702.
 17. **Basler, C. F., A. Mikulasova, L. Martinez-Sobrido, J. Paragas, E. Muhlberger, M. Bray, H. D. Klenk, P. Palese, and A. Garcia-Sastre.** 2003. The Ebola virus VP35 protein inhibits activation of interferon regulatory factor 3. *Journal of virology* **77**:7945-7956.
 18. **Basler, C. F., X. Wang, E. Muhlberger, V. Volchkov, J. Paragas, H. D. Klenk, A. Garcia-Sastre, and P. Palese.** 2000. The Ebola virus VP35 protein functions as a type I IFN antagonist. *Proceedings of the National Academy of Sciences of the United States of America* **97**:12289-12294.
 19. **Bates, P., J. A. Young, and H. E. Varmus.** 1993. A receptor for subgroup A Rous sarcoma virus is related to the low density lipoprotein receptor. *Cell* **74**:1043-1051.
 20. **Bavari, S., C. M. Bosio, E. Wiegand, G. Ruthel, A. B. Will, T. W. Geisbert, M. Hevey, C. Schmaljohn, A. Schmaljohn, and M. J. Aman.** 2002. Lipid raft microdomains: a gateway for compartmentalized trafficking of Ebola and Marburg viruses. *The Journal of experimental medicine* **195**:593-602.
 21. **Bego, M. G., E. Cote, N. Aschman, J. Mercier, W. Weissenhorn, and E. A. Cohen.** 2015. Vpu Exploits the Cross-Talk between BST2 and the ILT7 Receptor to Suppress Anti-HIV-1 Responses by Plasmacytoid Dendritic Cells. *PLoS pathogens* **11**:e1005024.
 22. **Bermejo, M., J. D. Rodriguez-Teijeiro, G. Illera, A. Barroso, C. Vila, and P. D. Walsh.** 2006. Ebola outbreak killed 5000 gorillas. *Science* **314**:1564.
 23. **Bhattacharyya, S., K. L. Warfield, G. Ruthel, S. Bavari, M. J. Aman, and T. J. Hope.** 2010. Ebola virus uses clathrin-mediated endocytosis as an entry pathway. *Virology* **401**:18-28.
 24. **Billcliff, P. G., O. A. Gorleku, L. H. Chamberlain, and G. Banting.** 2013. The cytosolic N-terminus of CD317/tetherin is a membrane microdomain exclusion motif. *Biol Open* **2**:1253-1263.
 25. **Billcliff, P. G., R. Rollason, I. Prior, D. M. Owen, K. Gaus, and G. Banting.** 2013. CD317/tetherin is an organiser of membrane microdomains. *Journal of cell science* **126**:1553-1564.
 26. **Binley, J. M., R. W. Sanders, B. Clas, N. Schuelke, A. Master, Y. Guo, F. Kajumo, D. J. Anselma, P. J. Maddon, W. C. Olson, and J. P. Moore.** 2000. A recombinant human immunodeficiency virus type 1 envelope glycoprotein complex stabilized by an intermolecular disulfide bond between the gp120 and gp41 subunits is an antigenic mimic of the trimeric virion-associated structure. *Journal of virology* **74**:627-643.
 27. **Blondeau, C., A. Pelchen-Matthews, P. Ilcochova, M. Marsh, R. S. Milne, and G. J. Towers.** 2013. Tetherin restricts herpes simplex virus 1 and is antagonized by glycoprotein M. *Journal of virology* **87**:13124-13133.
 28. **Bour, S., and K. Strebel.** 1996. The human immunodeficiency virus (HIV) type 2 envelope protein is a functional complement to HIV type 1 Vpu that enhances particle release of heterologous retroviruses. *Journal of virology* **70**:8285-8300.

29. **Brass, A. L., I. C. Huang, Y. Benita, S. P. John, M. N. Krishnan, E. M. Feeley, B. J. Ryan, J. L. Weyer, L. van der Weyden, E. Fikrig, D. J. Adams, R. J. Xavier, M. Farzan, and S. J. Elledge.** 2009. The IFITM proteins mediate cellular resistance to influenza A H1N1 virus, West Nile virus, and dengue virus. *Cell* **139**:1243-1254.
30. **Breman, J. G., K. M. Johnson, G. van der Groen, C. B. Robbins, M. V. Szczeniowski, K. Ruti, P. A. Webb, F. Meier, and D. L. Heymann.** 1999. A search for Ebola virus in animals in the Democratic Republic of the Congo and Cameroon: ecologic, virologic, and serologic surveys, 1979-1980. Ebola Virus Study Teams. *The Journal of infectious diseases* **179 Suppl 1**:S139-147.
31. **Bukreyev, A. A., V. E. Volchkov, V. M. Blinov, and S. V. Netesov.** 1993. The VP35 and VP40 proteins of filoviruses. Homology between Marburg and Ebola viruses. *FEBS Lett* **322**:41-46.
32. **Bwaka, M. A., M. J. Bonnet, P. Calain, R. Colebunders, A. De Roo, Y. Guimard, K. R. Katwiki, K. Kibadi, M. A. Kipasa, K. J. Kuvula, B. B. Mapanda, M. Massamba, K. D. Mupapa, J. J. Muyembe-Tamfum, E. Ndaberey, C. J. Peters, P. E. Rollin, and E. Van den Enden.** 1999. Ebola hemorrhagic fever in Kikwit, Democratic Republic of the Congo: clinical observations in 103 patients. *The Journal of infectious diseases* **179 Suppl 1**:S1-7.
33. **Cao, W., L. Bover, M. Cho, X. Wen, S. Hanabuchi, M. Bao, D. B. Rosen, Y. H. Wang, J. L. Shaw, Q. Du, C. Li, N. Arai, Z. Yao, L. L. Lanier, and Y. J. Liu.** 2009. Regulation of TLR7/9 responses in plasmacytoid dendritic cells by BST2 and ILT7 receptor interaction. *J Exp Med* **206**:1603-1614.
34. **Cardenas, W. B., Y. M. Loo, M. Gale, Jr., A. L. Hartman, C. R. Kimberlin, L. Martinez-Sobrido, E. O. Saphire, and C. F. Basler.** 2006. Ebola virus VP35 protein binds double-stranded RNA and inhibits alpha/beta interferon production induced by RIG-I signaling. *Journal of virology* **80**:5168-5178.
35. **Carette, J. E., M. Raaben, A. C. Wong, A. S. Herbert, G. Obernosterer, N. Mulherkar, A. I. Kuehne, P. J. Kranzusch, A. M. Griffin, G. Ruthel, P. Dal Cin, J. M. Dye, S. P. Whelan, K. Chandran, and T. R. Brummelkamp.** 2011. Ebola virus entry requires the cholesterol transporter Niemann-Pick C1. *Nature* **477**:340-343.
36. **Chandran, K., N. J. Sullivan, U. Felbor, S. P. Whelan, and J. M. Cunningham.** 2005. Endosomal proteolysis of the Ebola virus glycoprotein is necessary for infection. *Science* **308**:1643-1645.
37. **Chang, H. W., J. C. Watson, and B. L. Jacobs.** 1992. The E3L gene of vaccinia virus encodes an inhibitor of the interferon-induced, double-stranded RNA-dependent protein kinase. *Proceedings of the National Academy of Sciences of the United States of America* **89**:4825-4829.
38. **Chatterji, U., M. D. Bobardt, P. Gaskill, D. Sheeter, H. Fox, and P. A. Gallay.** 2006. Trim5alpha accelerates degradation of cytosolic capsid associated with productive HIV-1 entry. *The Journal of biological chemistry* **281**:37025-37033.
39. **Chen, Z., M. Zhu, X. Pan, Y. Zhu, H. Yan, T. Jiang, Y. Shen, X. Dong, N. Zheng, J. Lu, and S. Ying.** 2014. Inhibition of Hepatitis B virus replication by SAMHD1. *Biochem Biophys Res Commun* **450**:1462-1468.
40. **Clemens, M. J., and B. R. Williams.** 1978. Inhibition of cell-free protein synthesis by pppA2'p5'A2'p5'A: a novel oligonucleotide synthesized by interferon-treated L cell extracts. *Cell* **13**:565-572.
41. **Cocka, L. J.** 2015. Insight into Tetherin-Mediated Signaling via the Discover of a Novel Isoform with Biologically Distinct Properties. Available from Dissertations & Theses @ University of Pennsylvania; ProQuest Dissertations & Theses Global.

42. **Cocka, L. J., and P. Bates.** 2012. Identification of alternatively translated Tetherin isoforms with differing antiviral and signaling activities. *PLoS pathogens* **8**:e1002931.
43. **Cohen, E. A., E. F. Terwilliger, J. G. Sodroski, and W. A. Haseltine.** 1988. Identification of a protein encoded by the vpu gene of HIV-1. *Nature* **334**:532-534.
44. **Cote, M., J. Misasi, T. Ren, A. Bruchez, K. Lee, C. M. Filone, L. Hensley, Q. Li, D. Ory, K. Chandran, and J. Cunningham.** 2011. Small molecule inhibitors reveal Niemann-Pick C1 is essential for Ebola virus infection. *Nature* **477**:344-348.
45. **Dafa-Berger, A., A. Kuzmina, M. Fassler, H. Yitzhak-Asraf, Y. Shemer-Avni, and R. Taube.** 2012. Modulation of hepatitis C virus release by the interferon-induced protein BST-2/tetherin. *Virology*.
46. **Daffis, S., K. J. Szretter, J. Schriewer, J. Li, S. Youn, J. Errett, T. Y. Lin, S. Schneller, R. Zust, H. Dong, V. Thiel, G. C. Sen, V. Fensterl, W. B. Klimstra, T. C. Pierson, R. M. Buller, M. Gale, Jr., P. Y. Shi, and M. S. Diamond.** 2010. 2'-O methylation of the viral mRNA cap evades host restriction by IFIT family members. *Nature* **468**:452-456.
47. **Dang, Y., X. Wang, W. J. Esselman, and Y. H. Zheng.** 2006. Identification of APOBEC3DE as another antiretroviral factor from the human APOBEC family. *Journal of virology* **80**:10522-10533.
48. **Davies, M. V., H. W. Chang, B. L. Jacobs, and R. J. Kaufman.** 1993. The E3L and K3L vaccinia virus gene products stimulate translation through inhibition of the double-stranded RNA-dependent protein kinase by different mechanisms. *Journal of virology* **67**:1688-1692.
49. **Davies, M. V., O. Elroy-Stein, R. Jagus, B. Moss, and R. J. Kaufman.** 1992. The vaccinia virus K3L gene product potentiates translation by inhibiting double-stranded-RNA-activated protein kinase and phosphorylation of the alpha subunit of eukaryotic initiation factor 2. *Journal of virology* **66**:1943-1950.
50. **Douglas, J. L., K. Viswanathan, M. N. McCarroll, J. K. Gustin, K. Fruh, and A. V. Moses.** 2009. Vpu directs the degradation of the human immunodeficiency virus restriction factor BST-2/Tetherin via a {beta}TrCP-dependent mechanism. *Journal of virology* **83**:7931-7947.
51. **Dowell, S. F., R. Mukunu, T. G. Ksiazek, A. S. Khan, P. E. Rollin, and C. J. Peters.** 1999. Transmission of Ebola hemorrhagic fever: a study of risk factors in family members, Kikwit, Democratic Republic of the Congo, 1995. *Commission de Lutte contre les Epidemies a Kikwit. The Journal of infectious diseases* **179 Suppl 1**:S87-91.
52. **Dube, D., M. B. Brecher, S. E. Delos, S. C. Rose, E. W. Park, K. L. Schornberg, J. H. Kuhn, and J. M. White.** 2009. The primed ebolavirus glycoprotein (19-kilodalton GP1,2): sequence and residues critical for host cell binding. *Journal of virology* **83**:2883-2891.
53. **Dube, M., B. B. Roy, P. Guiot-Guillain, J. Mercier, J. Binette, G. Leung, and E. A. Cohen.** 2009. Suppression of Tetherin-restricting activity upon human immunodeficiency virus type 1 particle release correlates with localization of Vpu in the trans-Golgi network. *Journal of virology* **83**:4574-4590.
54. **Dull, T., R. Zufferey, M. Kelly, R. J. Mandel, M. Nguyen, D. Trono, and L. Naldini.** 1998. A third-generation lentivirus vector with a conditional packaging system. *Journal of virology* **72**:8463-8471.
55. **Falzarano, D., O. Krokhin, V. Wahl-Jensen, J. Seebach, K. Wolf, H. J. Schnittler, and H. Feldmann.** 2006. Structure-function analysis of the soluble glycoprotein, sGP, of Ebola virus. *Chembiochem* **7**:1605-1611.

56. **Farrell, P. J., K. Balkow, T. Hunt, R. J. Jackson, and H. Trachsel.** 1977. Phosphorylation of initiation factor eIF-2 and the control of reticulocyte protein synthesis. *Cell* **11**:187-200.
57. **Feeley, E. M., J. S. Sims, S. P. John, C. R. Chin, T. Pertel, L. M. Chen, G. D. Gaiha, B. J. Ryan, R. O. Donis, S. J. Elledge, and A. L. Brass.** 2011. IFITM3 inhibits influenza A virus infection by preventing cytosolic entry. *PLoS pathogens* **7**:e1002337.
58. **Feldmann, H., S. M. Jones, K. M. Daddario-DiCaprio, J. B. Geisbert, U. Stroher, A. Grolla, M. Bray, E. A. Fritz, L. Fernando, F. Feldmann, L. E. Hensley, and T. W. Geisbert.** 2007. Effective post-exposure treatment of Ebola infection. *PLoS pathogens* **3**:e2.
59. **Feldmann, H., E. Muhlberger, A. Randolph, C. Will, M. P. Kiley, A. Sanchez, and H. D. Klenk.** 1992. Marburg virus, a filovirus: messenger RNAs, gene order, and regulatory elements of the replication cycle. *Virus research* **24**:1-19.
60. **Feng, Z., M. Cerveny, Z. Yan, and B. He.** 2007. The VP35 protein of Ebola virus inhibits the antiviral effect mediated by double-stranded RNA-dependent protein kinase PKR. *Journal of virology* **81**:182-192.
61. **Fitzpatrick, K., M. Skasko, T. J. Deerinck, J. Crum, M. H. Ellisman, and J. Guatelli.** 2010. Direct restriction of virus release and incorporation of the interferon-induced protein BST-2 into HIV-1 particles. *PLoS Pathog* **6**:e1000701.
62. **Floyd-Smith, G., E. Slattery, and P. Lengyel.** 1981. Interferon action: RNA cleavage pattern of a (2'-5')oligoadenylate--dependent endonuclease. *Science* **212**:1030-1032.
63. **Francica, J. R., M. K. Matukonis, and P. Bates.** 2009. Requirements for cell rounding and surface protein down-regulation by Ebola virus glycoprotein. *Virology* **383**:237-247.
64. **Francica, J. R., A. Varela-Rohena, A. Medvec, G. Plesa, J. L. Riley, and P. Bates.** 2010. Steric shielding of surface epitopes and impaired immune recognition induced by the ebola virus glycoprotein. *PLoS pathogens* **6**:e1001098.
65. **Frese, M., G. Kochs, H. Feldmann, C. Hertkorn, and O. Haller.** 1996. Inhibition of bunyaviruses, phleboviruses, and hantaviruses by human MxA protein. *Journal of virology* **70**:915-923.
66. **Fritz, J. V., N. Tibroni, O. T. Keppler, and O. T. Fackler.** 2012. HIV-1 Vpu's lipid raft association is dispensable for counteraction of the particle release restriction imposed by CD317/Tetherin. *Virology* **424**:33-44.
67. **Galao, R. P., A. Le Tortorec, S. Pickering, T. Kueck, and S. J. Neil.** 2012. Innate sensing of HIV-1 assembly by Tetherin induces NFkappaB-dependent proinflammatory responses. *Cell host & microbe* **12**:633-644.
68. **Galao, R. P., S. Pickering, R. Curnock, and S. J. Neil.** 2014. Retroviral retention activates a Syk-dependent HemITAM in human tetherin. *Cell host & microbe* **16**:291-303.
69. **Geisbert, T. W., L. E. Hensley, T. Larsen, H. A. Young, D. S. Reed, J. B. Geisbert, D. P. Scott, E. Kagan, P. B. Jahrling, and K. J. Davis.** 2003. Pathogenesis of Ebola hemorrhagic fever in cynomolgus macaques: evidence that dendritic cells are early and sustained targets of infection. *Am J Pathol* **163**:2347-2370.
70. **Georges, A. J., E. M. Leroy, A. A. Renaut, C. T. Benissan, R. J. Nabias, M. T. Ngoc, P. I. Obiang, J. P. Lepage, E. J. Bertherat, D. D. Benoni, E. J. Wickings, J. P. Amblard, J. M. Lansoud-Soukate, J. M. Milleliri, S. Baize, and M. C. Georges-Courbot.** 1999. Ebola hemorrhagic fever outbreaks in Gabon, 1994-1997: epidemiologic and health control issues. *The Journal of infectious diseases* **179 Suppl 1**:S65-75.
71. **Gnirss, K., M. Fiedler, A. Kramer-Kuhl, S. Bolduan, E. Mittler, S. Becker, M. Schindler, and S. Pohlmann.** 2014. Analysis of determinants in filovirus glycoproteins required for tetherin antagonism. *Viruses* **6**:1654-1671.

72. **Gnirss, K., P. Zmora, P. Blazejewska, M. Winkler, A. Lins, I. Nehlmeier, S. Gartner, A. S. Moldenhauer, H. Hofmann-Winkler, T. Wolff, M. Schindler, and S. Pohlmann.** 2015. Tetherin sensitivity of influenza A viruses is strain specific: Role of hemagglutinin and neuraminidase. *Journal of virology*.
73. **Goebel, S. J., G. P. Johnson, M. E. Perkus, S. W. Davis, J. P. Winslow, and E. Paoletti.** 1990. The complete DNA sequence of vaccinia virus. *Virology* **179**:247-266, 517-263.
74. **Goldstone, D. C., V. Ennis-Adeniran, J. J. Hedden, H. C. Groom, G. I. Rice, E. Christodoulou, P. A. Walker, G. Kelly, L. F. Haire, M. W. Yap, L. P. de Carvalho, J. P. Stoye, Y. J. Crow, I. A. Taylor, and M. Webb.** 2011. HIV-1 restriction factor SAMHD1 is a deoxynucleoside triphosphate triphosphohydrolase. *Nature* **480**:379-382.
75. **Gomes, M. F., Y. P. A. Pastore, L. Rossi, D. Chao, I. Longini, M. E. Halloran, and A. Vespignani.** 2014. Assessing the international spreading risk associated with the 2014 west african ebola outbreak. *PLoS Curr* **6**.
76. **Gomis-Ruth, F. X., A. Dessen, J. Timmins, A. Bracher, L. Kolesnikowa, S. Becker, H. D. Klenk, and W. Weissenhorn.** 2003. The matrix protein VP40 from Ebola virus octamerizes into pore-like structures with specific RNA binding properties. *Structure* **11**:423-433.
77. **Gordien, E., O. Rosmorduc, C. Peltekian, F. Garreau, C. Brechot, and D. Kremsdorf.** 2001. Inhibition of hepatitis B virus replication by the interferon-inducible MxA protein. *Journal of virology* **75**:2684-2691.
78. **Goto, T., S. J. Kennel, M. Abe, M. Takishita, M. Kosaka, A. Solomon, and S. Saito.** 1994. A novel membrane antigen selectively expressed on terminally differentiated human B cells. *Blood* **84**:1922-1930.
79. **Gottlinger, H. G., T. Dorfman, E. A. Cohen, and W. A. Haseltine.** 1993. Vpu protein of human immunodeficiency virus type 1 enhances the release of capsids produced by gag gene constructs of widely divergent retroviruses. *Proceedings of the National Academy of Sciences of the United States of America* **90**:7381-7385.
80. **Goujon, C., O. Moncorge, H. Bauby, T. Doyle, C. C. Ward, T. Schaller, S. Hue, W. S. Barclay, R. Schulz, and M. H. Malim.** 2013. Human MX2 is an interferon-induced post-entry inhibitor of HIV-1 infection. *Nature* **502**:559-562.
81. **Gregory, S. M., E. Harada, B. Liang, S. E. Delos, J. M. White, and L. K. Tamm.** 2011. Structure and function of the complete internal fusion loop from Ebolavirus glycoprotein 2. *Proceedings of the National Academy of Sciences of the United States of America* **108**:11211-11216.
82. **Guerra, S., A. Caceres, K. P. Knobeloch, I. Horak, and M. Esteban.** 2008. Vaccinia virus E3 protein prevents the antiviral action of ISG15. *PLoS pathogens* **4**:e1000096.
83. **Guimard, Y., M. A. Bwaka, R. Colebunders, P. Calain, M. Massamba, A. De Roo, K. D. Mupapa, K. Kibadi, K. J. Kuvula, D. E. Ndaberey, K. R. Katwiki, B. B. Mapanda, O. B. Nkuku, Y. Fleerackers, E. Van den Enden, and M. A. Kipasa.** 1999. Organization of patient care during the Ebola hemorrhagic fever epidemic in Kikwit, Democratic Republic of the Congo, 1995. *The Journal of infectious diseases* **179 Suppl 1**:S268-273.
84. **Gunther, S., G. Sommer, U. Plikat, A. Iwanska, S. Wain-Hobson, H. Will, and A. Meyerhans.** 1997. Naturally occurring hepatitis B virus genomes bearing the hallmarks of retroviral G-->A hypermutation. *Virology* **235**:104-108.
85. **Guo, F., S. Cen, M. Niu, Y. Yang, R. J. Gorelick, and L. Kleiman.** 2007. The interaction of APOBEC3G with human immunodeficiency virus type 1 nucleocapsid inhibits tRNA³Lys annealing to viral RNA. *Journal of virology* **81**:11322-11331.

86. **Gupta, M., S. Mahanty, R. Ahmed, and P. E. Rollin.** 2001. Monocyte-derived human macrophages and peripheral blood mononuclear cells infected with ebola virus secrete MIP-1alpha and TNF-alpha and inhibit poly-IC-induced IFN-alpha in vitro. *Virology* **284**:20-25.
87. **Gupta, R. K., S. Hue, T. Schaller, E. Verschoor, D. Pillay, and G. J. Towers.** 2009. Mutation of a single residue renders human tetherin resistant to HIV-1 Vpu-mediated depletion. *PLoS Pathog* **5**:e1000443.
88. **Gupta, R. K., P. Mlcochova, A. Pelchen-Matthews, S. J. Petit, G. Mattiuzzo, D. Pillay, Y. Takeuchi, M. Marsh, and G. J. Towers.** 2009. Simian immunodeficiency virus envelope glycoprotein counteracts tetherin/BST-2/CD317 by intracellular sequestration. *Proc Natl Acad Sci U S A* **106**:20889-20894.
89. **Gustin, J. K., Y. Bai, A. V. Moses, and J. L. Douglas.** 2015. Ebola Virus Glycoprotein Promotes Enhanced Viral Egress by Preventing Ebola VP40 From Associating With the Host Restriction Factor BST2/Tetherin. *The Journal of infectious diseases*.
90. **Hacke, M., P. Bjorkholm, A. Hellwig, P. Himmels, C. R. de Almodovar, B. Brugger, F. Wieland, and A. M. Ernst.** 2015. Inhibition of Ebola virus glycoprotein-mediated cytotoxicity by targeting its transmembrane domain and cholesterol. *Nat Commun* **6**.
91. **Haines, K. M., N. H. Vande Burgt, J. R. Francica, R. L. Kaletsky, and P. Bates.** 2012. Chinese hamster ovary cell lines selected for resistance to ebolavirus glycoprotein mediated infection are defective for NPC1 expression. *Virology* **432**:20-28.
92. **Hammonds, J., L. Ding, H. Chu, K. Geller, A. Robbins, J. J. Wang, H. Yi, and P. Spearman.** 2012. The tetherin/BST-2 coiled-coil ectodomain mediates plasma membrane microdomain localization and restriction of particle release. *J Virol* **86**:2259-2272.
93. **Hammonds, J., J. J. Wang, H. Yi, and P. Spearman.** 2010. Immunoelectron microscopic evidence for Tetherin/BST2 as the physical bridge between HIV-1 virions and the plasma membrane. *PLoS Pathog* **6**:e1000749.
94. **Harris, R. S., K. N. Bishop, A. M. Sheehy, H. M. Craig, S. K. Petersen-Mahrt, I. N. Watt, M. S. Neuberger, and M. H. Malim.** 2003. DNA deamination mediates innate immunity to retroviral infection. *Cell* **113**:803-809.
95. **Hartlieb, B., T. Muziol, W. Weissenhorn, and S. Becker.** 2007. Crystal structure of the C-terminal domain of Ebola virus VP30 reveals a role in transcription and nucleocapsid association. *Proceedings of the National Academy of Sciences of the United States of America* **104**:624-629.
96. **Harty, R. N., M. E. Brown, G. Wang, J. Huibregtse, and F. P. Hayes.** 2000. A PPxY motif within the VP40 protein of Ebola virus interacts physically and functionally with a ubiquitin ligase: implications for filovirus budding. *Proc Natl Acad Sci U S A* **97**:13871-13876.
97. **Hashiguchi, T., M. L. Fusco, Z. A. Bornholdt, J. E. Lee, A. I. Flyak, R. Matsuoka, D. Kohda, Y. Yanagi, M. Hammel, J. E. Crowe, Jr., and E. O. Saphire.** 2015. Structural basis for Marburg virus neutralization by a cross-reactive human antibody. *Cell* **160**:904-912.
98. **Hatzioannou, T., D. Perez-Caballero, A. Yang, S. Cowan, and P. D. Bieniasz.** 2004. Retrovirus resistance factors Ref1 and Lv1 are species-specific variants of TRIM5alpha. *Proceedings of the National Academy of Sciences of the United States of America* **101**:10774-10779.
99. **Hauser, H., L. A. Lopez, S. J. Yang, J. E. Oldenburg, C. M. Exline, J. C. Guatelli, and P. M. Cannon.** 2010. HIV-1 Vpu and HIV-2 Env counteract BST-2/tetherin by sequestration in a perinuclear compartment. *Retrovirology* **7**:51.

100. **Helbig, K. J., D. T. Lau, L. Semendric, H. A. Harley, and M. R. Beard.** 2005. Analysis of ISG expression in chronic hepatitis C identifies viperin as a potential antiviral effector. *Hepatology* **42**:702-710.
101. **Henao-Restrepo, A. M., I. M. Longini, M. Egger, N. E. Dean, W. J. Edmunds, A. Camacho, M. W. Carroll, M. Doumbia, B. Draguez, S. Duraffour, G. Enwere, R. Grais, S. Gunther, S. Hossmann, M. K. Kondrachine, S. Kone, E. Kuisma, M. M. Levine, S. Mandal, G. Norheim, X. Riveros, A. Soumah, S. Trelle, A. S. Vicari, C. H. Watson, S. Kivimäki, M. P. Kieny, and J.-A. Ruyter.** Efficacy and effectiveness of an rVSV-vectored vaccine expressing Ebola surface glycoprotein: interim results from the Guinea ring vaccination cluster-randomised trial. *The Lancet*.
102. **Hensley, L. E., H. A. Young, P. B. Jahrling, and T. W. Geisbert.** 2002. Proinflammatory response during Ebola virus infection of primate models: possible involvement of the tumor necrosis factor receptor superfamily. *Immunol Lett* **80**:169-179.
103. **Hoenen, T., V. Volchkov, L. Kolesnikova, E. Mittler, J. Timmins, M. Ottmann, O. Reynard, S. Becker, and W. Weissenhorn.** 2005. VP40 octamers are essential for Ebola virus replication. *Journal of virology* **79**:1898-1905.
104. **Hood, C. L., J. Abraham, J. C. Boyington, K. Leung, P. D. Kwong, and G. J. Nabel.** 2010. Biochemical and structural characterization of cathepsin L-processed Ebola virus glycoprotein: implications for viral entry and immunogenicity. *Journal of virology* **84**:2972-2982.
105. **Hovanessian, A. G., R. E. Brown, and I. M. Kerr.** 1977. Synthesis of low molecular weight inhibitor of protein synthesis with enzyme from interferon-treated cells. *Nature* **268**:537-540.
106. **Hsiang, T. Y., C. Zhao, and R. M. Krug.** 2009. Interferon-induced ISG15 conjugation inhibits influenza A virus gene expression and replication in human cells. *Journal of virology* **83**:5971-5977.
107. **Hsiao, N. W., J. W. Chen, T. C. Yang, G. M. Orloff, Y. Y. Wu, C. H. Lai, Y. C. Lan, and C. W. Lin.** 2010. ISG15 over-expression inhibits replication of the Japanese encephalitis virus in human medulloblastoma cells. *Antiviral Res* **85**:504-511.
108. **Huang, I. C., C. C. Bailey, J. L. Weyer, S. R. Radoshitzky, M. M. Becker, J. J. Chiang, A. L. Brass, A. A. Ahmed, X. Chi, L. Dong, L. E. Longobardi, D. Boltz, J. H. Kuhn, S. J. Eledge, S. Bavari, M. R. Denison, H. Choe, and M. Farzan.** 2011. Distinct patterns of IFITM-mediated restriction of filoviruses, SARS coronavirus, and influenza A virus. *PLoS pathogens* **7**:e1001258.
109. **Huang, Y., L. Xu, Y. Sun, and G. J. Nabel.** 2002. The assembly of Ebola virus nucleocapsid requires virion-associated proteins 35 and 24 and posttranslational modification of nucleoprotein. *Mol Cell* **10**:307-316.
110. **Hui, D. J., C. R. Bhasker, W. C. Merrick, and G. C. Sen.** 2003. Viral stress-inducible protein p56 inhibits translation by blocking the interaction of eIF3 with the ternary complex eIF2.GTP.Met-tRNAⁱ. *The Journal of biological chemistry* **278**:39477-39482.
111. **Hunt, C. L., A. A. Kolokoltsov, R. A. Davey, and W. Maury.** 2011. The Tyro3 receptor kinase Axl enhances macropinocytosis of Zaire ebolavirus. *Journal of virology* **85**:334-347.
112. **Ilinskaya, A., D. Derse, S. Hill, G. Princler, and G. Heidecker.** 2013. Cell-cell transmission allows human T-lymphotropic virus 1 to circumvent tetherin restriction. *Virology* **436**:201-209.
113. **Ishikawa, J., T. Kaisho, H. Tomizawa, B. O. Lee, Y. Kobune, J. Inazawa, K. Oritani, M. Itoh, T. Ochi, K. Ishihara, and et al.** 1995. Molecular cloning and chromosomal

- mapping of a bone marrow stromal cell surface gene, BST2, that may be involved in pre-B-cell growth. *Genomics* **26**:527-534.
114. **Ito, H., S. Watanabe, A. Takada, and Y. Kawaoka.** 2001. Ebola virus glycoprotein: proteolytic processing, acylation, cell tropism, and detection of neutralizing antibodies. *Journal of virology* **75**:1576-1580.
 115. **Iwabu, Y., H. Fujita, M. Kinomoto, K. Kaneko, Y. Ishizaka, Y. Tanaka, T. Sata, and K. Tokunaga.** 2009. HIV-1 accessory protein Vpu internalizes cell-surface BST-2/tetherin through transmembrane interactions leading to lysosomes. *The Journal of biological chemistry* **284**:35060-35072.
 116. **Jaax, N. K., K. J. Davis, T. J. Geisbert, P. Vogel, G. P. Jaax, M. Topper, and P. B. Jahrling.** 1996. Lethal experimental infection of rhesus monkeys with Ebola-Zaire (Mayinga) virus by the oral and conjunctival route of exposure. *Arch Pathol Lab Med* **120**:140-155.
 117. **Jaffe, E. A., D. Armellino, G. Lam, C. Cordon-Cardo, H. W. Murray, and R. L. Evans.** 1989. IFN-gamma and IFN-alpha induce the expression and synthesis of Leu 13 antigen by cultured human endothelial cells. *Journal of immunology* **143**:3961-3966.
 118. **Jahrling, P. B., T. W. Geisbert, D. W. Dalgard, E. D. Johnson, T. G. Ksiazek, W. C. Hall, and C. J. Peters.** 1990. Preliminary report: isolation of Ebola virus from monkeys imported to USA. *Lancet* **335**:502-505.
 119. **Janvier, K., A. Pelchen-Matthews, J. B. Renaud, M. Caillet, M. Marsh, and C. Berlioz-Torrent.** 2011. The ESCRT-0 component HRS is required for HIV-1 Vpu-mediated BST-2/tetherin down-regulation. *PLoS pathogens* **7**:e1001265.
 120. **Jeffers, S. A., D. A. Sanders, and A. Sanchez.** 2002. Covalent modifications of the ebola virus glycoprotein. *Journal of virology* **76**:12463-12472.
 121. **Jia, B., R. Serra-Moreno, W. Neidermyer, A. Rahmberg, J. Mackey, I. B. Fofana, W. E. Johnson, S. Westmoreland, and D. T. Evans.** 2009. Species-specific activity of SIV Nef and HIV-1 Vpu in overcoming restriction by tetherin/BST2. *PLoS Pathog* **5**:e1000429.
 122. **Jiang, D., H. Guo, C. Xu, J. Chang, B. Gu, L. Wang, T. M. Block, and J. T. Guo.** 2008. Identification of three interferon-inducible cellular enzymes that inhibit the replication of hepatitis C virus. *Journal of virology* **82**:1665-1678.
 123. **Johnson, K. M., J. V. Lange, P. A. Webb, and F. A. Murphy.** 1977. Isolation and partial characterisation of a new virus causing acute haemorrhagic fever in Zaire. *Lancet* **1**:569-571.
 124. **Johnson, R. F., S. E. McCarthy, P. J. Godlewski, and R. N. Harty.** 2006. Ebola virus VP35-VP40 interaction is sufficient for packaging 3E-5E minigenome RNA into virus-like particles. *Journal of virology* **80**:5135-5144.
 125. **Jolly, C., N. J. Booth, and S. J. Neil.** 2010. Cell-cell spread of human immunodeficiency virus type 1 overcomes tetherin/BST-2-mediated restriction in T cells. *Journal of virology* **84**:12185-12199.
 126. **Jones, P. H., M. Maric, M. N. Madison, W. Maury, R. J. Roller, and C. M. Okeoma.** 2013. BST-2/tetherin-mediated restriction of chikungunya (CHIKV) VLP budding is counteracted by CHIKV non-structural protein 1 (nsP1). *Virology* **438**:37-49.
 127. **Jones, S. M., H. Feldmann, U. Stroher, J. B. Geisbert, L. Fernando, A. Grolla, H. D. Klenk, N. J. Sullivan, V. E. Volchkov, E. A. Fritz, K. M. Daddario, L. E. Hensley, P. B. Jahrling, and T. W. Geisbert.** 2005. Live attenuated recombinant vaccine protects nonhuman primates against Ebola and Marburg viruses. *Nat Med* **11**:786-790.
 128. **Jouvenet, N., S. J. Neil, M. Zhadina, T. Zang, Z. Kratovac, Y. Lee, M. McNatt, T. Hatzioannou, and P. D. Bieniasz.** 2009. Broad-spectrum inhibition of retroviral and filoviral particle release by tetherin. *J Virol* **83**:1837-1844.

129. **Kaletsky, R. L., J. R. Francica, C. Agrawal-Gamse, and P. Bates.** 2009. Tetherin-mediated restriction of filovirus budding is antagonized by the Ebola glycoprotein. *Proc Natl Acad Sci U S A* **106**:2886-2891.
130. **Kaletsky, R. L., G. Simmons, and P. Bates.** 2007. Proteolysis of the Ebola virus glycoproteins enhances virus binding and infectivity. *Journal of virology* **81**:13378-13384.
131. **Katzmann, D. J., M. Babst, and S. D. Emr.** 2001. Ubiquitin-dependent sorting into the multivesicular body pathway requires the function of a conserved endosomal protein sorting complex, ESCRT-I. *Cell* **106**:145-155.
132. **Keckesova, Z., L. M. Ylinen, and G. J. Towers.** 2004. The human and African green monkey TRIM5alpha genes encode Ref1 and Lv1 retroviral restriction factor activities. *Proceedings of the National Academy of Sciences of the United States of America* **101**:10780-10785.
133. **Kibuuka, H., N. M. Berkowitz, M. Millard, M. E. Enama, A. Tindikahwa, A. B. Sekiziyivu, P. Costner, S. Sitar, D. Glover, Z. Hu, G. Joshi, D. Stanley, M. Kunchai, L. A. Eller, R. T. Bailer, R. A. Koup, G. J. Nabel, J. R. Mascola, N. J. Sullivan, B. S. Graham, M. Roederer, N. L. Michael, M. L. Robb, and J. E. Ledgerwood.** 2015. Safety and immunogenicity of Ebola virus and Marburg virus glycoprotein DNA vaccines assessed separately and concomitantly in healthy Ugandan adults: a phase 1b, randomised, double-blind, placebo-controlled clinical trial. *Lancet* **385**:1545-1554.
134. **Kluge, S. F., K. Mack, S. S. Iyer, F. M. Pujol, A. Heigele, G. H. Learn, S. M. Usmani, D. Sauter, S. Joas, D. Hotter, F. Bibollet-Ruche, L. J. Plenderleith, M. Peeters, M. Geyer, P. M. Sharp, O. T. Fackler, B. H. Hahn, and F. Kirchhoff.** 2014. Nef proteins of epidemic HIV-1 group O strains antagonize human tetherin. *Cell host & microbe* **16**:639-650.
135. **Kobayashi, T., H. Ode, T. Yoshida, K. Sato, P. Gee, S. P. Yamamoto, H. Ebina, K. Strebel, H. Sato, and Y. Koyanagi.** 2011. Identification of amino acids in the human tetherin transmembrane domain responsible for HIV-1 Vpu interaction and susceptibility. *Journal of virology* **85**:932-945.
136. **Kolesnikova, L., B. Berghofer, S. Bamberg, and S. Becker.** 2004. Multivesicular bodies as a platform for formation of the Marburg virus envelope. *Journal of virology* **78**:12277-12287.
137. **Kong, W. S., T. Irie, A. Yoshida, R. Kawabata, T. Kadoi, and T. Sakaguchi.** 2012. Inhibition of virus-like particle release of Sendai virus and Nipah virus, but not that of mumps virus, by tetherin/CD317/BST-2. *Hiroshima J Med Sci* **61**:59-67.
138. **Kuhl, A., C. Banning, A. Marzi, J. Votteler, I. Steffen, S. Bertram, I. Glowacka, A. Konrad, M. Sturzl, J. T. Guo, U. Schubert, H. Feldmann, G. Behrens, M. Schindler, and S. Pohlmann.** 2011. The Ebola virus glycoprotein and HIV-1 Vpu employ different strategies to counteract the antiviral factor tetherin. *J Infect Dis* **204 Suppl 3**:S850-860.
139. **Kuhn, J. H., S. Becker, H. Ebihara, T. W. Geisbert, K. M. Johnson, Y. Kawaoka, W. I. Lipkin, A. I. Negredo, S. V. Netesov, S. T. Nichol, G. Palacios, C. J. Peters, A. Tenorio, V. E. Volchkov, and P. B. Jahrling.** 2010. Proposal for a revised taxonomy of the family Filoviridae: classification, names of taxa and viruses, and virus abbreviations. *Arch Virol* **155**:2083-2103.
140. **Kupzig, S., V. Korolchuk, R. Rollason, A. Sugden, A. Wilde, and G. Banting.** 2003. Bst-2/HM1.24 is a raft-associated apical membrane protein with an unusual topology. *Traffic* **4**:694-709.
141. **Lamb, R. A., and C. J. Lai.** 1980. Sequence of interrupted and uninterrupted mRNAs and cloned DNA coding for the two overlapping nonstructural proteins of influenza virus. *Cell* **21**:475-485.

142. **Le Guenzo, B., P. Formenty, M. Wyers, P. Gounon, F. Walker, and C. Boesch.** 1995. Isolation and partial characterisation of a new strain of Ebola virus. *Lancet* **345**:1271-1274.
143. **Le Tortorec, A., and S. J. Neil.** 2009. Antagonism to and intracellular sequestration of human tetherin by the human immunodeficiency virus type 2 envelope glycoprotein. *J Virol* **83**:11966-11978.
144. **Ledgerwood, J. E., A. D. DeZure, D. A. Stanley, L. Novik, M. E. Enama, N. M. Berkowitz, Z. Hu, G. Joshi, A. Ploquin, S. Sitar, I. J. Gordon, S. A. Plummer, L. A. Holman, C. S. Hendel, G. Yamshchikov, F. Roman, A. Nicosia, S. Colloca, R. Cortese, R. T. Bailer, R. M. Schwartz, M. Roederer, J. R. Mascola, R. A. Koup, N. J. Sullivan, and B. S. Graham.** 2014. Chimpanzee Adenovirus Vector Ebola Vaccine - Preliminary Report. *N Engl J Med*.
145. **Lee, J. E., M. L. Fusco, A. J. Hessel, W. B. Oswald, D. R. Burton, and E. O. Saphire.** 2008. Structure of the Ebola virus glycoprotein bound to an antibody from a human survivor. *Nature* **454**:177-182.
146. **Lefebvre, A., C. Fiet, C. Belpois-Duchamp, M. Tiv, K. Astruc, and L. S. Aho Glele.** 2014. Case fatality rates of Ebola virus diseases: a meta-analysis of World Health Organization data. *Med Mal Infect* **44**:412-416.
147. **Lennemann, N. J., B. A. Rhein, E. Ndungo, K. Chandran, X. Qiu, and W. Maury.** 2014. Comprehensive functional analysis of N-linked glycans on Ebola virus GP1. *MBio* **5**:e00862-00813.
148. **Leroy, E. M., A. Epelboin, V. Mondonge, X. Pourrut, J. P. Gonzalez, J. J. Muyembe-Tamfum, and P. Formenty.** 2009. Human Ebola outbreak resulting from direct exposure to fruit bats in Luebo, Democratic Republic of Congo, 2007. *Vector Borne Zoonotic Dis* **9**:723-728.
149. **Leroy, E. M., B. Kumulungui, X. Pourrut, P. Rouquet, A. Hassanin, P. Yaba, A. Delicat, J. T. Paweska, J. P. Gonzalez, and R. Swanepoel.** 2005. Fruit bats as reservoirs of Ebola virus. *Nature* **438**:575-576.
150. **Leroy, E. M., P. Rouquet, P. Formenty, S. Souquiere, A. Kilbourne, J. M. Froment, M. Bermejo, S. Smit, W. Karesh, R. Swanepoel, S. R. Zaki, and P. E. Rollin.** 2004. Multiple Ebola virus transmission events and rapid decline of central African wildlife. *Science* **303**:387-390.
151. **Li, Q., A. Lau, T. J. Morris, L. Guo, C. B. Fordyce, and E. F. Stanley.** 2004. A syntaxin 1, Galpha(o), and N-type calcium channel complex at a presynaptic nerve terminal: analysis by quantitative immunocolocalization. *J Neurosci* **24**:4070-4081.
152. **Li, X., D. Kaloyanova, M. van Eijk, R. Eerland, G. van der Goot, V. Oorschot, J. Klumperman, F. Lottspeich, V. Starkuviene, F. T. Wieland, and J. B. Helms.** 2007. Involvement of a Golgi-resident GPI-anchored protein in maintenance of the Golgi structure. *Mol Biol Cell* **18**:1261-1271.
153. **Li, X. Y., F. Guo, L. Zhang, L. Kleiman, and S. Cen.** 2007. APOBEC3G inhibits DNA strand transfer during HIV-1 reverse transcription. *The Journal of biological chemistry* **282**:32065-32074.
154. **Licata, J. M., R. F. Johnson, Z. Han, and R. N. Harty.** 2004. Contribution of ebola virus glycoprotein, nucleoprotein, and VP24 to budding of VP40 virus-like particles. *Journal of virology* **78**:7344-7351.
155. **Licata, J. M., M. Simpson-Holley, N. T. Wright, Z. Han, J. Paragas, and R. N. Harty.** 2003. Overlapping motifs (PTAP and PPEY) within the Ebola virus VP40 protein function independently as late budding domains: involvement of host proteins TSG101 and VPS-4. *Journal of virology* **77**:1812-1819.

156. **Lilly, F.** 1967. Susceptibility to two strains of Friend leukemia virus in mice. *Science* **155**:461-462.
157. **Lindenmann, J.** 1962. Resistance of mice to mouse-adapted influenza A virus. *Virology* **16**:203-204.
158. **Liu, Y., S. Luo, S. He, M. Zhang, P. Wang, C. Li, W. Huang, B. Hu, G. E. Griffin, R. J. Shattock, and Q. Hu.** 2015. Tetherin restricts HSV-2 release and is counteracted by multiple viral glycoproteins. *Virology* **475**:96-109.
159. **Liu, Z., Q. Pan, S. Ding, J. Qian, F. Xu, J. Zhou, S. Cen, F. Guo, and C. Liang.** 2013. The interferon-inducible MxB protein inhibits HIV-1 infection. *Cell host & microbe* **14**:398-410.
160. **Lopez, L. A., S. J. Yang, C. M. Exline, S. Rengarajan, K. G. Haworth, and P. M. Cannon.** 2012. Anti-Tetherin Activities of HIV-1 Vpu and Ebola Virus Glycoprotein Do Not Involve Removal of Tetherin from Lipid Rafts. *J Virol* **86**:5467-5480.
161. **Lopez, L. A., S. J. Yang, H. Hauser, C. M. Exline, K. G. Haworth, J. Oldenburg, and P. M. Cannon.** 2010. Ebola virus glycoprotein counteracts BST-2/Tetherin restriction in a sequence-independent manner that does not require tetherin surface removal. *J Virol* **84**:7243-7255.
162. **Lu, Y., M. Wambach, M. G. Katze, and R. M. Krug.** 1995. Binding of the influenza virus NS1 protein to double-stranded RNA inhibits the activation of the protein kinase that phosphorylates the eIF-2 translation initiation factor. *Virology* **214**:222-228.
163. **Lv, M., J. Wang, X. Wang, T. Zuo, Y. Zhu, W. Kong, and X. Yu.** 2011. Polarity changes in the transmembrane domain core of HIV-1 Vpu inhibits its anti-tetherin activity. *PLoS One* **6**:e20890.
164. **Lyon, G. M., A. K. Mehta, J. B. Varkey, K. Brantly, L. Plyler, A. K. McElroy, C. S. Kraft, J. S. Towner, C. Spiropoulou, U. Stroher, T. M. Uyeki, and B. S. Ribner.** 2014. Clinical care of two patients with Ebola virus disease in the United States. *N Engl J Med* **371**:2402-2409.
165. **MacNeil, A., E. C. Farnon, O. W. Morgan, P. Gould, T. K. Boehmer, D. D. Blaney, P. Wiersma, J. W. Tappero, S. T. Nichol, T. G. Ksiazek, and P. E. Rollin.** 2011. Filovirus outbreak detection and surveillance: lessons from Bundibugyo. *The Journal of infectious diseases* **204 Suppl 3**:S761-767.
166. **Mangeat, B., G. Gers-Huber, M. Lehmann, M. Zufferey, J. Luban, and V. Piguet.** 2009. HIV-1 Vpu neutralizes the antiviral factor Tetherin/BST-2 by binding it and directing its beta-TrCP2-dependent degradation. *PLoS pathogens* **5**:e1000574.
167. **Mangeat, B., P. Turelli, G. Caron, M. Friedli, L. Perrin, and D. Trono.** 2003. Broad antiretroviral defence by human APOBEC3G through lethal editing of nascent reverse transcripts. *Nature* **424**:99-103.
168. **Mansouri, M., K. Viswanathan, J. L. Douglas, J. Hines, J. Gustin, A. V. Moses, and K. Fruh.** 2009. Molecular mechanism of BST2/tetherin downregulation by K5/MIR2 of Kaposi's sarcoma-associated herpesvirus. *J Virol* **83**:9672-9681.
169. **Marin, M., K. M. Rose, S. L. Kozak, and D. Kabat.** 2003. HIV-1 Vif protein binds the editing enzyme APOBEC3G and induces its degradation. *Nat Med* **9**:1398-1403.
170. **Martin-Serrano, J., T. Zang, and P. D. Bieniasz.** 2001. HIV-1 and Ebola virus encode small peptide motifs that recruit Tsg101 to sites of particle assembly to facilitate egress. *Nat Med* **7**:1313-1319.
171. **Marzi, A., A. Akhavan, G. Simmons, T. Gramberg, H. Hofmann, P. Bates, V. R. Lingappa, and S. Pohlmann.** 2006. The signal peptide of the ebolavirus glycoprotein influences interaction with the cellular lectins DC-SIGN and DC-SIGNR. *Journal of virology* **80**:6305-6317.

172. **Masuyama, N., T. Kuronita, R. Tanaka, T. Muto, Y. Hirota, A. Takigawa, H. Fujita, Y. Aso, J. Amano, and Y. Tanaka.** 2009. HM1.24 is internalized from lipid rafts by clathrin-mediated endocytosis through interaction with alpha-adaptin. *J Biol Chem* **284**:15927-15941.
173. **McNatt, M. W., T. Zang, T. Hatzioannou, M. Bartlett, I. B. Fofana, W. E. Johnson, S. J. Neil, and P. D. Bieniasz.** 2009. Species-specific activity of HIV-1 Vpu and positive selection of tetherin transmembrane domain variants. *PLoS Pathog* **5**:e1000300.
174. **Min, J. Y., and R. M. Krug.** 2006. The primary function of RNA binding by the influenza A virus NS1 protein in infected cells: Inhibiting the 2'-5' oligo (A) synthetase/RNase L pathway. *Proceedings of the National Academy of Sciences of the United States of America* **103**:7100-7105.
175. **Mitchell, R. S., C. Katsura, M. A. Skasko, K. Fitzpatrick, D. Lau, A. Ruiz, E. B. Stephens, F. Margottin-Goguet, R. Benarous, and J. C. Guatelli.** 2009. Vpu antagonizes BST-2-mediated restriction of HIV-1 release via beta-TrCP and endolysosomal trafficking. *PLoS Pathog* **5**:e1000450.
176. **Mohan, G. S., W. Li, L. Ye, R. W. Compans, and C. Yang.** 2012. Antigenic subversion: a novel mechanism of host immune evasion by Ebola virus. *PLoS pathogens* **8**:e1003065.
177. **Muhlberger, E., M. Weik, V. E. Volchkov, H. D. Klenk, and S. Becker.** 1999. Comparison of the transcription and replication strategies of marburg virus and Ebola virus by using artificial replication systems. *Journal of virology* **73**:2333-2342.
178. **Mupapa, K., M. Massamba, K. Kibadi, K. Kuvula, A. Bwaka, M. Kipasa, R. Colebunders, and J. J. Muyembe-Tamfum.** 1999. Treatment of Ebola hemorrhagic fever with blood transfusions from convalescent patients. *International Scientific and Technical Committee. The Journal of infectious diseases* **179 Suppl 1**:S18-23.
179. **Nanbo, A., M. Imai, S. Watanabe, T. Noda, K. Takahashi, G. Neumann, P. Halfmann, and Y. Kawaoka.** 2010. Ebolavirus is internalized into host cells via macropinocytosis in a viral glycoprotein-dependent manner. *PLoS pathogens* **6**:e1001121.
180. **Narayan, S., R. J. Barnard, and J. A. Young.** 2003. Two retroviral entry pathways distinguished by lipid raft association of the viral receptor and differences in viral infectivity. *Journal of virology* **77**:1977-1983.
181. **Ndambi, R., P. Akamituna, M. J. Bonnet, A. M. Tukadila, J. J. Muyembe-Tamfum, and R. Colebunders.** 1999. Epidemiologic and clinical aspects of the Ebola virus epidemic in Mosango, Democratic Republic of the Congo, 1995. *The Journal of infectious diseases* **179 Suppl 1**:S8-10.
182. **Negredo, A., G. Palacios, S. Vazquez-Moron, F. Gonzalez, H. Dopazo, F. Molero, J. Juste, J. Quetglas, N. Savji, M. de la Cruz Martinez, J. E. Herrera, M. Pizarro, S. K. Hutchison, J. E. Echevarria, W. I. Lipkin, and A. Tenorio.** 2011. Discovery of an ebolavirus-like filovirus in europe. *PLoS pathogens* **7**:e1002304.
183. **Neil, S. J., V. Sandrin, W. I. Sundquist, and P. D. Bieniasz.** 2007. An interferon-alpha-induced tethering mechanism inhibits HIV-1 and Ebola virus particle release but is counteracted by the HIV-1 Vpu protein. *Cell host & microbe* **2**:193-203.
184. **Neil, S. J., T. Zang, and P. D. Bieniasz.** 2008. Tetherin inhibits retrovirus release and is antagonized by HIV-1 Vpu. *Nature* **451**:425-430.
185. **Neumann, G., H. Ebihara, A. Takada, T. Noda, D. Kobasa, L. D. Jasenosky, S. Watanabe, J. H. Kim, H. Feldmann, and Y. Kawaoka.** 2005. Ebola virus VP40 late domains are not essential for viral replication in cell culture. *Journal of virology* **79**:10300-10307.

186. **Newman, E. N., R. K. Holmes, H. M. Craig, K. C. Klein, J. R. Lingappa, M. H. Malim, and A. M. Sheehy.** 2005. Antiviral function of APOBEC3G can be dissociated from cytidine deaminase activity. *Curr Biol* **15**:166-170.
187. **Nisole, S., M. A. Maroui, X. H. Mascle, M. Aubry, and M. K. Chelbi-Alix.** 2013. Differential Roles of PML Isoforms. *Front Oncol* **3**:125.
188. **Noda, T., H. Sagara, E. Suzuki, A. Takada, H. Kida, and Y. Kawaoka.** 2002. Ebola virus VP40 drives the formation of virus-like filamentous particles along with GP. *J Virol* **76**:4855-4865.
189. **Noda, T., S. Watanabe, H. Sagara, and Y. Kawaoka.** 2007. Mapping of the VP40-binding regions of the nucleoprotein of Ebola virus. *Journal of virology* **81**:3554-3562.
190. **Okumura, A., P. M. Pitha, and R. N. Harty.** 2008. ISG15 inhibits Ebola VP40 VLP budding in an L-domain-dependent manner by blocking Nedd4 ligase activity. *Proceedings of the National Academy of Sciences of the United States of America* **105**:3974-3979.
191. **Ono, K., T. Ohtomo, K. Yoshida, Y. Yoshimura, S. Kawai, Y. Koishihara, S. Ozaki, M. Kosaka, and M. Tsuchiya.** 1999. The humanized anti-HM1.24 antibody effectively kills multiple myeloma cells by human effector cell-mediated cytotoxicity. *Mol Immunol* **36**:387-395.
192. **Ozaki, K., S. Ozaki, M. Kosaka, and S. Saito.** 1996. Localization and imaging of human plasmacytoma xenografts in severe combined immunodeficiency mice by a new murine monoclonal antibody, anti-HM1.24. *Tokushima J Exp Med* **43**:7-15.
193. **Pan, X. B., J. C. Han, X. Cong, and L. Wei.** 2012. BST2/tetherin inhibits dengue virus release from human hepatoma cells. *PLoS One* **7**:e51033.
194. **Panchal, R. G., G. Ruthel, T. A. Kenny, G. H. Kallstrom, D. Lane, S. S. Badie, L. Li, S. Bavari, and M. J. Aman.** 2003. In vivo oligomerization and raft localization of Ebola virus protein VP40 during vesicular budding. *Proceedings of the National Academy of Sciences of the United States of America* **100**:15936-15941.
195. **Pardieu, C., R. Vigan, S. J. Wilson, A. Calvi, T. Zang, P. Bieniasz, P. Kellam, G. J. Towers, and S. J. Neil.** 2010. The RING-CH ligase K5 antagonizes restriction of KSHV and HIV-1 particle release by mediating ubiquitin-dependent endosomal degradation of tetherin. *PLoS pathogens* **6**:e1000843.
196. **Pavlovic, J., O. Haller, and P. Staeheli.** 1992. Human and mouse Mx proteins inhibit different steps of the influenza virus multiplication cycle. *Journal of virology* **66**:2564-2569.
197. **Pavlovic, J., T. Zurcher, O. Haller, and P. Staeheli.** 1990. Resistance to influenza virus and vesicular stomatitis virus conferred by expression of human MxA protein. *Journal of virology* **64**:3370-3375.
198. **Perez-Caballero, D., T. Zang, A. Ebrahimi, M. W. McNatt, D. A. Gregory, M. C. Johnson, and P. D. Bieniasz.** 2009. Tetherin inhibits HIV-1 release by directly tethering virions to cells. *Cell* **139**:499-511.
199. **Pichlmair, A., C. Lassnig, C. A. Eberle, M. W. Gorna, C. L. Baumann, T. R. Burkard, T. Burckstummer, A. Stefanovic, S. Krieger, K. L. Bennett, T. Rulicke, F. Weber, J. Colinge, M. Muller, and G. Superti-Furga.** 2011. IFIT1 is an antiviral protein that recognizes 5'-triphosphate RNA. *Nat Immunol* **12**:624-630.
200. **Pincetic, A., Z. Kuang, E. J. Seo, and J. Leis.** 2010. The interferon-induced gene ISG15 blocks retrovirus release from cells late in the budding process. *Journal of virology* **84**:4725-4736.

201. **Piqueras, B., J. Connolly, H. Freitas, A. K. Palucka, and J. Banchereau.** 2006. Upon viral exposure, myeloid and plasmacytoid dendritic cells produce 3 waves of distinct chemokines to recruit immune effectors. *Blood* **107**:2613-2618.
202. **Pourrut, X., B. Kumulungui, T. Wittmann, G. Moussavou, A. Delicat, P. Yaba, D. Nkoghe, J. P. Gonzalez, and E. M. Leroy.** 2005. The natural history of Ebola virus in Africa. *Microbes Infect* **7**:1005-1014.
203. **Prins, K. C., W. B. Cardenas, and C. F. Basler.** 2009. Ebola virus protein VP35 impairs the function of interferon regulatory factor-activating kinases IKKepsilon and TBK-1. *Journal of virology* **83**:3069-3077.
204. **Qiu, X., G. Wong, J. Audet, A. Bello, L. Fernando, J. B. Alimonti, H. Fausther-Bovendo, H. Wei, J. Aviles, E. Hiatt, A. Johnson, J. Morton, K. Swope, O. Bohorov, N. Bohorova, C. Goodman, D. Kim, M. H. Pauly, J. Velasco, J. Pettitt, G. G. Olinger, K. Whaley, B. Xu, J. E. Strong, L. Zeitlin, and G. P. Kobinger.** 2014. Reversion of advanced Ebola virus disease in nonhuman primates with ZMapp. *Nature* **514**:47-53.
205. **Radoshitzky, S. R., L. Dong, X. Chi, J. C. Clester, C. Retterer, K. Spurgers, J. H. Kuhn, S. Sandwick, G. Ruthel, K. Kota, D. Boltz, T. Warren, P. J. Kranzusch, S. P. Whelan, and S. Bavari.** 2010. Infectious Lassa virus, but not filoviruses, is restricted by BST-2/tetherin. *J Virol* **84**:10569-10580.
206. **Rampling, T., K. Ewer, G. Bowyer, D. Wright, E. B. Imoukhuede, R. Payne, F. Hartnell, M. Gibani, C. Bliss, A. Minhinnick, M. Wilkie, N. Venkatraman, I. Poulton, N. Lella, R. Roberts, K. Sierra-Davidson, V. Krahling, E. Berrie, F. Roman, I. De Ryck, A. Nicosia, N. J. Sullivan, D. A. Stanley, J. E. Ledgerwood, R. M. Schwartz, L. Siani, S. Colloca, A. Folgori, S. Di Marco, R. Cortese, S. Becker, B. S. Graham, R. A. Koup, M. M. Levine, V. Moorthy, A. J. Pollard, S. J. Draper, W. R. Ballou, A. Lawrie, S. C. Gilbert, and A. V. Hill.** 2015. A Monovalent Chimpanzee Adenovirus Ebola Vaccine - Preliminary Report. *N Engl J Med*.
207. **Ratner, L., W. Haseltine, R. Patarca, K. J. Livak, B. Starcich, S. F. Josephs, E. R. Doran, J. A. Rafalski, E. A. Whitehorn, K. Baumeister, and et al.** 1985. Complete nucleotide sequence of the AIDS virus, HTLV-III. *Nature* **313**:277-284.
208. **Regad, T., A. Saib, V. Lallemand-Breitenbach, P. P. Pandolfi, H. de The, and M. K. Chelbi-Alix.** 2001. PML mediates the interferon-induced antiviral state against a complex retrovirus via its association with the viral transactivator. *Embo J* **20**:3495-3505.
209. **Regules, J. A., J. H. Beigel, K. M. Paolino, J. Voell, A. R. Castellano, P. Munoz, J. E. Moon, R. C. Ruck, J. W. Bennett, P. S. Twomey, R. L. Gutierrez, S. A. Remich, H. R. Hack, M. L. Wisniewski, M. D. Josleyn, S. A. Kwilas, N. Van Deusen, O. T. Mbaya, Y. Zhou, D. A. Stanley, R. L. Bliss, D. Cebrik, K. S. Smith, M. Shi, J. E. Ledgerwood, B. S. Graham, N. J. Sullivan, L. L. Jagodzinski, S. A. Peel, J. B. Alimonti, J. W. Hooper, P. M. Silvera, B. K. Martin, T. P. Monath, W. J. Ramsey, C. J. Link, H. C. Lane, N. L. Michael, R. T. Davey, Jr., and S. J. Thomas.** 2015. A Recombinant Vesicular Stomatitis Virus Ebola Vaccine - Preliminary Report. *N Engl J Med*.
210. **Reid, S. P., L. W. Leung, A. L. Hartman, O. Martinez, M. L. Shaw, C. Carbonnelle, V. E. Volchkov, S. T. Nichol, and C. F. Basler.** 2006. Ebola virus VP24 binds karyopherin alpha1 and blocks STAT1 nuclear accumulation. *Journal of virology* **80**:5156-5167.
211. **Reth, M.** 1989. Antigen receptor tail clue. *Nature* **338**:383-384.
212. **Rice, G. I., J. Bond, A. Asipu, R. L. Brunette, I. W. Manfield, I. M. Carr, J. C. Fuller, R. M. Jackson, T. Lamb, T. A. Briggs, M. Ali, H. Gornall, L. R. Couthard, A. Aeby, S. P. Attard-Montalto, E. Bertini, C. Bodemer, K. Brockmann, L. A. Brueton, P. C. Corry, I. Desguerre, E. Fazzi, A. G. Cazorla, B. Gener, B. C. Hamel, A. Heiberg, M. Hunter, M. S. van der Knaap, R. Kumar, L. Lagae, P. G. Landrieu, C. M. Lourenco, D.**

- Marom, M. F. McDermott, W. van der Merwe, S. Orcesi, J. S. Prendiville, M. Rasmussen, S. A. Shalev, D. M. Soler, M. Shinawi, R. Spiegel, T. Y. Tan, A. Vanderver, E. L. Wakeling, E. Wassmer, E. Whittaker, P. Lebon, D. B. Stetson, D. T. Bonthron, and Y. J. Crow.** 2009. Mutations involved in Aicardi-Goutieres syndrome implicate SAMHD1 as regulator of the innate immune response. *Nat Genet* **41**:829-832.
213. **Rollason, R., V. Korolchuk, C. Hamilton, M. Jepson, and G. Banting.** 2009. A CD317/tetherin-RICH2 complex plays a critical role in the organization of the subapical actin cytoskeleton in polarized epithelial cells. *J Cell Biol* **184**:721-736.
214. **Rong, L., J. Zhang, J. Lu, Q. Pan, R. P. Lorgeoux, C. Aloysius, F. Guo, S. L. Liu, M. A. Wainberg, and C. Liang.** 2009. The transmembrane domain of BST-2 determines its sensitivity to down-modulation by human immunodeficiency virus type 1 Vpu. *J Virol* **83**:7536-7546.
215. **Ryabchikova, E. I., L. V. Kolesnikova, and S. V. Luchko.** 1999. An analysis of features of pathogenesis in two animal models of Ebola virus infection. *The Journal of infectious diseases* **179 Suppl 1**:S199-202.
216. **Saeed, M. F., A. A. Kolokoltsov, T. Albrecht, and R. A. Davey.** 2010. Cellular entry of ebola virus involves uptake by a macropinocytosis-like mechanism and subsequent trafficking through early and late endosomes. *PLoS pathogens* **6**:e1001110.
217. **Sakuma, T., T. Noda, S. Urata, Y. Kawaoka, and J. Yasuda.** 2009. Inhibition of Lassa and Marburg virus production by tetherin. *J Virol* **83**:2382-2385.
218. **Samelson, L. E., and R. D. Klausner.** 1992. Tyrosine kinases and tyrosine-based activation motifs. Current research on activation via the T cell antigen receptor. *The Journal of biological chemistry* **267**:24913-24916.
219. **Sanchez, A., and M. P. Kiley.** 1987. Identification and analysis of Ebola virus messenger RNA. *Virology* **157**:414-420.
220. **Sanchez, A., M. P. Kiley, B. P. Holloway, and D. D. Auperin.** 1993. Sequence analysis of the Ebola virus genome: organization, genetic elements, and comparison with the genome of Marburg virus. *Virus Res* **29**:215-240.
221. **Sanchez, A., M. P. Kiley, B. P. Holloway, J. B. McCormick, and D. D. Auperin.** 1989. The nucleoprotein gene of Ebola virus: cloning, sequencing, and in vitro expression. *Virology* **170**:81-91.
222. **Sanchez, A., S. G. Trappier, B. W. Mahy, C. J. Peters, and S. T. Nichol.** 1996. The virion glycoproteins of Ebola viruses are encoded in two reading frames and are expressed through transcriptional editing. *Proc Natl Acad Sci U S A* **93**:3602-3607.
223. **Sanchez, A., Z. Y. Yang, L. Xu, G. J. Nabel, T. Crews, and C. J. Peters.** 1998. Biochemical analysis of the secreted and virion glycoproteins of Ebola virus. *Journal of virology* **72**:6442-6447.
224. **Sauter, D., M. Schindler, A. Specht, W. N. Landford, J. Munch, K. A. Kim, J. Votteler, U. Schubert, F. Bibollet-Ruche, B. F. Keele, J. Takehisa, Y. Ogando, C. Ochsenbauer, J. C. Kappes, A. Ayouba, M. Peeters, G. H. Learn, G. Shaw, P. M. Sharp, P. Bieniasz, B. H. Hahn, T. Hatziioannou, and F. Kirchhoff.** 2009. Tetherin-driven adaptation of Vpu and Nef function and the evolution of pandemic and nonpandemic HIV-1 strains. *Cell Host Microbe* **6**:409-421.
225. **Schornerberg, K., S. Matsuyama, K. Kabsch, S. Delos, A. Bouton, and J. White.** 2006. Role of endosomal cathepsins in entry mediated by the Ebola virus glycoprotein. *Journal of virology* **80**:4174-4178.
226. **Schubert, H. L., Q. Zhai, V. Sandrin, D. M. Eckert, M. Garcia-Maya, L. Saul, W. I. Sundquist, R. A. Steiner, and C. P. Hill.** 2010. Structural and functional studies on the

- extracellular domain of BST2/tetherin in reduced and oxidized conformations. *Proc Natl Acad Sci U S A* **107**:17951-17956.
227. **Scianimanico, S., G. Schoehn, J. Timmins, R. H. Ruigrok, H. D. Klenk, and W. Weissenhorn.** 2000. Membrane association induces a conformational change in the Ebola virus matrix protein. *Embo J* **19**:6732-6741.
228. **Sebastian, S., and J. Luban.** 2005. TRIM5alpha selectively binds a restriction-sensitive retroviral capsid. *Retrovirology* **2**:40.
229. **Serra-Moreno, R., K. Zimmermann, L. J. Stern, and D. T. Evans.** 2013. Tetherin/BST-2 antagonism by Nef depends on a direct physical interaction between Nef and tetherin, and on clathrin-mediated endocytosis. *PLoS pathogens* **9**:e1003487.
230. **Sheehy, A. M., N. C. Gaddis, J. D. Choi, and M. H. Malim.** 2002. Isolation of a human gene that inhibits HIV-1 infection and is suppressed by the viral Vif protein. *Nature* **418**:646-650.
231. **Sheehy, A. M., N. C. Gaddis, and M. H. Malim.** 2003. The antiretroviral enzyme APOBEC3G is degraded by the proteasome in response to HIV-1 Vif. *Nat Med* **9**:1404-1407.
232. **Shimajima, M., A. Takada, H. Ebihara, G. Neumann, K. Fujioka, T. Irimura, S. Jones, H. Feldmann, and Y. Kawaoka.** 2006. Tyro3 family-mediated cell entry of Ebola and Marburg viruses. *Journal of virology* **80**:10109-10116.
233. **Siekierka, J., T. M. Mariano, P. A. Reichel, and M. B. Mathews.** 1985. Translational control by adenovirus: lack of virus-associated RNAI during adenovirus infection results in phosphorylation of initiation factor eIF-2 and inhibition of protein synthesis. *Proceedings of the National Academy of Sciences of the United States of America* **82**:1959-1963.
234. **Simmons, G., J. D. Reeves, C. C. Grogan, L. H. Vandenberghe, F. Baribaud, J. C. Whitbeck, E. Burke, M. J. Buchmeier, E. J. Soilleux, J. L. Riley, R. W. Doms, P. Bates, and S. Pohlmann.** 2003. DC-SIGN and DC-SIGNR bind ebola glycoproteins and enhance infection of macrophages and endothelial cells. *Virology* **305**:115-123.
235. **Simmons, G., R. J. Wool-Lewis, F. Baribaud, R. C. Netter, and P. Bates.** 2002. Ebola virus glycoproteins induce global surface protein down-modulation and loss of cell adherence. *Journal of virology* **76**:2518-2528.
236. **Simons, K., and E. Ikonen.** 1997. Functional rafts in cell membranes. *Nature* **387**:569-572.
237. **Skasko, M., Y. Wang, Y. Tian, A. Tokarev, J. Munguia, A. Ruiz, E. B. Stephens, S. J. Opella, and J. Guatelli.** 2012. HIV-1 Vpu protein antagonizes innate restriction factor BST-2 via lipid-embedded helix-helix interactions. *The Journal of biological chemistry* **287**:58-67.
238. **Stanley, D. A., A. N. Honko, C. Asiedu, J. C. Trefry, A. W. Lau-Kilby, J. C. Johnson, L. Hensley, V. Ammendola, A. Abbate, F. Grazioli, K. E. Foulds, C. Cheng, L. Wang, M. M. Donaldson, S. Colloca, A. Folgori, M. Roederer, G. J. Nabel, J. Mascola, A. Nicosia, R. Cortese, R. A. Koup, and N. J. Sullivan.** 2014. Chimpanzee adenovirus vaccine generates acute and durable protective immunity against ebolavirus challenge. *Nat Med* **20**:1126-1129.
239. **Stopak, K., C. de Noronha, W. Yonemoto, and W. C. Greene.** 2003. HIV-1 Vif blocks the antiviral activity of APOBEC3G by impairing both its translation and intracellular stability. *Mol Cell* **12**:591-601.
240. **Strebel, K., T. Klimkait, and M. A. Martin.** 1988. A novel gene of HIV-1, vpu, and its 16-kilodalton product. *Science* **241**:1221-1223.
241. **Stremlau, M., M. Perron, M. Lee, Y. Li, B. Song, H. Javanbakht, F. Diaz-Griffero, D. J. Anderson, W. I. Sundquist, and J. Sodroski.** 2006. Specific recognition and

- accelerated uncoating of retroviral capsids by the TRIM5alpha restriction factor. Proceedings of the National Academy of Sciences of the United States of America **103**:5514-5519.
242. **Sze, A., S. M. Belgnaoui, D. Olagnier, R. Lin, J. Hiscott, and J. van Grevenynghe.** 2013. Host restriction factor SAMHD1 limits human T cell leukemia virus type 1 infection of monocytes via STING-mediated apoptosis. *Cell host & microbe* **14**:422-434.
243. **Takada, A., S. Watanabe, H. Ito, K. Okazaki, H. Kida, and Y. Kawaoka.** 2000. Downregulation of beta1 integrins by Ebola virus glycoprotein: implication for virus entry. *Virology* **278**:20-26.
244. **Tavano, B., R. P. Galao, D. R. Graham, S. J. Neil, V. N. Aquino, D. Fuchs, and A. Boasso.** 2013. Ig-like transcript 7, but not bone marrow stromal cell antigen 2 (also known as HM1.24, tetherin, or CD317), modulates plasmacytoid dendritic cell function in primary human blood leukocytes. *Journal of immunology* **190**:2622-2630.
245. **Terenzi, F., P. Saikia, and G. C. Sen.** 2008. Interferon-inducible protein, P56, inhibits HPV DNA replication by binding to the viral protein E1. *Embo J* **27**:3311-3321.
246. **Timmins, J., G. Schoehn, C. Kohlhaas, H. D. Klenk, R. W. Ruigrok, and W. Weissenhorn.** 2003. Oligomerization and polymerization of the filovirus matrix protein VP40. *Virology* **312**:359-368.
247. **Timmins, J., G. Schoehn, S. Ricard-Blum, S. Scianimanico, T. Vernet, R. W. Ruigrok, and W. Weissenhorn.** 2003. Ebola virus matrix protein VP40 interaction with human cellular factors Tsg101 and Nedd4. *J Mol Biol* **326**:493-502.
248. **Tokarev, A., M. Suarez, W. Kwan, K. Fitzpatrick, R. Singh, and J. Guatelli.** 2013. Stimulation of NF-kappaB activity by the HIV restriction factor BST2. *Journal of virology* **87**:2046-2057.
249. **Tokarev, A. A., J. Munguia, and J. C. Guatelli.** 2011. Serine-threonine ubiquitination mediates downregulation of BST-2/tetherin and relief of restricted virion release by HIV-1 Vpu. *Journal of virology* **85**:51-63.
250. **Towers, G., M. Bock, S. Martin, Y. Takeuchi, J. P. Stoye, and O. Danos.** 2000. A conserved mechanism of retrovirus restriction in mammals. Proceedings of the National Academy of Sciences of the United States of America **97**:12295-12299.
251. **Turelli, P., B. Mangeat, S. Jost, S. Vianin, and D. Trono.** 2004. Inhibition of hepatitis B virus replication by APOBEC3G. *Science* **303**:1829.
252. **Uchil, P. D., B. D. Quinlan, W. T. Chan, J. M. Luna, and W. Mothes.** 2008. TRIM E3 ligases interfere with early and late stages of the retroviral life cycle. *PLoS pathogens* **4**:e16.
253. **Van Damme, N., D. Goff, C. Katsura, R. L. Jorgenson, R. Mitchell, M. C. Johnson, E. B. Stephens, and J. Guatelli.** 2008. The interferon-induced protein BST-2 restricts HIV-1 release and is downregulated from the cell surface by the viral Vpu protein. *Cell Host Microbe* **3**:245-252.
254. **Venkatesh, S., and P. D. Bieniasz.** 2013. Mechanism of HIV-1 virion entrapment by tetherin. *PLoS pathogens* **9**:e1003483.
255. **Vigan, R., and S. J. Neil.** 2010. Determinants of tetherin antagonism in the transmembrane domain of the human immunodeficiency virus type 1 Vpu protein. *Journal of virology* **84**:12958-12970.
256. **Villinger, F., P. E. Rollin, S. S. Brar, N. F. Chikkala, J. Winter, J. B. Sundstrom, S. R. Zaki, R. Swanepoel, A. A. Ansari, and C. J. Peters.** 1999. Markedly elevated levels of interferon (IFN)-gamma, IFN-alpha, interleukin (IL)-2, IL-10, and tumor necrosis factor-alpha associated with fatal Ebola virus infection. *The Journal of infectious diseases* **179 Suppl 1**:S188-191.

257. **Viswanathan, K., M. S. Smith, D. Malouli, M. Mansouri, J. A. Nelson, and K. Fruh.** 2011. BST2/Tetherin enhances entry of human cytomegalovirus. *PLoS pathogens* **7**:e1002332.
258. **Volchkov, V. E., S. Becker, V. A. Volchkova, V. A. Ternovoj, A. N. Kotov, S. V. Netesov, and H. D. Klenk.** 1995. GP mRNA of Ebola virus is edited by the Ebola virus polymerase and by T7 and vaccinia virus polymerases. *Virology* **214**:421-430.
259. **Volchkov, V. E., H. Feldmann, V. A. Volchkova, and H. D. Klenk.** 1998. Processing of the Ebola virus glycoprotein by the proprotein convertase furin. *Proc Natl Acad Sci U S A* **95**:5762-5767.
260. **Volchkov, V. E., V. A. Volchkova, A. A. Chepurinov, V. M. Blinov, O. Dolnik, S. V. Netesov, and H. Feldmann.** 1999. Characterization of the L gene and 5' trailer region of Ebola virus. *The Journal of general virology* **80 (Pt 2)**:355-362.
261. **Volchkova, V. A., H. D. Klenk, and V. E. Volchkov.** 1999. Delta-peptide is the carboxy-terminal cleavage fragment of the nonstructural small glycoprotein sGP of Ebola virus. *Virology* **265**:164-171.
262. **Wang, X., E. R. Hinson, and P. Cresswell.** 2007. The interferon-inducible protein viperin inhibits influenza virus release by perturbing lipid rafts. *Cell host & microbe* **2**:96-105.
263. **Watanabe, R., G. P. Leser, and R. A. Lamb.** 2011. Influenza virus is not restricted by tetherin whereas influenza VLP production is restricted by tetherin. *Virology* **417**:50-56.
264. **Wauquier, N., P. Becquart, C. Padilla, S. Baize, and E. M. Leroy.** 2010. Human fatal zaire ebola virus infection is associated with an aberrant innate immunity and with massive lymphocyte apoptosis. *PLoS Negl Trop Dis* **4**.
265. **Weidner, J. M., D. Jiang, X. B. Pan, J. Chang, T. M. Block, and J. T. Guo.** 2010. Interferon-induced cell membrane proteins, IFITM3 and tetherin, inhibit vesicular stomatitis virus infection via distinct mechanisms. *J Virol* **84**:12646-12657.
266. **Weik, M., J. Modrof, H. D. Klenk, S. Becker, and E. Muhlberger.** 2002. Ebola virus VP30-mediated transcription is regulated by RNA secondary structure formation. *Journal of virology* **76**:8532-8539.
267. **Weinelt, J., and S. J. Neil.** 2014. Differential sensitivities of tetherin isoforms to counteraction by primate lentiviruses. *Journal of virology* **88**:5845-5858.
268. **Weissenhorn, W., L. J. Calder, S. A. Wharton, J. J. Skehel, and D. C. Wiley.** 1998. The central structural feature of the membrane fusion protein subunit from the Ebola virus glycoprotein is a long triple-stranded coiled coil. *Proceedings of the National Academy of Sciences of the United States of America* **95**:6032-6036.
269. **Weissenhorn, W., A. Carfi, K. H. Lee, J. J. Skehel, and D. C. Wiley.** 1998. Crystal structure of the Ebola virus membrane fusion subunit, GP2, from the envelope glycoprotein ectodomain. *Mol Cell* **2**:605-616.
270. **Wills, J. W., C. E. Cameron, C. B. Wilson, Y. Xiang, R. P. Bennett, and J. Leis.** 1994. An assembly domain of the Rous sarcoma virus Gag protein required late in budding. *Journal of virology* **68**:6605-6618.
271. **Wool-Lewis, R. J., and P. Bates.** 1999. Endoproteolytic processing of the ebola virus envelope glycoprotein: cleavage is not required for function. *Journal of virology* **73**:1419-1426.
272. **Wreschner, D. H., J. W. McCauley, J. J. Skehel, and I. M. Kerr.** 1981. Interferon action--sequence specificity of the ppp(A2'p)nA-dependent ribonuclease. *Nature* **289**:414-417.
273. **Yang, Z. Y., H. J. Duckers, N. J. Sullivan, A. Sanchez, E. G. Nabel, and G. J. Nabel.** 2000. Identification of the Ebola virus glycoprotein as the main viral determinant of vascular cell cytotoxicity and injury. *Nat Med* **6**:886-889.

274. **Yondola, M. A., F. Fernandes, A. Belicha-Villanueva, M. Uccellini, Q. Gao, C. Carter, and P. Palese.** 2011. Budding capability of the influenza virus neuraminidase can be modulated by tetherin. *J Virol* **85**:2480-2491.
275. **Yu, X., Y. Yu, B. Liu, K. Luo, W. Kong, P. Mao, and X. F. Yu.** 2003. Induction of APOBEC3G ubiquitination and degradation by an HIV-1 Vif-Cul5-SCF complex. *Science* **302**:1056-1060.
276. **Zhang, F., W. N. Landford, M. Ng, M. W. McNatt, P. D. Bieniasz, and T. Hatziioannou.** 2011. SIV Nef proteins recruit the AP-2 complex to antagonize Tetherin and facilitate virion release. *PLoS Pathog* **7**:e1002039.
277. **Zhang, F., S. J. Wilson, W. C. Landford, B. Virgen, D. Gregory, M. C. Johnson, J. Munch, F. Kirchhoff, P. D. Bieniasz, and T. Hatziioannou.** 2009. Nef proteins from simian immunodeficiency viruses are tetherin antagonists. *Cell Host Microbe* **6**:54-67.
278. **Zhang, H., B. Yang, R. J. Pomerantz, C. Zhang, S. C. Arunachalam, and L. Gao.** 2003. The cytidine deaminase CEM15 induces hypermutation in newly synthesized HIV-1 DNA. *Nature* **424**:94-98.
279. **Zola, H., B. Swart, I. Nicholson, B. Aasted, A. Bensussan, L. Bomsell, C. Buckley, G. Clark, K. Drbal, P. Engel, D. Hart, V. Horejsi, C. Isacke, P. Macardle, F. Malavasi, D. Mason, D. Olive, A. Saalmueller, S. F. Schlossman, R. Schwartz-Albiez, P. Simmons, T. F. Tedder, M. Uguccioni, and H. Warren.** 2005. CD molecules 2005: human cell differentiation molecules. *Blood* **106**:3123-3126.